

THE UPTAKE OF SILICIC ACID BY DIATOMS
IN THE BERING SEA

RECOMMENDED:

William S. Kuylenstierna

John G. Guering

Chairman, Advisory Committee

John G. Guering

Head, Marine Science Program

W. S. Kuylenstierna

Director, Division of Marine Sciences

APPROVED:

K. B. Gathman

Vice Chancellor for Research and Advanced Study

Sept. 8, 1983.

Date

THE UPTAKE OF SILICIC ACID BY DIATOMS
IN THE BERING SEA

A
THESIS

Presented to the Faculty of the University of Alaska
in Partial Fulfillment of the Requirements
for the Degree of

Master of Science

by
Susan Banahan, B. S.

Fairbanks, Alaska

September 1983

ABSTRACT

Silicic acid uptake rates and biogenic silica concentrations were measured on the southeastern Bering Sea shelf. Specific uptake velocities were low throughout the spring phytoplankton bloom on both middle and outer shelves. Average concentrations of biogenic silica were 300 and 400 mmol Si m⁻² in the middle and coastal domains, respectively. The lower concentration in the outer shelf, 100 mmol Si m⁻², was a result of the greater grazing stress on diatom phytoplankton in that area. Average kinetic constants for silicic acid uptake were K_s = 3.2 μM and V_{max} = 0.009 h⁻¹. Cellular composition of shelf phytoplankton reflected N-limitation more than Si-limitation. Estimated annual production of biogenic silica is 2.87 mol Si m⁻² yr⁻¹ for the middle shelf and 1.64 mol Si m⁻² yr⁻¹ for the outer shelf. The accumulation rate of silica in outer shelf sediments equals ~50% of the annual production, diffusion of silicic acid from the sediments equals ~15% and the remaining 35% is assumed to recycle in the water column.

TABLE OF CONTENTS

ABSTRACT.	iii
LIST OF FIGURES	vi
LIST OF TABLES.	ix
ACKNOWLEDGEMENTS.	xi
CHAPTER I. INTRODUCTION.	1
<u>Diatoms in Primary Production and the</u> <u>Biogenic Silica Cycle.</u>	1
<u>The PROBES Study of the Southeastern Bering Sea.</u>	5
<u>Research in Silicic Acid Uptake.</u>	6
<u>Thesis Objectives.</u>	7
<u>The Study Area</u>	9
CHAPTER II. SILICIC ACID UPTAKE BY DIATOMS IN THE BERING SEA . . .	16
<u>Methods and Materials.</u>	16
<u>Results.</u>	23
Vertical Profiles of Silica and Silicic Acid Uptake . . .	23
Cross-Shelf Variations in Silica and Silicic	
Acid Uptake	27
A Time Series Study	30
Light and Kinetic Experiments	36
<u>Discussion</u>	41
Grazing and the Distribution of Silica.	41
Concentration Kinetics.	43
Light Response.	49
Nutrient Limitation on the Middle Shelf	50
Silica and Carbon Productivity.	57
A Comparison of Biogenic Silica and Silicic Acid	
Uptake in the Bering Sea and Three Upwelling	
Systems	61
CHAPTER III. A BIOGENIC SILICA BUDGET FOR THE OUTER	
SHELF OF THE BERING SEA	67
<u>Methods and Materials.</u>	67
<u>Results.</u>	71

TABLE OF CONTENTS (continued)

<u>Discussion</u>	75
The Flux of Silicic Acid from Sediments	75
The Deposition of Carbon and Silica	86
CHAPTER IV. SUMMARY, CONCLUSIONS AND RECOMMENDATIONS	93
<u>A List of Study Results.</u>	95
<u>Recommendations for Further Study.</u>	96
LITERATURE CITED.	99
APPENDIX A. Station locations, silicic acid uptake data and biogenic silica concentrations at selected PROBES productivity stations.	111
APPENDIX B. The equations from the linear geometric mean regressions of carbon, nitrogen and chlorophyll-a versus silicon.	121

LIST OF FIGURES

Figure 1a.	Map of the hydrographic regimes of the south-eastern Bering Sea shelf. Stations 1-12 of the PROBES A-line are indicated on the larger map; the entire A-line section and the three fronts are shown in the insert. From Coachman (1982b).	11
Figure 1b.	Schematic of the hydrographic domains and fronts in vertical section along the southeastern Bering Sea shelf. From Coachman (1982b)	13
Figure 1c.	Estimated mean circulation on the Bering Sea shelf. From Kinder and Schumacher (1981b)	13
Figure 2.	The averaged profiles of particulate silicon (PSi), specific uptake velocity (Vo) and absolute uptake of silicic acid (Ro) from six stations in the coastal domain	25
Figure 3a,b.	The averaged profiles of particulate silicon (PSi), specific uptake velocity (Vo) and absolute uptake of silicic acid (Ro) from six stations in the middle domain during the period of April to mid May (a) and eight stations during the period mid May to July (b)	26
Figure 4a,b.	Profiles of particulate silicon (PSi), specific uptake velocity (Vo) and absolute uptake of silicic acid (Ro) from two stations in the outer domain	28
Figure 4c,d.	Profiles of particulate silicon (PSi), specific uptake velocity (Vo) and absolute uptake of silicic acid (Ro) from two stations near the outer front.	29
Figure 5a,b,c,d.	Station 12 time series of May 1979. Figures a, b, c and d are the vertical profiles of particulate silicon (PSi) and specific uptake velocity of silicic acid (Vo) from four sampling dates during the series.	33

LIST OF FIGURES (continued)

Figure 5e.	A record of the absolute speed of the wind from daily measurements on the R/V THOMPSON (Niebauer, 1982) during May 1979. The depths of the wind mixed layer are also plotted.	33
Figure 6a,b.	Least squares fit hyperbolas from six experiments where a clear concentration dependence of silicic acid uptake is evident. Station numbers are indicated to the right of the respective curve.	37
Figure 7a,b,c,d.	Specific uptake of silicic acid (V_o) as a function of percent of the surface photo-synthetically active radiation.	39
Figure 8.	Two diurnal experiments. The 4-hour average specific uptake of silicic acid (V_o) throughout a 24-hour period from Stations 2090, 17 May 1979 and 3117, 8 June 1979.	40
Figure 9a,b.	The distribution of silicic acid (a) and nitrate (b) along the PROBES A-line during 11-14 May 1979. From Whitledge and Reeburgh(1980).	45
Figure 10.	Normalized kinetic data as summarized in Table 6, plotted with the idealized Michaelis-Menten hyperbola.	47
Figure 11a,b.	Time series contours of silicic acid at middle domain A-line Station 14 (a) and outer domain A-line Station 5 (b) as drawn from 1979-81 data by T. Whitledge (unpublished data)	59
Figure 12.	Station locations of cores collected in 1979 and 1982 from the outer domain	68
Figure 13.	Profiles of interstitial silicic acid concentration in four cores from the outer domain. The large crosses represent an averaged profile; the vertical line is the length of the average section, the horizontal line indicates \pm one standard deviation.	72

LIST OF FIGURES (continued)

Figure 14.	Porosity profiles for 1982 outer domain cores PB-4 and PB-5.	73
Figure 15.	Profiles of percent particulate organic nitrogen (org N) and particulate organic carbon (org C) for 1982 outer domain cores PB-4 and PB-5. The numbers 4 and 5 in the legend correspond to the data for cores PB-4 and PB-5 respectively.	74
Figure 16a,b.	Profiles of percent amorphous silica for the 1982 outer domain cores PB-4 and PB-5. Figure 16a and 16b represent companion cores; Figure 16b was derived from the analysis of the same cores resulting in Figures 14 and 15.	76
Figure 17a.	Excess ^{210}Pb activity (dpm g^{-1}) versus the cumulative mass of sediment (g cm^{-2}) for core PB-4. The line is the linear least squares regression with a slope equivalent to a sedimentation rate of $877 \text{ g m}^{-2} \text{ yr}^{-1}$	77
Figure 17b.	Profile of total ^{210}Pb activity versus depth in the sediment for core PB-4.	77
Figure 17c.	Excess ^{210}Pb activity (dpm g^{-1}) versus the cumulative mass of sediment (g cm^{-2}) for core PB-5. The line is the linear least squares regression with a slope equivalent to a sedimentation rate of $706 \text{ g m}^{-2} \text{ yr}^{-1}$	78
Figure 17d.	Profile of total ^{210}Pb activity versus depth in the sediment for core PB-5.	78
Figure 18.	Percent amorphous silica content versus the estimated average age of each core section from the companion cores to PB-4 and PB-5. The lines are the linear least squares regressions with slopes equivalent to first order dissolution constants, k in s^{-1}	85
Figure 19.	Summary of the biogenic silica budget for the outer domain of the Bering Shelf	92

LIST OF TABLES

Table 1.	The isotopic composition of the ^{28}Si standard (diatom silica) and the ^{29}Si and ^{30}Si tracer solutions as determined in this study compared to the specifications given by the isotope supplier, Oak Ridge National Laboratory.	22
Table 2.	Biogenic silica integrated to the 0.01% SPAR depth on the southeastern Bering Sea shelf. The mean values of each domain are compared using the Student's test	31
Table 3.	Mean integrated specific velocity, \bar{V}_o , for the middle and outer shelves. Values were integrated to the 0.01% SPAR depth. These means are not different at the 95% confidence level.	32
Table 4.	Mean integrated absolute uptake, \bar{R}_o , for the middle and outer shelves. Values were integrated to the 0.01% SPAR depth.	32
Table 5.	Absolute uptake of silicic acid, R_o , specific uptake, V_o , and biogenic silica, PSi , integrated to the bottom (70 m) for the 1979 Station 12 time series.	35
Table 6.	Summary of Bering Sea kinetic experiments. V_1 is the specific uptake rate measured at S_1 , the highest concentration of silicic acid in the experiment series. V_{max} and K_s are the theoretical maximum uptake rate and half saturation constant, respectively	38
Table 7.	Summary of the recent zooplankton biomass and ingestion studies done in the PROBES study area.	42
Table 8.	The slopes from linear geometric mean regressions of carbon, nitrogen and chlorophyll-a versus silicon. These slopes are expressed as mole ratios, with the 95% confidence intervals enclosed in parentheses. the Si:chl-a ratios are in grams	52
Table 9.	Cellular chemical composition of three marine diatoms expressed as ratios (by moles), except Si:chl-a which is in grams. From Harrison <u>et al.</u> (1977).	52

LIST OF TABLES (continued)

Table 10.	Data used to estimate the annual production of biogenic silica and carbon on the south-eastern Bering Sea shelf	60
Table 11.	Average integrated biogenic silica (integrated to the 1% SPAR depth) in the PROBES study area and three upwelling systems.	63
Table 12.	Nutrient concentrations and surface temperatures in the PROBES study area and three upwelling systems . .	65
Table 13.	Location, depth, bottom and air temperatures for cores collected in the outer domain of the Bering Sea	68
Table 14.	Sedimentation rates, ^{210}Pb activities and ^{210}Pb flux rates to surface sediments for outer domain cores PB-14 and PB-5, June 1982. The 95% confidence intervals for sedimentation rates are enclosed in parentheses	79
Table 15.	Silicic acid flux rate estimates and first order dissolution constants based on pore water gradients of silicic acid in outer domain cores PB-4 and PB-5, June 1982	82
Table 16.	A summary of studies estimating or measuring the flux of silicic acid from sediments.	83
Table 17.	Data used to estimate the accumulation rate of particulate organic carbon (ACCUM C) and biogenic silica (ACCUM Si) in outer shelf sediments.	87

ACKNOWLEDGEMENTS

Thanks to my graduate committee, all of whom helped me in everything from collecting samples to greatly improving the text of this thesis. I was slow in maturing as a student and I'm grateful to Dr. John Goering for his patience. Dr. R. T. Cooney was always available for helpful discussions during the drafting of this thesis. Special thanks to Dr. William Reeburgh for all his help at sea and most of all for his friendship and encouragement.

I owe much of my analytical success to Douglas McIntosh who solved my tougher problems in mass spectrometry. Thanks to David Boisseau who by example showed me how to work efficiently at sea. Credit for the success of my first Bering Sea cruise is due to Dave. Thanks to Bunny Blank who made getting this thesis in on time possible and thank you Mary Alford for letting me use the office.

Special thanks to Jeffrey Cornwell for close friendship, support and an infectious enthusiasm for sediment chemistry. Thanks to Susan Sugai for polishing both my thesis text and presentation. To all my friends, I've benefitted both personally and academically knowing you. Finally, thanks to my parents Emily and Andrew Banahan. I sometimes doubted my abilities; they never did.

This work was supported by the National Science Foundation Grant #DDP7623340, the Processes and Resources of the Bering Sea Shelf Project.

CHAPTER I. INTRODUCTION

Diatoms in Primary Production and the Biogenic Silica Cycle

Diatoms, the dominant phytoplankton of intense upwelling regions (Dugdale, 1972; Walsh *et al.*, 1974; Nelson, Goering and Boisseau, 1981; Broecker and Peng, 1982) and temperate continental shelves (Russell-Hunter, 1970), are responsible for an estimated 20-25% of the world's net primary production (Werner, 1977a). On maps of oceanic carbon production (Koblentz-Mishke, Volkovinski and Kabanova, 1970) the regions of high productivity are also the regions of high opal deposition (Lisitzin, 1972; Schink, Fanning and Pilson, 1974; Johnson, 1976; Broecker and Peng, 1982). These regions are the Antarctic Convergence, the upwelling areas off western North America, Northwest Africa and Peru, the westward band of the Equatorial Divergence and the northernmost Pacific. DeMaster (1981) calculated that opal deposition in the subarctic Pacific, including the Bering Sea and Sea of Okhotsk, is equivalent to ~10% of the combined dissolved input to the world's oceans. He concluded that as a sink for biogenic silica, the deep Bering Sea is second only to the sediments beneath the Antarctic Convergence.

Silicon is the second most abundant element in the earth's crust, equivalent to 25.7% by weight. The most common isotope is ^{28}Si (>90%) with lesser abundances of stable ^{29}Si and ^{30}Si and some rare radioisotopes. Pure elemental silicon does not exist in nature and is found almost exclusively in the +4 oxidation state. Silicon is nonmetallic

and, like its cogener carbon, can form extensive heteropolymers with oxygen. These -Si-O-Si- chains can be cross-linked and substituted as in pyroxenes, amphiboles, kaolinite, feldspars, zeolites and other silicate minerals (Huheey, 1972).

Dissolved silicon in neutral aqueous solutions is nonionized monomeric silicic acid, $\text{Si}(\text{OH})_4$. Autopolycondensation does occur under conditions of low pH, freezing or saturation, however the process is reversible (Alexander, 1954). Amorphous hydrated silicon dioxide ($\text{SiO}_2 \cdot n\text{H}_2\text{O}$), referred to as silica or opal, is the result of the polycondensation of the silicic acid or volcanic processes.

Silicon is important in several biological systems. Trace quantities of silicon are required for vertebrate bone and soft tissue formation, for structural support in sponges and some vascular plants and for the synthesis of protective structures in diatoms, silicoflagellates and some protozoans (Simpson and Volcani, 1981). The form of biogenic silicon is amorphous silica.

The major sources of silicic acid to the oceans are terrestrial weathering of rocks transported by rivers and submarine volcanism (DeMaster, 1981). The mean residence time of dissolved Si in the oceans is ~20,000 years (Broecker and Peng, 1982).

All diatoms have an absolute requirement for silicon, most needing an intact test for normal growth (Darley, 1974). Silicification is an intracellular process, using energy in the translocation of silicic acid through the cell membrane (Lewin and Reimann, 1969; Sullivan, 1976; Werner, 1977b). Wall formation occurs by the polycondensation

of silicic acid onto newly exposed cytoplasmic surfaces (Lewin, 1962; Werner, 1977b). Originally thought to be a largely inorganic process, recent study shows that actual wall formation is also linked to metabolic activity (Sullivan, 1980). The single mineral phase formed is amorphous silica or opal (Darley, 1974).

Culture studies of Navicula pelliculosa, Cylindrotheca fusiformis and Ditylum brightwellii show that transport of silicic acid is highly influenced by the stages of the cellular division cycle. Higher rates of transport occur during the biprotoplastic phase, just before cell separation (Darley, 1974), and are a function of de novo protein synthesis during that phase (Sullivan, 1977).

Silicic acid starvation has been used as a method to synchronize cell division in cultures (Darley and Volcani, 1971; Sullivan, 1977). The division cycle is arrested at the biprotoplastic phase and complete deprivation leads to eventual cessation of most metabolic activity (Werner, 1977b). Under nonlimiting conditions, 10-50% of a diatom's dry weight is silica (Lewin, 1962; Werner, 1977b). The thickness of the test varies with species, silicic acid availability and the rate of cell division.

Diatom tests eventually sink to the bottom, become entrained in downwelling water masses or become "packaged" in fecal material that sinks to the bottom. A high fraction of silica can redissolve before burial; up to 55% in the top 100 m (Nelson and Gordon, 1982) and as much as 99% in the deep ocean (Hurd, 1973; Heath, 1974; Cobler and Dymond, 1980). The packaging of diatom tests into membrane enclosed

fecal pellets increases the sinking rate up to 1000 times the rate of individual cells (Smayda, 1971; Schrader, 1971). Some more weakly silicified diatoms, like Chaetoceros and Rhizosolenia, are broken up during passage through the grazer's gut and their dissolution may actually be accelerated. However, more heavily silicified species (Fragilariopsis, Thalassiosira, Coscinodiscus) can remain intact even after repeated passage through pelagic and benthic grazers (Smayda, 1971). Nelson et al. (1981) suggest diatom ingestion by the anchoveta and fecal pellet sinking are responsible for the low rate of water column dissolution and consequent silicic acid limitation in the Peru upwelling system.

The dissolution of biogenic silica continues after deposition. Two universal features in marine sediments are the enrichment of interstitial waters in silicic acid (up to 800 μM beneath highly productive waters) and undersaturation with respect to amorphous opal (Siever, Beck and Berner, 1965; Fanning and Pilson, 1971; Hurd, 1973; Schink et al., 1974; Emerson et al., 1980; Sayles, 1981; Jahnke et al., 1982; Wakefield, 1982). Although the overall concentration of silicic acid in the ocean may be influenced by equilibrium with silicate minerals (Mackenzie and Garrels, 1965; Mackenzie et al., 1967; Willey, 1978), the high interstitial levels found in sediments beneath productive areas far exceed the equilibrium concentrations for those clays. The source of the enrichment in those sediments is the continued dissolution of biogenic silica making the sediments a potentially important source of silicic acid (Hurd, 1973; Schink et al., 1975;

Fanning and Pilson, 1974; Aller and Benninger, 1981; Wakefield, 1982). The maximum summer flux of silicic acid from sediments in Long Island Sound is equivalent to that laterally transported into the Sound (Aller and Benninger, 1981). Edmond et al. (1979) found silicic acid anomalies in the bottom waters of the Antarctic, Indian and North Pacific Oceans consistent with fluxes estimated from pore water gradients. Tsunogai et al. (1979) modeled deep Bering Sea profiles and attributed the deep silicic acid anomaly to diffusion from the sediments.

Research in silicic acid and biogenic silica in the Bering Sea has been concentrated in the deeper basins (Tsunogai et al., 1979; Toggweiler and Broecker, unpublished manuscript). Maps of the distribution of amorphous silica and silica production were compiled by Lisitzin (1972) for the entire North Pacific, including the southeastern Bering Sea shelf. However, his estimates of production and accumulation were based on assumptions about carbon production and a constant C:Si ratio derived from an Antarctic diatom sample. There have been no direct measurements of silicic acid uptake (biogenic silica production) in the Bering Sea.

The PROBES Study of the Southeastern Bering Sea Shelf

The southeastern Bering Sea is a highly productive region supporting well developed fin and shellfish fisheries and large populations of birds and marine mammals (Iverson, et al., 1979). The focus of the Processes and Resources of the Bering Sea Shelf Project (PROBES) has been to investigate mass and energy transfer from the primary producers

(phytoplankton) to the higher trophic levels (zooplankton, pelagic fish, benthic organisms and birds). In an effort to understand the dynamics of shelf ecosystems, the PROBES group has concentrated on the study of the relationships between hydrodynamics, nutrients, phytoplankton and zooplankton.

Several approaches have been used to quantify primary production on the southeast Bering Sea shelf. Direct measurements include the uptake of inorganic nitrogen and carbon by phytoplankton and the identification of species responsible for production in different areas of the shelf. Extensive nutrient and dissolved inorganic carbon data collected in the PROBES study area also provide indirect estimates of production. This study, as part of the PROBES Project, looks at production by diatom phytoplankton, specifically the production of biogenic silica and its accumulation in the sediments. The intent is to construct a budget for biogenic silica in the PROBES study area and discuss the silica cycle in the context of the Bering Sea shelf ecosystem.

Research in Silicic Acid Uptake

Silicic acid uptake and its potential as a limiting nutrient in primary production has been studied in laboratory and natural systems. Estimates of net biomineralization (uptake minus dissolution) have been based on the mass balances of system nutrients (Cooper, 1933; Paasche and Ostergren, 1980). Monitoring silicic acid concentrations under the controlled conditions of continuous culture has produced

precise net uptake rates (Paasche, 1973a,b; Conway, Harrison and Davis, 1976; Harrison, Conway and Dugdale, 1976).

Germanium has an outer shell electron configuration analogous to silicon and is potentially a diatom poison (Lewin and Reimann, 1969). However, germanic acid is used in very low concentrations ($\text{Ge:Si} < 10^{-6}$) as a tracer of silicic acid uptake. The radioisotope ^{68}Ge is used in short term experiments with good results in cultured and natural phytoplankton (Sullivan, 1976; Azam and Chisholm, 1976).

Studies of silicic acid uptake in Baja, California, northwest Africa and Peru upwelling areas (Nelson, Goering and Carter, 1973; Nelson and Goering, 1978; Nelson and Conway, 1979; Nelson *et al.*, 1981) have been done using the stable isotope method described in Nelson (1975) and Nelson and Goering (1977a). This method uses high purity ^{30}Si as a tracer of silicic acid uptake by the particulate fraction (diatoms) or as a label in the soluble fraction to measure dissolution. This is the method used in this study.

Thesis Objectives

The following questions about silicic acid uptake, as it pertains to diatom ecology, are addressed:

1. What is the distribution of biogenic silica in the surface waters of the southeastern Bering Sea shelf and what influences that distribution?
2. What is the vertical distribution of silicic acid uptake in the euphotic zone?

3. How tightly is uptake coupled to light and mixing events?
4. Does silicic acid limitation occur and, if it does, how significant is this limitation to diatom growth?
5. Do estimates of carbon production based on silicic acid uptake measurements agree with ^{14}C measurements?

Profiles of silicic acid uptake, consisting of rate measurements spaced throughout the euphotic zone, provide estimates of total surface silica production and the vertical variation in rates. The short term effects (<1 day) of light on uptake are studied in two types of experiments; light perturbations in which phytoplankton from low light conditions are exposed to increased light and diurnal incubations consisting of a series of uptake rate measurements made throughout a 24-hour period. The passing of a storm was followed in a time series of profile experiments to observe the effect of mixing on uptake. Whether silicic acid uptake is sensitive to ambient concentrations is investigated through Michaelis-Menten type kinetic experiments. The suite of carbon and nitrogen uptake data generated by PROBES investigators is used to determine a Si:C ratio for Bering Sea diatoms. This ratio is then used to convert Si-production to C-production.

The fate of biogenic silica, once produced, leads to the next two questions for this study:

6. What is the accumulation rate of biogenic silica in the sediments?

7. How much of the silica produced is recycled by dissolution before and after deposition?

These estimates are made using data from a series of analyses on cores taken from the outer shelf of the Bering Sea. Biogenic silica accumulation rates are obtained from ^{210}Pb derived sedimentation rates and the amorphous silica content of outer shelf surface sediments. The budget for biogenic silica is completed by a steady state assumption. Silica dissolution in the outer shelf must equal the annual production minus the annual accumulation. Silicic acid diffusing from the sediments is estimated from pore water gradients in silicic acid concentration. Silica dissolution in the water column is then derived from a mass balance.

The Study Area

The Bering Sea is located between 52-66°N latitude and 162°E to 157°W longitude, covering an area of $2.25 \times 10^6 \text{ km}^2$. It is bounded by the land masses of subarctic Siberia and Alaska on the west and east, the Aleutian Arc to the south and Bering Strait to the north. The unusually wide continental shelf, 500-800 km, accounts for about half the total area (Sharma, 1979). The shelf is relatively featureless, gradually deepening to the ~170 m shelf break. The other half of the Bering Sea is abyssal plain generally over 3500 m deep (Kinder, 1981). A comprehensive description of Bering Shelf hydrography and circulation is given in Kinder and Schumacher (1981a,b). A brief review is given here.

The southeastern Bering Sea shelf has been divided into three hydrographic domains as distinguished by their persistent vertical structure in properties such as salinity, temperature and nutrients. These domains are the coastal, middle and outer domains. The absolute values of these properties vary interannually but the cross-shelf pattern of contours remains essentially the same, a manifestation of the different mixing regimes (Coachman, 1982a). Mean flow on the shelf is less than 2 cm s^{-1} so these mixing regimes are a result of buoyancy input, tidal energy and wind mixing.

The coastal domain is adjacent to the Alaska mainland and extends to roughly the 50-m isobath (Figure 1a). The water column in this domain is homogeneous, a result of tidal mixing extending to the surface. The region between the 50- and 100-m isobaths approximates the middle domain. The middle domain is a two-layered system during the spring, summer and fall. The bottom mixed layer reaches ~50 m into the water column and the wind mixed layer ranges 15-50 m thick. The sharp pycnocline between these two layers is best developed in summer when decreased winds and increased insolation enhance stratification.

The outer shelf domain is located between the 100- and 200-m isobaths. The greater water depths in this domain separate the wind mixed and tidally mixed layers, with stratification occurring at mid depth. Warmer, saltier Alaska Stream/Bering Sea water mixes with the fresher, colder shelf water in the outer domain. The stability in the middle layer and the similar densities of the two water masses causes the interleaving of those water masses. This is observed as

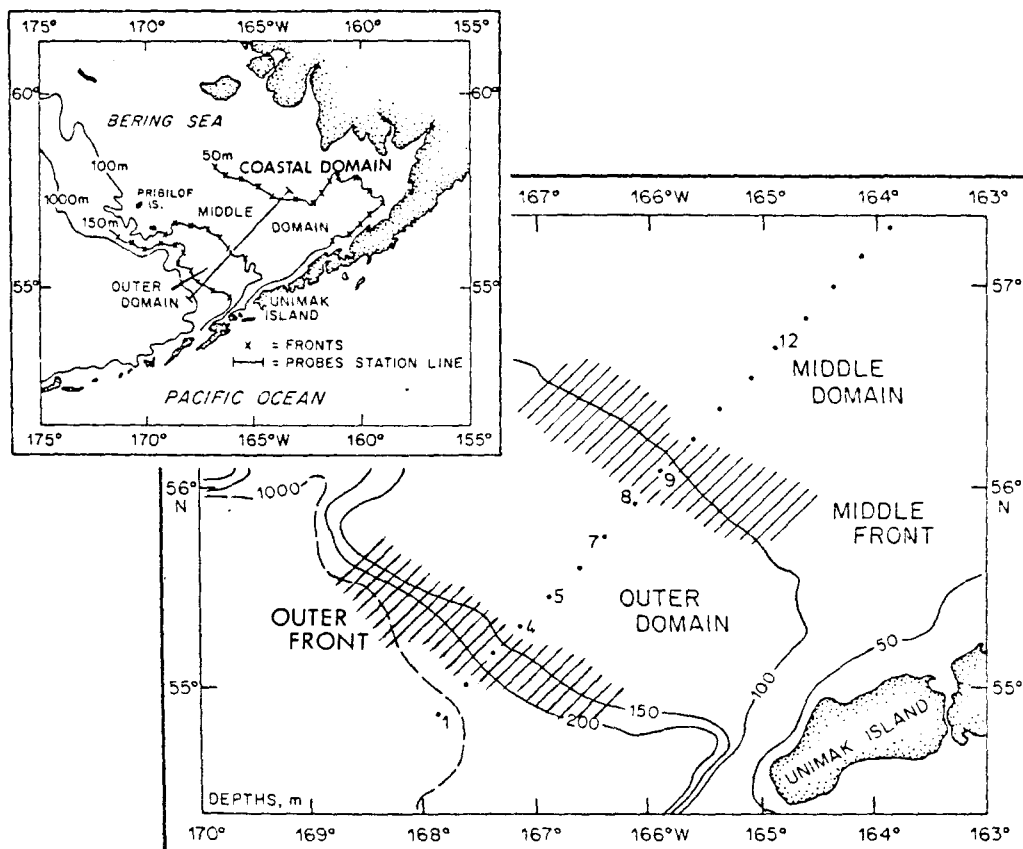


Figure 1a. Map of the hydrographic regimes of the southeastern Bering Sea shelf. Stations 1-12 of the PROBES A-line are indicated on the larger map; the entire A-line section and the three fronts are shown in the insert. From Coachman (1982b).

fine structure in the vertical distribution of temperature and salinity (Coachman and Charnell, 1979). Lateral interleaving is a major mixing mechanism in the outer shelf (Kinder and Schumacher, 1981a).

The transition regions between the hydrographic domains are called fronts. The Bering Shelf fronts are broad zones of intensified horizontal property gradients (Coachman, 1982a). The coastal or inner front is the narrow transition area between the homogeneous coastal domain and the two-layered middle domain (Figure 1b). This front is ~10 km wide, approximately following the 50 m contour. The inner front does not exist in winter because the middle domain is not stratified at that time. The fronts separating the middle, outer and oceanic domains are broader transitional regions about 50 km wide. The middle front, roughly following the 100 m isobath, is discernible in cross-shelf contours of temperature, salinity and nutrients by steeper horizontal gradients in the bottom 30-50 m layer (Figure 1b). The middle front is also characterized by higher concentrations of chlorophyll-a in the spring and summer. The outer front is centered over the 200 m shelf break. It is defined throughout the year as the beginning of the horizontal gradient in salinity that extends across the shelf.

Like the hydrographic domains, there are three distinct flow regimes (Kinder and Schumacher, 1981b). These flow regimes are bounded by the hydrographic fronts (Figure 1c). The source of kinetic energy on the shelf is largely tidal; ~60% tidal at the shelf break and >90% tidal in the coastal domain. Though mean flow is slow, particularly in the middle domain, tidal speeds are $20\text{--}25\text{ cm s}^{-1}$ and even faster

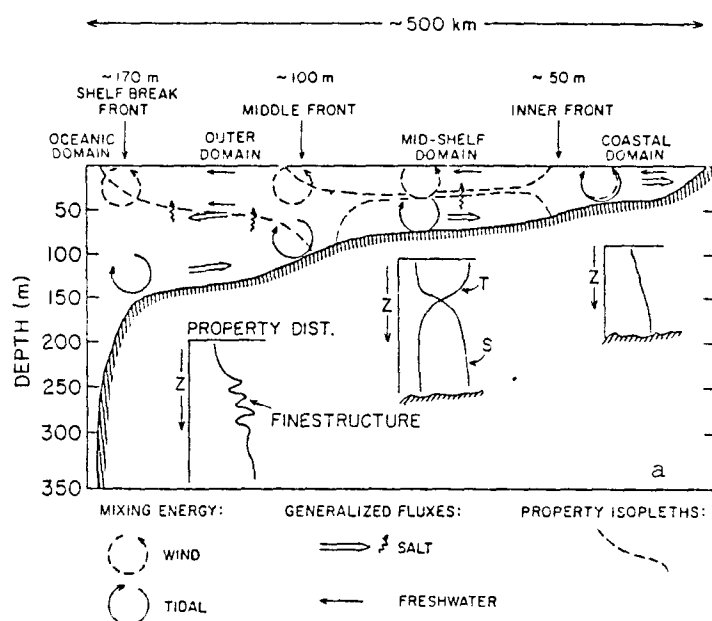


Figure 1b. Schematic of the hydrographic domains and fronts in vertical section along the southeastern Bering Sea shelf. From Coachman (1982b).

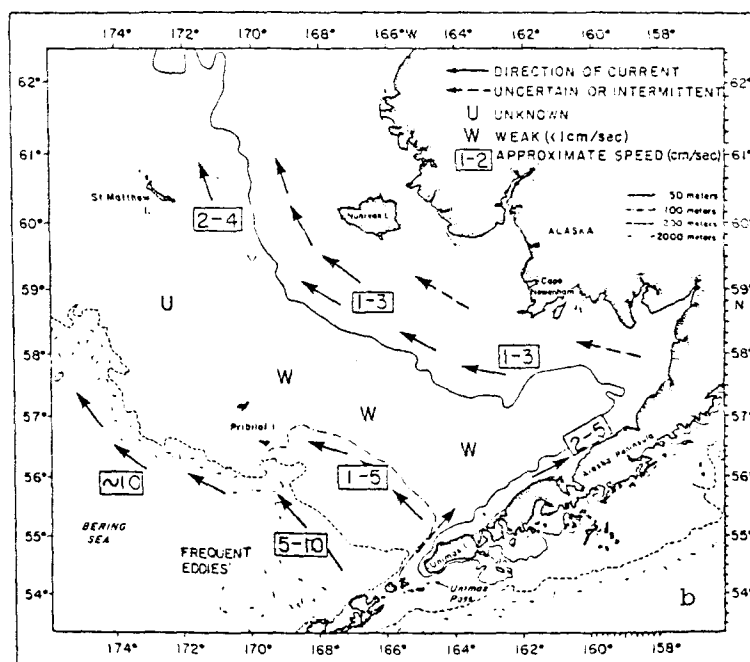


Figure 1c. Estimated mean circulation on the Bering Sea shelf. From Kinder and Schumacher (1981b).

inshore. Wind forcing can generate high energy, short term currents in the middle and coastal domains, especially in winter when storms are frequent. Storms can generate maximum 5-day speeds of up to 30 cm s^{-1} in the outer shelf (Schumacher and Kinder, 1983).

The overall mean flow on the southeastern shelf of the Bering Sea is to the northwest. The mean flow in the coastal and outer domains is statistically greater than the middle domain. A somewhat faster current, $1\text{-}10 \text{ cm s}^{-1}$, runs northwest along the shelf break, toward the Pribilof Islands.

There are two biological subsystems on the southeastern Bering Sea shelf, characterized by different phytoplankton and zooplankton communities. The middle front effectively divides these middle and outer shelf subsystems. The grazing community of the outer shelf is dominated by large oceanic copepods Neocalanus plumcrus, N. cristatus, Metridia pacifica and Eucalanus bungii (Cooney and Coyle, 1982; Vidal and Smith, unpublished manuscript). Migration of these large copepods inshore is limited by the $32^\circ/\text{‰}$ isohaline (S. Smith, personal communication). The grazing stress, particularly on diatoms (S. Smith, personal communication) results in a phytoplankton community dominated by the nonsiliceous haptophyte Pheocystis poucheti (Iverson *et al.*, 1979; Goering and Iverson, 1981).

Inshore of the 100 m contour, middle shelf herbivores are mostly small species of copepods like Calanus marshallae, Pseudocalanus spp., Acartia sp. and euphausiids (Cooney, 1981; Cooney and Coyle, 1982). These smaller copepods do not seem to prey on the larger, chain-forming

and spine-forming diatoms of the middle shelf (Chaetoceros spp., Thalassiosira spp., Rhizosolenia sp.). Most of the carbon production in the middle and coastal domains sinks passively to the bottom and supports a high density benthic community (Iverson et al., 1979). The middle shelf phytoplankton community goes through three stages of species succession (Goering and Iverson, 1981), while the outer shelf is held static at the first stage by grazing (Kocur, 1982).

CHAPTER II. SILICIC ACID UPTAKE BY DIATOMS IN THE BERING SEA

Methods and Materials

Water samples were collected with 30-liter Niskin bottles (General Oceanics) mounted on a rosette sampler. Sampling depths were selected for 100, 50, 30, 15, 5, 1, 0.1 and 0.01 percent penetration of the surface photosynthetically active radiation (% SPAR). These "light" depths were determined at each station using light transmission data collected with an LI-192S underwater quantum sensor and LI-185 quantum meter (Lambda Instrument Corporation).

The ^{30}Si silicic acid solution was prepared using high purity ^{30}Si silicon dioxide (Oak Ridge National Laboratory, Isotope Sales Division). The ^{30}Si silicon dioxide was converted into a silicic acid solution by sodium carbonate fusion and dilution with distilled water to a concentration of $20\ \mu\text{mol ml}^{-1}$ (Nelson and Goering, 1977a). A $10\ \mu\text{mol ml}^{-1}$ solution of ^{29}Si silicic acid used in sample analysis was also prepared this way.

Three types of silicic acid uptake experiments were done: 1) water column profiles to measure the specific uptake rates and particulate silicon concentrations at intervals throughout the euphotic zone, 2) kinetic experiments to determine the degree of dependence of silicic acid uptake on ambient silicic acid concentration and, 3) light perturbation and diurnal uptake experiments to examine how uptake is influenced by changing light conditions. All experiments were done in bottles manufactured of clear plastic to avoid possible silicic acid

contamination from glass bottles. The bottles used were covered with neutral density screens (Perforated Products Incorporated) and cooled with circulating seawater in white-bottomed, clear-sided plexiglas incubators. These incubators were situated on an unshaded part of the ship's deck. The specified open areas of the screens were 100%, 50%, 30%, 15%, 5% and 1% to approximate the light at the collection depths; 0.1% and 0.01% bottles were opaqued with black tape. The 1978 samples were incubated in 1.2-liter plexiglas bottles sealed with plastic-wrapped rubber stoppers; 1979, 1980 and 1981 experiments were done in 1.2-liter virgin polystyrene bottles with screwcaps (Corning Glass Works). All bottles were soaked in seawater for 2-3 days to precondition the plastic before their use in experiments. No obvious differences were seen in results from 1978 and 1979-81 incubations, however, a specific test for differences in the properties of the two sets of bottles was not done.

Water column profiles required 4-liter samples from all eight light depths. Samples from the higher light levels, 100-15%, were held in white 4-liter polypropylene bottles; these bottles passed 50% of the ambient light. Deeper samples, 15-0.01%, were held in opaque polypropylene bottles. Four ml of $20 \mu\text{mol ml}^{-1}$ silicic acid was added and mixed into each 4-liter bottle. Two screened bottles per light depth were rinsed twice and filled with the labeled water. A ~ 100 ml bubble was left in all incubation bottles to facilitate mixing. The two sets of screened bottles were then placed in the incubators on deck. Tank temperature was maintained to within 5°C of sea surface

temperature with circulating seawater. One set was incubated for 20-24 h, the other for 6, 8, 10 or 12 h.

Incubations were ended by filtering each 1.2-liter sample through a 0.8- μ m polycarbonate filter (Nucleopore). The filter funnels used were made of polystyrene. Vacuum pressure was \sim 0.2 atm. Each filter was folded and stored in a polystyrene petri dish. The particulate material on the filter was then analyzed for silica content and isotopic composition (described later in this section).

Light and concentration experiments required somewhat different sampling than profiles. Thirty-liter samples taken from the chlorophyll-a maximum were used for the light experiments. A subsample was poured into a 5-gal plastic container, labeled and mixed. The labeled sample was then transferred to a series of screened bottles (100%, 50%, ..., to 0% SPAR). These incubations lasted 6 h.

Two diurnal incubations were also done using water from a single depth. A 2-3 gal surface sample was kept in a 5-gal container cooled with circulating seawater. Duplicate 50% bottles were filled from that container, labeled and filtered 4 h later. This procedure was repeated throughout a 24 h period, a maximum of six measurements, in duplicate, in the series.

The concentration kinetic experiments required surface water depleted in silicic acid ($<1 \mu$ M). The collected water was homogenized in a 5-gal container, poured into 50% screened bottles and labeled with various amounts of ^{30}Si tracer. Like light experiments, kinetic incubations lasted 6 h; filtration was conducted as described for profiles.

All experiments were usually started within 1.5 h of sample collection. Except for the kinetic experiments, most final label concentrations were $\sim 20 \mu\text{M}$, which was considered saturating for uptake. All tracer additions were made with adjustable or fixed volume microliter pipettes.

Particulate material was prepared for isotope analysis by the procedure of Nelson and Goering (1977a) for all types of experiments. Filters were ashed at 900°C , digested in concentrated hydrofluoric acid and precipitated as barium hexafluorosilicate in aqueous barium chloride. During HF digestion, $10 \mu\text{mol}$ of ^{29}Si tracer was added to each sample for determination of particulate silicon by isotope dilution (Nelson, 1975).

Isotope analyses were performed using either a Finnigan 3100D or Hewlett Packard 5930A mass spectrometer; both have quadrupole type mass filters. Samples, as BaSiF_6 powder, were loaded into glass capillary tubes and introduced into the mass spectrometer on a pyrolytic probe. Electron bombardment at $350\text{--}400^\circ\text{C}$ produced the molecular ion of interest, SiF_3^+ . The ion currents of mass to charge ratios (m/e) 85, 86 and 87 were recorded. These m/e values correspond to the ^{28}Si , ^{29}Si and ^{30}Si ion fragments (Nelson and Goering, 1977a).

Like particulate samples, the tracer solutions of ^{29}Si and ^{30}Si silicic acid were precipitated as barium hexafluorosilicate and isotopically analyzed to verify their enrichments as specified by Oak Ridge. A standard for the natural abundances of ^{28}Si , ^{29}Si and ^{30}Si was prepared from a plankton net sample of Bering Sea diatoms. This

"standard" sample was treated as an uptake sample with the ^{29}Si tracer addition omitted. These standards and some samples were run and rerun periodically to check for instrument drift. Departures from "established" ratios were corrected by refocusing the electron source or retuning the quadrupole.

I used equations #1 through #11 of Nelson and Goering (1977a) to calculate the end-time values for particulate silicon concentration and specific uptake velocity. Equation #10 defines the end-time velocity, V_t , as follows:

$$V_t = (A_f,30 - A_n,30) / t(A_i,30 - A_n,30) \quad 1$$

where V_t is the specific uptake velocity of silicic acid in h^{-1} , $A_f,30$ is the atom percent of ^{30}Si in the final (end of incubation) particulate material, $A_n,30$ is the natural abundance of ^{30}Si , $A_i,30$ is the initial atom percent of ^{30}Si of the total silicic acid pool (ambient plus label) and t is the duration of the experiment in hours.

To be consistent with other PROBES productivity data (Niebauer et al., 1982), V_o , the uptake velocity based on the initial ($t=0$) particulate silicon concentration was calculated using the equation below.

$$V_o = (A_f,30 - A_n,30) / t(A_i,30 - A_f,30) \quad 2$$

The initial particulate silicon, PSi , was then back calculated from R_o , the absolute uptake in $\mu\text{mol l}^{-1} \text{h}^{-1}$.

$$\text{PSi} = R_o / V_o \quad 3$$

Ratios of the two tracer solutions used were constant but different from those given in the Oak Ridge specifications (see Table 1). Contamination with ^{28}Si by other reagents, i.e. BaCl_2 , HF , Na_2CO_3 or distilled water, did not seem likely. The ^{30}Si tracer was more enriched in my measurements than in Oak Ridge specifications. I would have expected the rarer isotopes, ^{29}Si and ^{30}Si , to decrease in purity by dilution with ^{28}Si . The ^{29}Si tracer was less enriched but with no increase in its ^{30}Si content. If there was contamination, it was by different isotopes in the different labels. The ^{28}Si standard made from Bering Sea diatoms matched the literature isotopic composition (Beynon, Saunders and Williams, 1968). I concluded the ^{29}Si and ^{30}Si tracers were not as given in the Oak Ridge specifications and used my measured ratios in the uptake calculations.

The precision for five replicate samples (from Station 4013, June 29, 1981, 32 m) was similar to that quoted for this method by Nelson and Goering (1977a). Their standard deviation for specific velocity (V_o) was 4%, for particulate silicon (PSi) 6% and for absolute uptake (R_o) 6.5%. The standard deviations for the Bering Sea replicates were 5% for V_o , 2% for PSi and 5.4% for R_o . The precision for PSi in kinetic experiments was 3% for PSi $>10\text{ }\mu\text{M}$ ($n = 36$) and 8% for PSi $<10\text{ }\mu\text{M}$ ($n = 60$). The assumption that particulate silicon does not change during the incubation period is still acceptable with a plus or minus 10% margin. Overall, this agrees with the Nelson and Goering (1977a) assessment.

Table 1. The isotopic composition of the ^{28}Si standard (diatom silica) and the ^{29}Si and ^{30}Si tracer solutions as determined in this study compared to the specifications given by the isotope supplier, Oak Ridge National Laboratory.

	MEAN VALUES OF 9 DETERMINATIONS			OAK RIDGE SPECIFICATIONS		
	atom % ^{28}Si	atom % ^{29}Si	atom % ^{30}Si	atom % ^{28}Si	atom % ^{29}Si	atom % ^{30}Si
^{28}Si standard	92.10 ± 0.11	4.77 ± 0.04	3.13 ± 0.08	92.18*	4.71*	3.12*
^{29}Si tracer	4.99 ± 0.06	94.66 ± 0.08	0.34 ± 0.05	4.35 ± 0.10	95.28 ± 0.05	0.36 ± 0.10
^{30}Si tracer	3.39 ± 0.03	1.01 ± 0.04	95.01 ± 0.04	4.71 ± 0.10	0.64 ± 0.05	94.65 ± 0.10

* From Beynon et al. (1968), p. 476.

Results

All uptake measured by the tracer method was assumed to be by live diatoms. Paasche and Ostergren (1980) found no detectable uptake of silicic acid in samples of killed diatoms. It was also assumed that no silicic acid was incorporated by nonbiogenic silica phases (Goering *et al.*, 1973; Nelson and Goering, 1977).

Simultaneous long (>20 h) and short (<12 h) term incubations were compared at 13 stations. Experiments of 8-12 h duration correlated well with companion long experiments. Daily uptake rates were estimated from the shorter term rates with the following regression equation:

$$V_{0,24 \text{ h}} = 0.772 V_{0,8,10,12 \text{ h}} \quad r^2 = 0.880 \quad 4$$

The intercept, $+0.0001 \text{ h}^{-1}$ was considered negligible. The 6-h experiments did not correlate significantly with the long term experiments and were not extrapolated to daily rates.

Data from the 33 stations used to characterize particulate silicon concentration and silicic acid uptake are listed in Appendix A. Inclusion of a station into a domain of the Bering Sea was based simply on its location.

Vertical Profiles of Silica and Silicic Acid Uptake

At most stations, potential specific uptake, V_0 , was detectable at the deepest light depth sampled (0.01% SPAR). Significant uptake below the 0.01% SPAR depth was measured in one extended profile at

Station 4070, May 30, 1980 (Appendix A). The greatest potential uptake observed was a surface rate of 0.026 h^{-1} at Station 2057, May 12, 1979. This specific uptake rate is equivalent to a growth rate of 0.9 divisions per day. The combined inorganic nitrogen and silicic acid at this station were ~ 13 and $\sim 35 \text{ } \mu\text{M}$, respectively. This high V_o , in light of essentially nonlimiting nutrients, was likely a good approximation of an in situ V_o . However, this V_o was twice as large as the other high surface values observed.

Specific uptake rates in the coastal domain were generally low and did not have large shallow maxima (Figure 2). Greater particulate silicon concentrations were found at depth in all coastal profiles so there were also no large surface maxima in absolute uptake. Particulate silicon seemed to be uniformly distributed at all sampling depths during the early bloom. At later May stations, particulate silicon had accumulated at, or below the mixed layer.

Silica values were high and evenly distributed in the upper 30 m of the water column at middle domain and middle front stations (Figure 3a). Both specific and absolute uptake values had definite shallow maxima between the 100% and 30% light depths. By late May, middle shelf profiles (Figure 3b) resembled the coastal profiles; absolute and specific uptake were more uniform with depth than at stations earlier in the bloom while particulate silicon concentrations increased with depth. The single exception, Station 4070 on May 30, 1980, had 30% depth maxima in uptake and particulate silicon (see Appendix A).

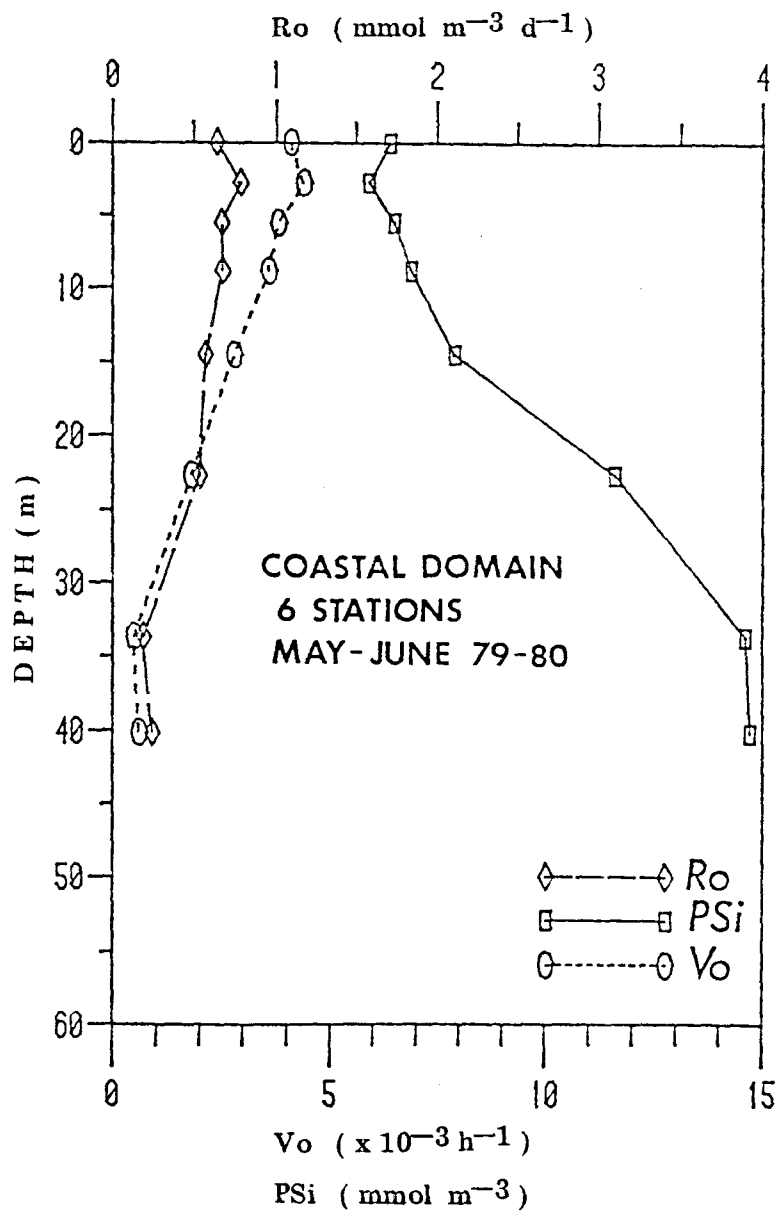


Figure 2. The averaged profiles of particulate silicon (PSi), specific uptake velocity (Vo) and absolute uptake of silicic acid (Ro) from six stations in the coastal domain.

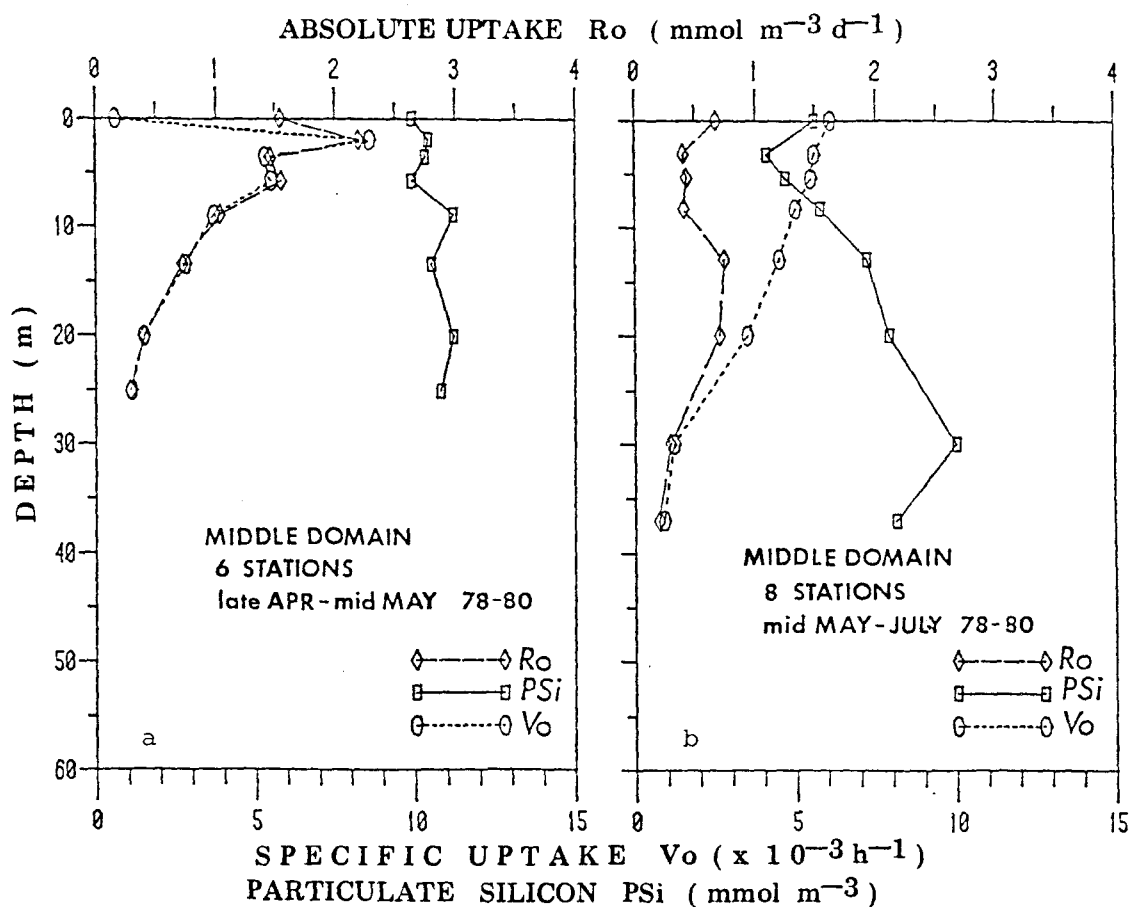


Figure 3a,b. The averaged profiles of particulate silicon (PSi), specific uptake velocity (V_o) and absolute uptake of silicic acid (R_o) from six stations in the middle domain during the period of April to mid May (a) and eight stations during the period mid May to July (b).

Particulate silicon in the outer shelf domain was low and generally uniform with depth (Figure 4a,b). Specific uptake rates had definite maxima in the 100-15% light depth range. Like particulate silicon, absolute uptake rates were usually low throughout the water column. Two outer front stations, 3001 on May 25, 1979 and 4052 on July 7, 1981, had surface maxima in specific uptake, absolute uptake and particulate silicon (Figure 4d,e).

Cross-Shelf Variations in Silica and Silicic Acid Uptake

The greatest integrated concentrations of particulate silicon were observed in the coastal and middle shelf domains. During the early bloom as much as $680 \text{ mmol Si m}^{-2}$ was measured at coastal domain Station 2019 of the PROBES A-line (May 5, 1979). Coastal domain concentrations of silica ranged from 300 to $400 \text{ mmol Si m}^{-2}$ in late May and June. The middle shelf stations had concentrations of $300\text{--}500 \text{ mmol Si m}^{-2}$ in early May and dropped to less than $300 \text{ mmol Si m}^{-2}$ by June. At outer shelf and outer front stations, particulate silicon was usually one third that found at inshore stations. A high of $252 \text{ mmol Si m}^{-2}$ was measured at outer shelf domain Station 3031 (May 31, 1978), but the characteristic concentration in that area was $\sim 100 \text{ mmol Si m}^{-2}$. Approximately $100 \text{ mmol Si m}^{-2}$ was found in the outer front as late as July (Stations 4052, July 7, and 4125, July 19, both in 1981).

Concentrations of particulate silicon were three to four times greater inshore of the 100-m isobath than those in the outer shelf. Coastal and middle shelf integrated mean particulate silicon

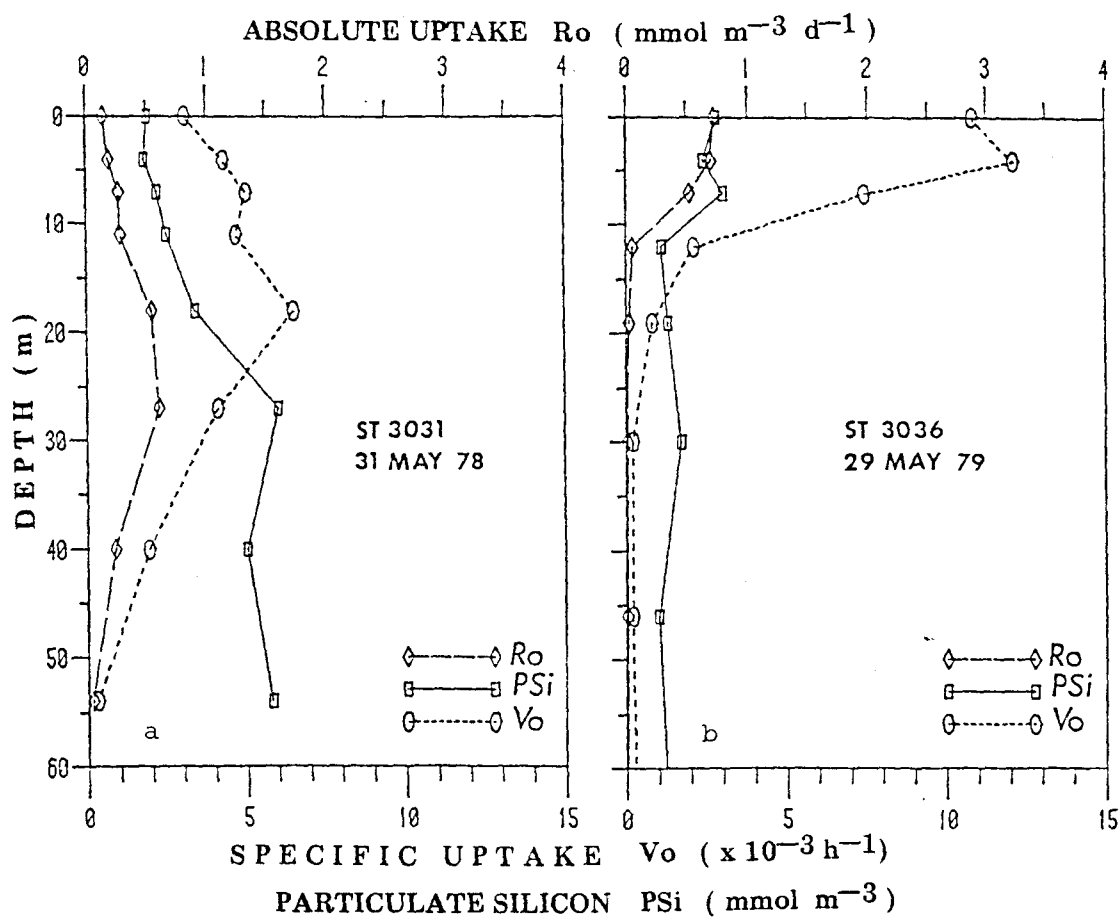


Figure 4a,b. Profiles of particulate silicon (PSi), specific uptake velocity (V_o) and absolute uptake of silicic acid (R_o) from two stations in the outer domain.

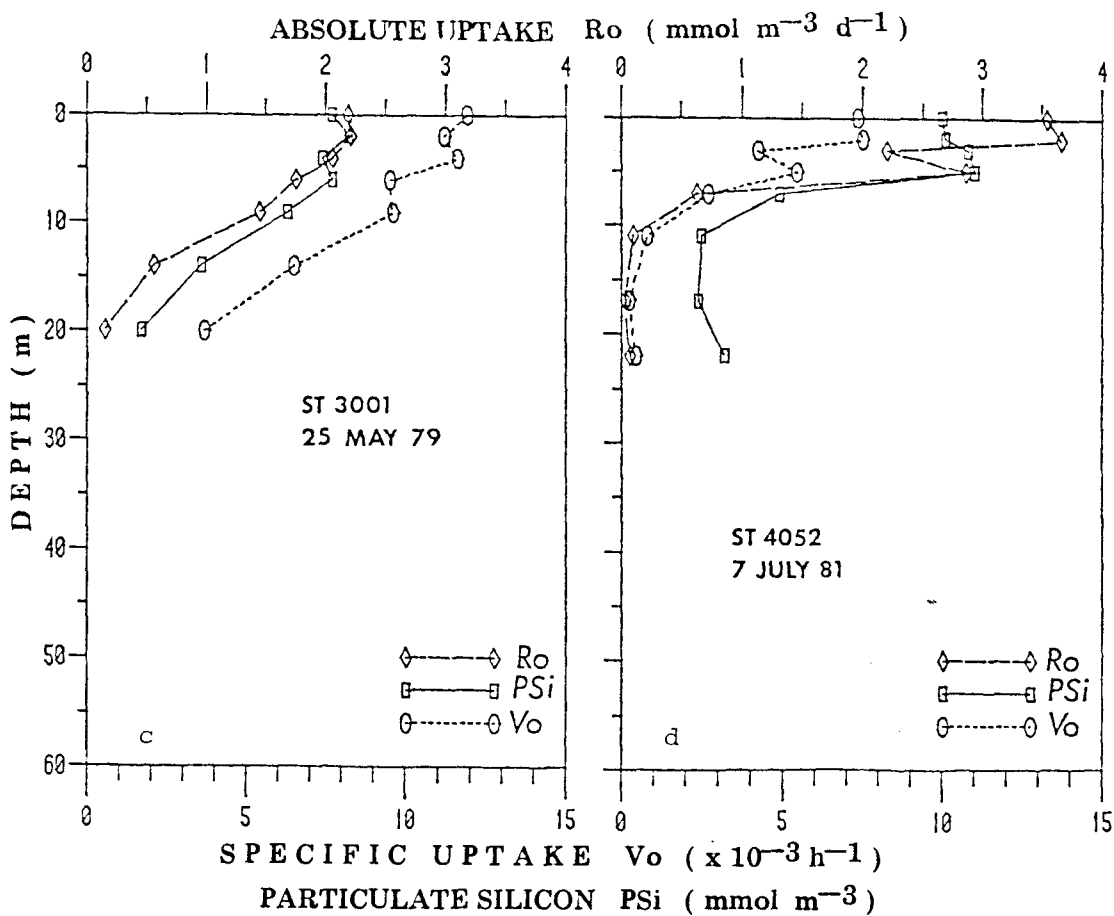


Figure 4c,d. Profiles of particulate silicon (PSi), specific uptake velocity (V_o) and absolute uptake of silicic acid (R_o) from two stations near the outer front.

concentrations, 429 and 299 mmol Si m^{-2} , respectively, are significantly greater than the outer shelf mean of 91 mmol Si m^{-2} at the 99% confidence level (Table 2). The mean concentration for the coastal zone was only greater than the middle shelf mean at the 97.5% level.

The means of integrated specific uptake for the coastal and middle shelf domains were not different at the 95% confidence level (Table 3). No difference, even at the 95% level, was found between the integrated V_o 's of any domain. The mean value of integrated absolute uptake for the outer shelf is about half that of the middle shelf, but these means are only different at the 97.5% confidence level (Table 4). As specific uptake across the shelf was fairly constant, the variation in absolute uptake on the shelf was simply a reflection of the onshore increase in particulate silicon.

A Time Series Study

Station 12 of the PROBES A-line (Figure 1a) was occupied four times during May 1979. Silicic acid uptake profiles were taken, in addition to chlorophyll-a and nutrient profiles, to observe the progression of uptake and silica accumulation through the peak bloom period and the effect of mixing events on both.

Particulate silicon, chlorophyll-a and nutrients were evenly distributed throughout the water column on May 4, 1979 (Station 2012). Specific uptake rates were $\sim 0.007 \text{ h}^{-1}$ in the top 6 m (the 15% light depth) and lower but significant to 20 m (Figure 5a). During the

Table 2. Biogenic silica integrated to the 0.01% SPAR depth on the southeastern Bering Sea shelf. The mean values of each domain are compared using the Student's t test.

	No. stations	mmol Si m ⁻²		SD
COASTAL DOMAIN	6	428.8		138.1
MIDDLE DOMAIN	18	299.0		202.4
OUTER DOMAIN & OUTER FRONT	10	91.3		62.9

COMPARISON TESTED	df	t	t*	confidence level
Mean P <i>S</i> i of the coastal domain is greater than the middle domain mean.	22	2.07	2.49	97.5
Mean P <i>S</i> i of the coastal domain is greater than the outer shelf mean.	14	2.98	6.76	99.5
Mean P <i>S</i> i of the middle domain is greater than the outer shelf mean.	26	2.78	5.86	99.5

Table 3. Mean integrated specific velocity, \bar{V}_o , for the middle and outer shelves. Values were integrated to the 0.01% SPAR depth. These means are not different at the 95% confidence level.

	No. stations	\bar{V}_o ($\text{m}^{-2} \text{h}^{-1}$)	SD
All stations inshore of the middle front.	22	0.104	0.055
All stations seaward of the middle front.	8*	0.110	0.049

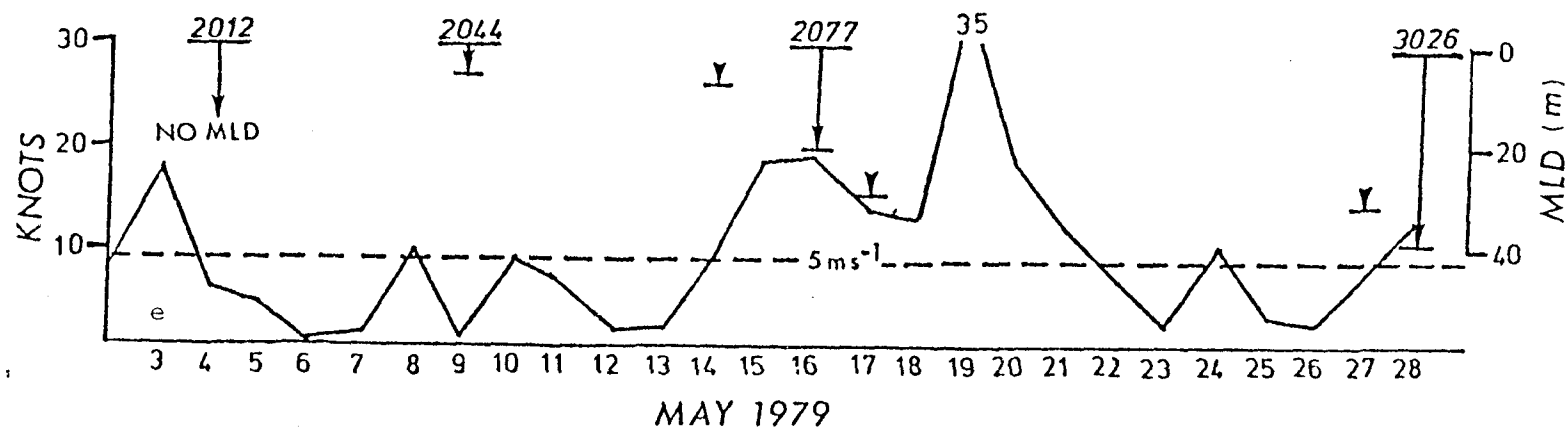
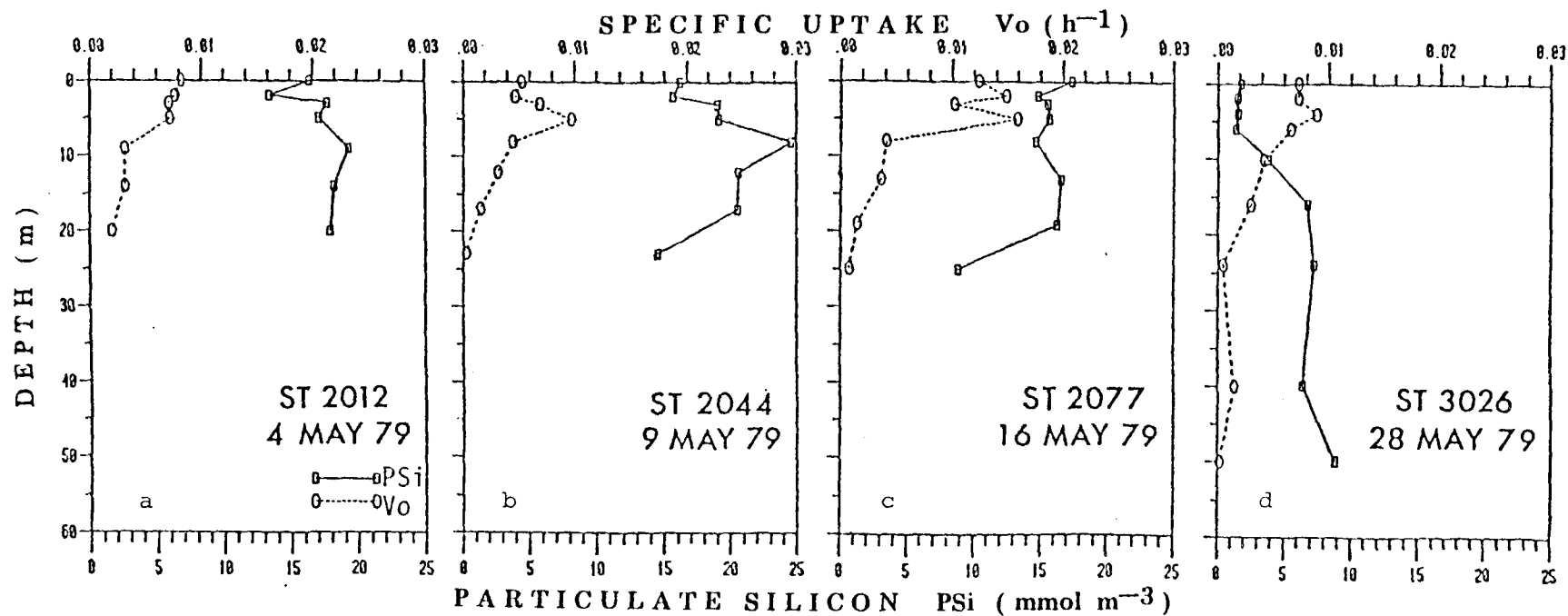
*Station 2057 (May 12, 1979) had unusually high V_o values and was not included in the outer shelf mean.

Table 4. Mean integrated absolute uptake, \bar{R}_o , for the middle and outer shelves. Values were integrated to the 0.01% SPAR depth.

	No. stations	\bar{R}_o ($\text{mmol m}^{-2} \text{d}^{-1}$)	SD
All stations inshore of the middle front.	22	20.9	13.3
All stations seaward of the middle front.	8	10.1	9.5

Figure 5a,b,c,d. Station 12 time series of May 1979. Figures a, b, c and d are the vertical profiles of particulate silicon (PSi) and specific uptake velocity of silicic acid (V_o) from four sampling dates during the series.

Figure 5e. A record of the absolute speed of the wind from daily measurements on the R/V Thompson (Niebauer, 1982) during May 1979. The depths of the wind mixed layer are also plotted.



period of May 4 to May 7, the wind speed remained <10 kt and the mixed layer depth shallowed to 5 m. Nitrate was depleted and silicic acid levels dropped from ~25 to ~6 μM in that layer; by May 9 (Station 2044) both nutrients were present only in trace amounts. Potential silicic acid uptake was lower at the surface than on May 4 (Station 2012). However, there was a peak in V_o at 5 m (Figure 5b) such that the integrated potential uptake in the top 20 m was essentially the same as May 4 (Table 5). Both particulate silicon and chlorophyll-a profiles had subsurface maxima just below the mixed layer.

Increased winds deepened the mixed layer to 20 m by May 16 (Station 2077). Specific uptake also peaked at 5 m, but with rates apparently greater throughout the euphotic zone than those of May 7 and May 9 (Figure 5c). On May 17 (Station 2090), a high V_o of 0.018 h^{-1} and in situ rate of 0.015 h^{-1} (MacIsaac and Dugdale, 1972) were observed at the surface. Both rates are higher than any seen in the time series. The surface particulate silicon concentration of the preceding stations, $16\text{--}17 \text{ mmol m}^{-3}$, dropped to 10 mmol m^{-3} .

A calm period around May 25 was followed by moderate winds (Figure 5e). The mixed layer deepened again on May 28, Station 3026. Specific uptake still had a subsurface maximum at 4 m with values higher than on calm days May 4 and May 9 (Stations 2012 and 2044), but not as high as those of May 16 and May 17 (Stations 2077 and 2090). Both particulate silicon and chlorophyll-a were mixed out of the top 20 m (Figure 5d).

Table 5. Absolute uptake of silicic acid, R_o , specific uptake, V_o , and biogenic silica, PSi , integrated to the bottom (70 m) for the 1979 Station 12 time series.

Station	Date	R_o ($\text{mmol m}^{-2} \text{d}^{-1}$)	V_o ($\text{m}^{-2} \text{h}^{-1}$)	PSi (mmol m^{-2})
2012	4 May	47.1	0.098	1308
2044	9 May	46.0	0.081	936
2077	16 May	55.7	0.137	664
3026	28 May	18.3	0.110	638

Light and Kinetic Experiments

Six of the eight kinetic experiments done in low ($<1 \mu\text{M}$) silicic acid surface waters, displayed concentration dependence of uptake suggesting a Michaelis-Menten hyperbola (see Figure 6a,b). Theoretical maximum velocities, V_{max} , and half saturation constants, K_s , derived from a least squares fit to the Michaelis-Menten equation (Cleland, 1967) are listed in Table 6. The averaged values for V_{max} and K_s are 0.009 h^{-1} ($\text{SD} = 0.004 \text{ h}^{-1}$) and $3.2 \mu\text{M}$ ($\text{SD} = 1.6 \mu\text{M}$), respectively.

The results of eight light perturbation experiments are in Figure 7a-d. Specific uptake increased with increased light in five of eight experiments. Two lower light samples showed no definite increase in uptake with increased light (Stations 2052 and 2073). The 50% sample at Station 3017 displayed no decrease in V_o with decreased light. Silicic acid uptake was detected in the dark bottles of all experiments. When rectangular hyperbolas were fitted to the data of experiments with positive responses to light, half saturation values were all less than 5% SPAR.

Diurnal incubations using surface phytoplankton were done at middle shelf domain Stations 2090 (May 17, 1979) and 3117 (June 8, 1979). The measured uptake at night in the Station 2090 experiment was comparable to the day rates (Figure 8).

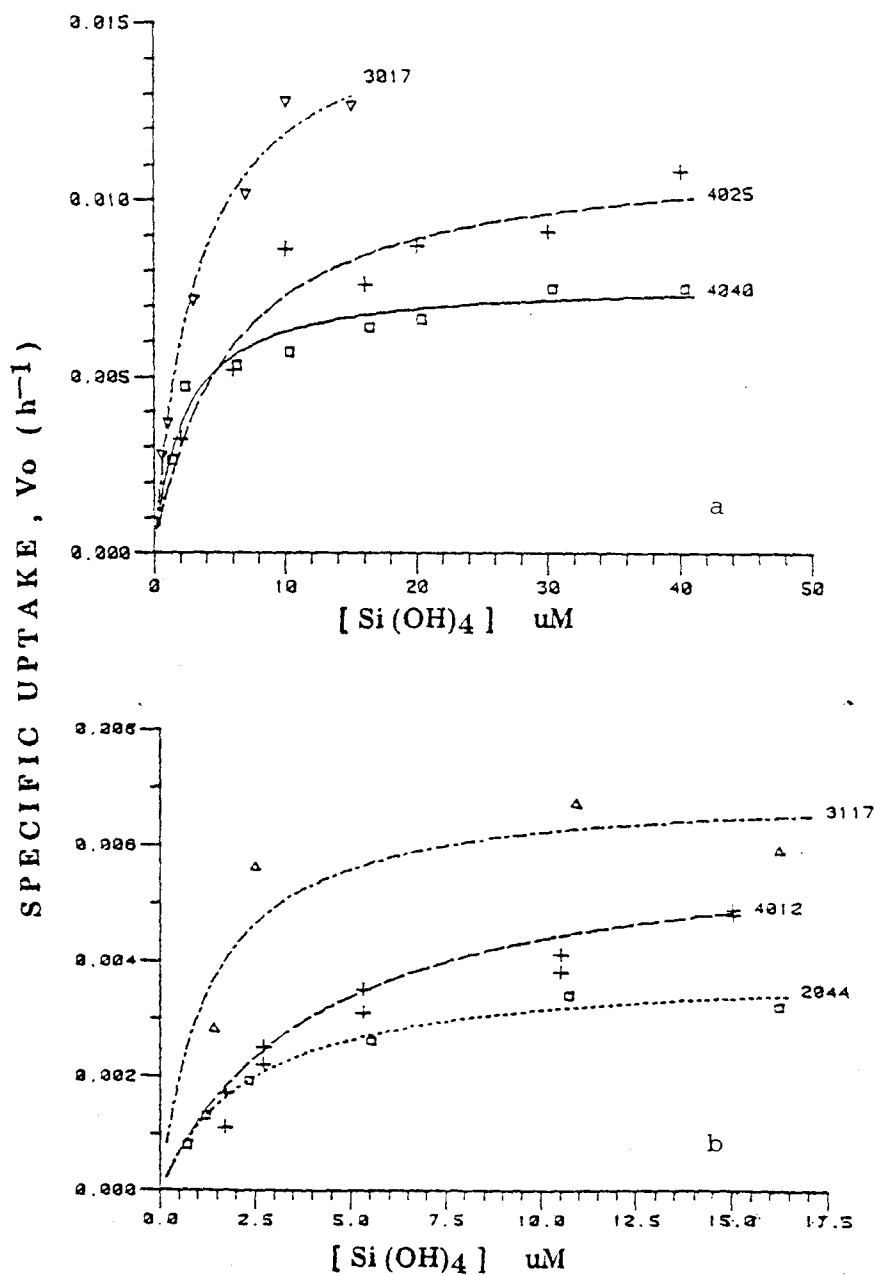


Figure 6a,b. Least squares fit hyperbolas from six experiments where a clear concentration dependence of silicic acid uptake is evident. Station numbers are indicated to the right of the respective curve.

Table 6. Summary of Bering Sea kinetic experiments. V_l is the specific uptake rate measured at S_l , the highest concentration of silicic acid in the experiment series. V_{max} and K_s are the theoretical maximum uptake rate and half saturation constant, respectively.

	STATION	V_l (h^{-1})	S_l (μM)	V_{max} (h^{-1})	K_s (μM)
3031	31 May 1978	0.0021	15.4	-	-
2044	9 May 1979	0.0032	16.2	0.0039	2.4
3017	27 May 1979	0.0127	15.0	0.0158	3.3
3117	8 June 1979	0.0059	16.2	0.0070	1.3
4012	23 May 1980	0.0050	15.1	0.0087	4.1
4025	1 July 1981	0.0108	40.0	0.0114	5.8
4040	4 July 1981	0.0080	40.3	0.0070	2.3
4052	7 July 1981	0.0083	40.6	-	-

- Kinetic constants could not be calculated for these experiments because there was no apparent concentration dependence.

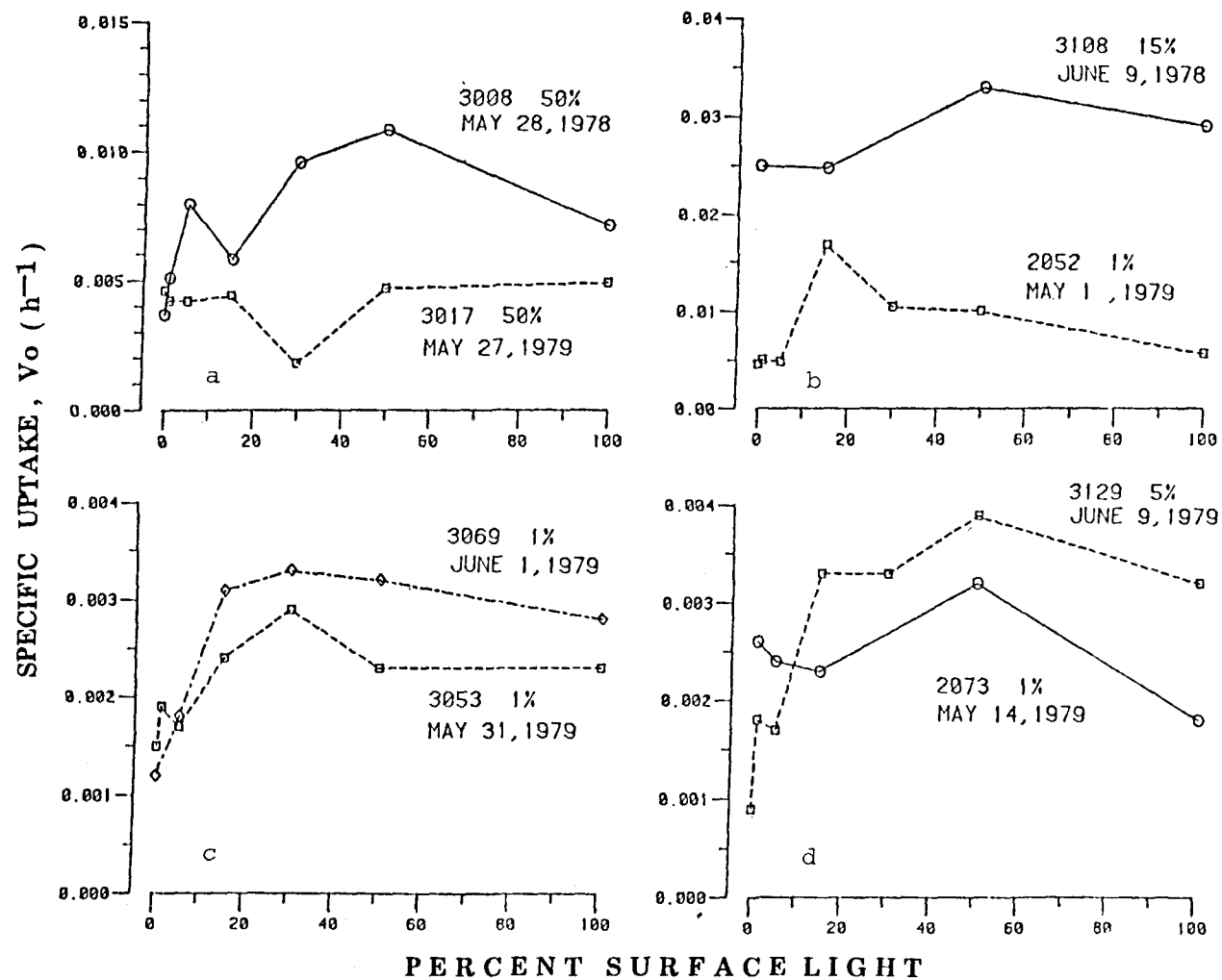


Figure 7a,b,c,d. Specific uptake of silicic acid (V_o) as a function of percent of the surface photo-synthetically active radiation.

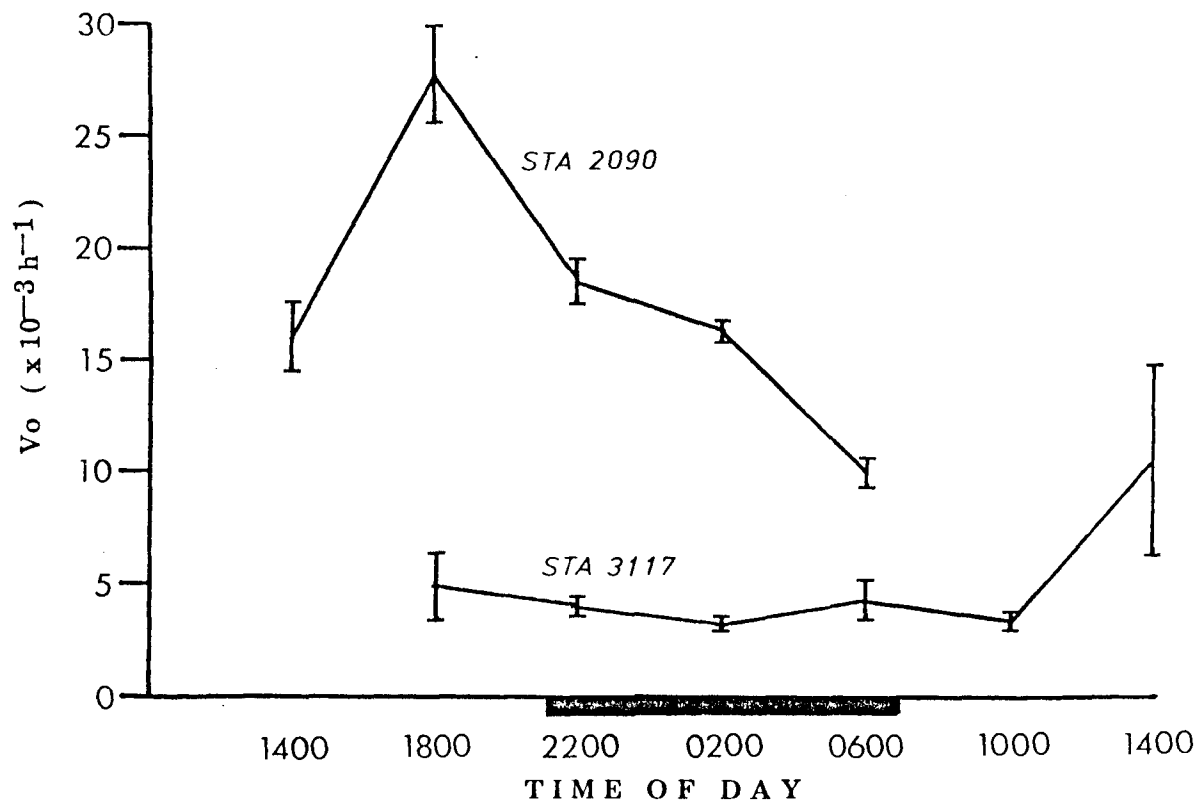


Figure 8. Two diurnal experiments. The 4-hour average specific uptake of silicic acid (V_o) throughout a 24-hour period from Stations 2090, 17 May 1979 and 3117, 8 June 1979. The bars are \pm one standard deviation from the average of two 4-hour incubations. The dark bar on the X axis indicates night.

Discussion

Grazing and the Distribution of Biogenic Silica

There was a striking cross-shelf gradient in particulate silicon, ~100 mmol Si m⁻² in the outer shelf increasing to 300-400 mmol Si m⁻² in the middle shelf and coastal domains. This gradient reflects the compositional difference between the outer and middle shelf phytoplankton communities. In the middle shelf, diatoms are responsible for most of the primary production while outer shelf production is dominated by Pheocystis poucheti, a non-siliceous colonial phytoplankton (Goering and Iverson, 1979; Kocur, 1982).

The dominance of Pheocystis in the outer shelf is attributed to the greater grazing stress on the diatom portion of that community (Goering and Iverson, 1981). Analogous to the two phytoplankton communities, there are two distinct zooplankton communities, apparently separated by the middle front. Middle shelf grazers are mostly small species of copepods and euphausiids; beyond the 100-m isobath large oceanic copepods are the dominant grazers (Cooney, 1981; Cooney and Coyle, 1982).

Recent studies in zooplankton biomass and consumption on the Bering Shelf are summarized in Table 7. Cooney and Coyle (1982) and Dagg (personal communication) seem to agree that up to 30% of the primary production, as carbon fixed by phytoplankton, is consumed on the outer shelf while only about 5% is consumed on the middle shelf. This agreement may be fortuitous. These studies involved different

Table 7. Summary of the recent zooplankton biomass and

TYPE OF MEASUREMENT OF ESTIMATE	MIDDLE SHELF
ingestion	80 mg C m ⁻² d ⁻¹ (5% of PP)*
ingestion	25% of PP
ingestion	110 mg C m ⁻² d ⁻¹ (5% of PP)
biomass	0.78 g C m ⁻²
biomass	0.9 g C m ⁻²
growth	40-150 mg C m ⁻² d ⁻¹
total growth	2.5 g C m ⁻² yr ⁻¹

Species accounting for most of
the total growth.

Thysanoessa raschi
Calanus marshallae

* PP = primary production, as carbon production.

ingestion studies done in the PROBES study area.

OUTER SHELF	REFERENCE
282 mg C m ⁻² d ⁻¹ (20-30% of PP)	Cooney & Coyle (1982)
18% of PP	Dagg <u>et al.</u> (1982)
630 mg C m ⁻² d ⁻¹ (30% of PP)	M. Dagg (personal communication)
5.3 g C m ⁻²	J. Vidal & S. Smith (personal communication)
5.8 g C m ⁻²	Vidal & Smith (unpub- lished manuscript)
200-300 mg C m ⁻² d ⁻¹	Vidal & Smith (unpub- lished manuscript)
10.4 g C m ⁻² yr ⁻¹	Vidal & Smith (unpub- lished manuscript)
<u>Neocalanus plumcrus</u>	Vidal & Smith (unpub- lished manuscript)
<u>N. cristatus</u>	
<u>Metridia pacifica</u>	
<u>Eucalanus bungii</u>	
euphausiids	

methods and assumptions, specifically, different estimates of primary production. The Cooney and Coyle (1982) ingestion rate is based on annual estimates of grazing and primary production, the Dagg (personal communication) estimate on peak bloom grazing and primary production. The difference in the Dagg et al. (1982) and Dagg (personal communication) ingestion as percent of primary production, in part, reflects an adjustment in the PROBES estimates of carbon fixation rates.

Both biomass and grazing experiments do suggest that consumption of organic carbon is three (Cooney and Coyle, 1982; Vidal and Smith, unpublished manuscript) to six times (Dagg, personal communication) greater on the outer shelf than on the middle shelf. A tripled grazing stress in the outer shelf would explain the three to four times greater integrated particulate silicon observed in the middle shelf. Grazing, especially by large copepods, effectively removes silica from the surface layers; after ingestion, diatom tests become incorporated into fast sinking fecal material (Schrader, 1971; Bishop et al., 1977; Honjo, Manganini and Cole, 1982). As V_o varies little over the whole shelf, herbivory is probably the major controller in the cross-shelf distribution of biogenic silica.

Concentration Kinetics

The V_{max} values in Table 6 are in the range of potential surface uptakes observed in profile experiments (Appendix A). Despite the lack of correlation in short versus long uptakes, the internal agreement between kinetic and profile rates allows comparison of these data with

data in the literature. Values of V_{max} are comparable to the higher surface rates measured.

The general pattern in surface silicic acid (and nitrate) concentrations in the middle shelf and coastal domains is a decrease from the 20-30 μM levels observed in early April to $<5 \mu M$ by mid-May (Figure 9a,b). The six stations that had a Michaelis-Menten type response were located in the middle shelf and inner front regions. Most kinetic experiments were done in late May, June and July. The nutrient fields and the kinetic results suggest silicic acid limitation does occur in middle and coastal domain surface waters.

Characterizing the outer shelf domain in terms of silicic acid dependence is difficult because the two experiments done in that area showed no clear dependence of uptake on silicic acid concentration. Harrison et al. (1976) found the uptake of silicic acid proportional to the cell quota of nitrogen in batch cultures grown under ammonium limitation. The total inorganic N in all kinetic experiments was $<1 \mu M$, so some other factor in addition to N-limitation was involved.

The uniformly low silicic acid uptake velocities at Station 3031 on May 31, 1978 (see Table 6) may suggest a senescent diatom population; absolute uptake of nitrate and carbon were also low. The high uptake at Station 4052 (July 7, 1981) may indicate a K_s much less than $0.6 \mu M$, the ambient silicic acid concentration at that station. As only two experiments were done, the question of silicic acid limitation in the outer shelf is left unresolved. The rest of this discussion is

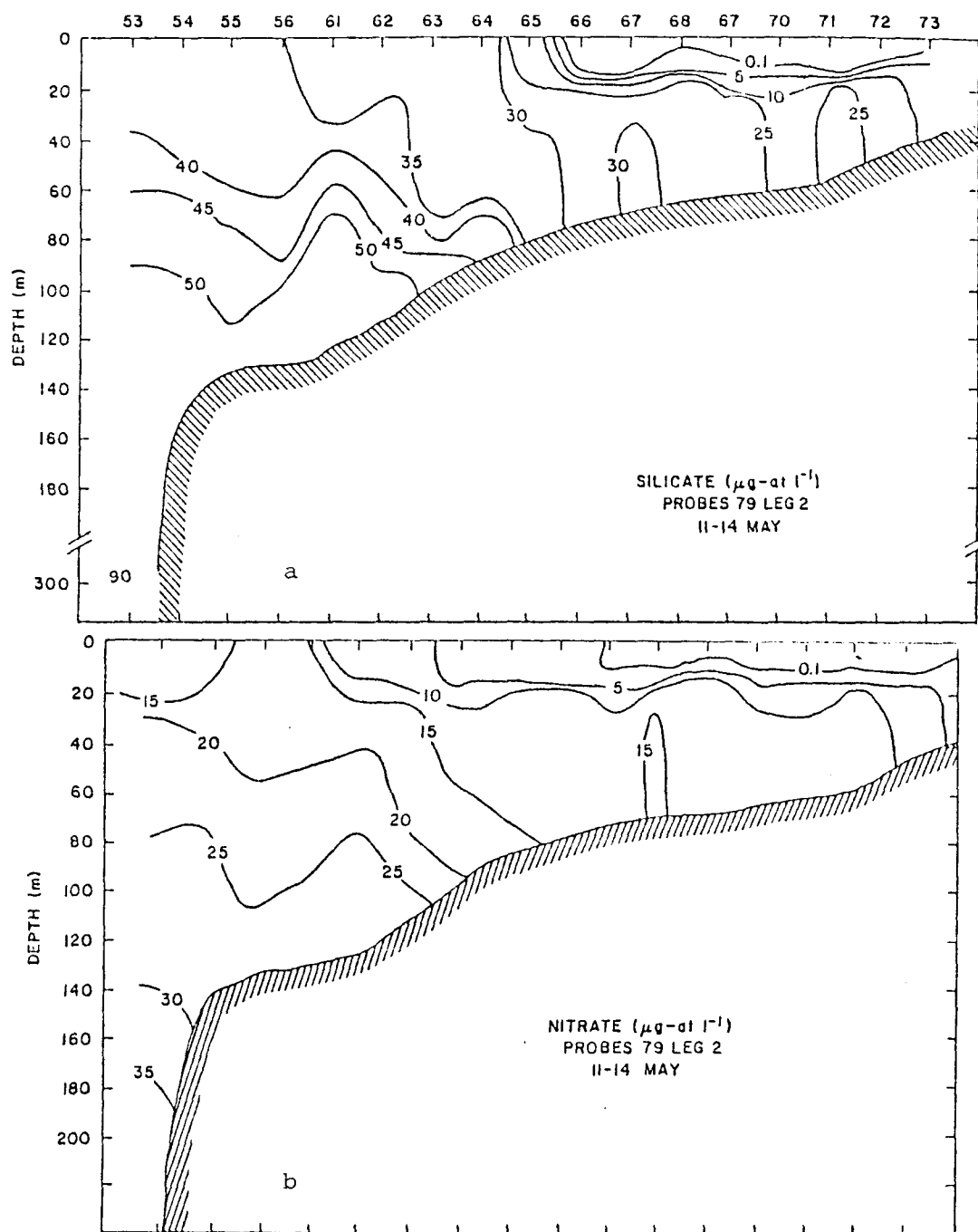


Figure 9a,b. The distribution of silicic acid (a) and nitrate (b) along the PROBES A-line during 11-14 May 1979. From Whitledge and Reeburgh (1980).

thus restricted to the results of the middle shelf and coastal domain experiments.

Nelson et al. (1981) summarize the results of 22 experiments in silicic acid uptake kinetics. The range of K_s from field and unialgal culture studies is 0.8-6.1 μM and the mean for all experiments is 2.38 μM . My range of K_s for the middle shelf and coastal domain of 1.3-5.8 μM , falls within those literature values.

Nelson et al. (1981) feel the Michaelis-Menten equation underestimates silicic acid uptake at nonlimiting concentrations ($>2K_s$). They suggest maximum rates of uptake are actually reached after $5K_s$, not approached asymptotically as the Michaelis-Menten equation predicts. I have plotted the Bering Sea kinetic data in a manner analogous to that of Nelson et al. (1981) to see how well the Michaelis-Menten hyperbola fits the Bering Sea data. In Figure 10, V_o is divided by the calculated V_{max} and plotted against the silicic acid concentration at that velocity divided by the calculated K_s . The theoretical V_{max} was used rather than the Nelson et al. (1981) V_1 , defined as the uptake measured at the highest concentration of silicic acid used in the experiment. Using the fit parameter, V_{max} , seems consistent with the idea of testing the predictability of the given equation. Plotted with the data, not fitted to it, is an idealized Michaelis-Menten hyperbola. At silicic acid concentrations $<2K_s$, the curve is an accurate predictor of V_o . There is scatter in the points beyond $2K_s$, but not a large systematic departure of normalized V_o from the idealized curve. The

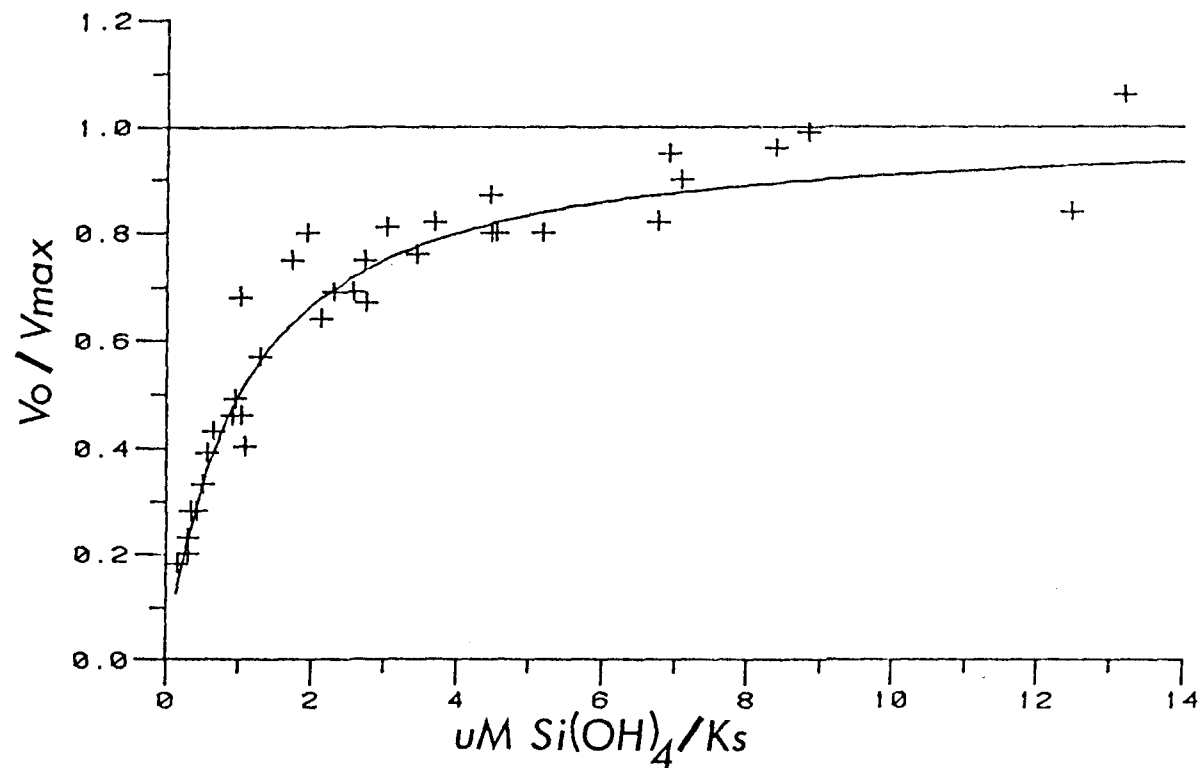


Figure 10. Normalized kinetic data as summarized in Table 6, plotted with the idealized Michaelis-Menten hyperbola. Experimental specific uptake rates (V_o) have been divided by each experiment's theoretical maximum velocity (V_{max}) and the corresponding concentration of silicic acid has been divided by the theoretical half saturation constant (K_s).

Michaelis-Menten equation seems adequate for estimating V_o up to 6.5 K_s , about 20 μM .

Paasche (1973b) found the form of the Michaelis-Menten equation used here oversimplified for his work and included a term for the threshold concentration, a concentration of silicic acid below which uptake does not occur. In the Bering Sea experiments there was uptake at levels as low as 0.7 μM . The nearly undetectable levels of silicic acid observed at some stations suggests that a threshold concentration on the order observed by Paasche (1973b), 0.3-1.3 μM , may not apply in the Bering Sea. This seems consistent with the low but definite response at Station 2044, May 9, 1979 (Figure 6b). Davis, Breitner and Harrison (1978) suggest the threshold concentration for Skeletonema costatum, if it exists, is probably less than 0.2 μM . This threshold may have been beyond the sensitivity of their silicic acid method.

The achieved V_{max} that Nelson et al. (1981) refer to is probably not equivalent to the internal or enzyme-regulated uptake (Conway et al., 1976). In field studies, nitrogen limitation often occurs with or before silicic acid limitation (Paasche and Ostergren, 1980; Nelson et al., 1981; this study). The V_{max} values measured are probably not a maximum theoretical uptake, but a potential uptake under specific conditions of N, Si and light stress. It is best to think of these reported K_s values as transport constants rather than mechanistic half-saturation constants (Goering et al., 1973).

Light Response

Silicic acid uptake was measurable in the dark bottles of all the light experiments. This is in agreement with the uptake measured at the 0.1% and 0.01% SPAR depths of most vertical profiles (Appendix A). Nelson and Goering (1978) feel that the lower light rates are representative of night uptake. As in the diurnal experiments, substantial dark uptake has been observed in natural populations off California (Azam and Chisholm, 1976; Nelson and Goering, 1978), in the Peru upwelling region (Goering et al., 1973) and off northwest Africa (Nelson and Conway, 1979). The sharp increase in V_o observed in most of the light experiments occurred between the 5% and 15% SPAR depths (see Figure 7). This agrees with the general pattern in vertical profiles of V_o ; the transition between relatively high and low rates was indicated in the 5% and 15% SPAR samples.

The extremes of total light dependence or independence in V_o were not observed in either light perturbation or diurnal experiments. Similar mixed responses are discussed by Nelson and Conway (1979) and Nelson et al. (1981). Silicic acid uptake precedes cell separation and is an ATP requiring process (Werner, 1977b cites several references). The ability for dark uptake of silicic acid may be dependent upon a population's cellular energy reserves (Nelson and Conway, 1979). Taxonomically similar populations residing at different depths are in different physiological states. Diatoms living at shallower depths can build up sufficient energy reserves during better light conditions to maintain higher levels of silicic acid uptake during low light. "

Populations living at low levels long enough to exhaust those reserves have a diminished ability for dark uptake.

Most of the light experiments done in this study do not address the question of mixing and uptake. Phytoplankton samples taken from lower light depths, in most cases, exhibited a positive response to increased light within 6 h. These experiments confirm that light does influence V_o on the Bering Shelf, but do not provide information on a population's light history or infer anything about its physiological state. The results of Stations 3008 and 3017 (see Figure 7a) demonstrate that decreased light may or may not inhibit the uptake of silicic acid. The diurnal experiments showed that though uptake may decrease at night, it does not stop.

Nutrient Limitation on the Middle Shelf

Silicic acid uptake can be inhibited by nitrogen or other nutrient stress even at nonlimiting concentrations of silicic acid (Conover, 1975b; Conway *et al.*, 1976; Harrison *et al.*, 1976; Davis *et al.*, 1978; Slawyk, 1979). The lower growth rates generally measured in marine diatom populations, compared to their cultured forms, are attributed to N-limitation (Paasche and Ostergren, 1980). A similar situation exists for freshwater diatoms; growth and silicic acid uptake are lower under phosphorus limitation (Mechling and Kilham, 1982).

During May, before silicic acid becomes limiting, nitrate is present only in trace quantities in surface waters of the middle shelf (see Figure 9b). The major source of nitrogen then becomes ammonium

regenerated at mid to bottom depths. Input of that ammonium (or new nitrate) to the upper layer is limited by diffusion across the pycnocline during periods of high water column stability (Coachman and Walsh, 1981). Deep wind mixing events do occur, such as the one on May 19 in the 1979 time series (Figure 5e), but they can be weeks apart. Sambrotto and Goering (1981) report evidence of N-limitation in the middle shelf during May of 1979 and 1980. By the end of May, middle shelf diatoms grow under a combination of nitrogen and silicon limitation.

Researchers have looked at the compositional ratios of major elements (C, N, Si, P and chl-a) in natural and cultured phytoplankton, relating their composition to assimilation rates of those elements (Slawyk et al., 1978; Eppley, Renger and Harrison, 1979; Slawyk, 1979). The elemental composition of phytoplankton is also linked to the availability of those elements as dissolved nutrients (Thomas and Dodson, 1972; Conover, 1975a; Harrison et al., 1976; Harrison et al., 1977; Rhee, 1978). Table 8 and Appendix B contain the results of linear, geometric mean regressions of particulate C and N (or the absolute uptake of) and chl-a versus particulate Si (or its absolute uptake). The data are from stations within the coastal domain, middle domain and outer shelf region; discrete data from all light depths were used.

The phytoplankton population is mixed over all regions of the southeastern Bering Sea shelf (Kocur, 1982). Outer shelf Pheocystis poucheti is also found in the diatom dominated middle shelf. The

Table 8. The slopes from linear geometric mean regressions of carbon, nitrogen and chlorophyll-a versus silicon. These slopes are expressed as mole ratios, with the 95% confidence intervals enclosed in parentheses. The Si:chl-a ratios are in grams.

REGION	Si:chl-a	N:Si	C:Si
COASTAL DOMAIN	41 (32-50)	0.70 (0.52-0.88) ^u	9.1 (3.9-14.2) ^u
MIDDLE SHELF	16 (14-18)	0.51 (0.44-0.58) ^p	6.4 (5.0-7.8) ^u
OUTER FRONT	23 (19-26)	1.30 (0.89-1.71) ^p	9.6 (6.4-12.7) ^u

^u Regression of absolute uptake data.

^p Regression of particulate concentration data.

Table 9. Cellular chemical composition of three marine diatoms expressed as ratios (by moles), except Si:chl-a which is in grams. From Harrison *et al.* (1977).

SPECIES	LIMITATION	Si:chl-a	N:Si	C:Si
<u>Skeletonema costatum</u>	Si-starved	11.4	2.8	36.5
	Si-limited	5.5	4.1	27.7
	nonlimited	15.0	1.9	9.4
	NH ₄ -limited	21.6	0.8	7.8
	NH ₄ -starved	20.8	0.8	11.9
<u>Chaetoceros debilis</u>	Si-starved	9.0	4.8	19.6
	Si-limited	5.8	4.1	22.5
	nonlimited	13.0	1.8	5.8
	NH ₄ -limited	36.3	0.5	3.0
	NH ₄ -starved	28.1	0.9	3.6
<u>Thalassiosira gravida</u>	Si-starved	2.4	8.5	39.2
	Si-limited	3.3	6.0	24.4
	nonlimited	9.8	2.3	6.3
	NH ₄ -limited	17.1	0.6	7.6
	NH ₄ -starved	50.7	1.4	3.5

slopes of the geometric mean regressions were used to approximate the elemental ratios of diatoms. The reasons for using this approach are: 1) natural phytoplankton samples contain an unknown amount of nondiatom C and N (microzooplankton, nonsiliceous phytoplankton and detritus), and 2) Banse (1977) has used slopes of C to chl-a regressions to remove the bias on the true ratio caused by detritus.

A functional linear regression, the geometric mean, was used because all the parameters involved are dependent variables; error is associated with all the measurements. The geometric mean algorithm minimizes the sum of the horizontal and vertical distance from each point and represents the mean slope of "X versus Y" and "Y versus X" (Ricker, 1973). Some of the equations in Appendix B have positive intercepts large enough to indicate detrital silica. This approach has no real theoretical basis but is a better approximation to the real diatom elemental composition than simple bulk ratios.

No significant correlations of particulate C, N or chl-a versus particulate Si were found in the data from the outer shelf. This was not surprising as diatoms are a minor portion of the phytoplankton population there.

Harrison et al. (1977), working with diatoms in unialgal cultures, measured a suite of particulate elemental ratios in various stages of ammonium and silicic acid limitation. They concluded that the sensitive indicators for determining N- or Si-limitation are C:Si, N:Si and Si:chl-a. Table 9 is a condensed version of the Harrison et al. (1977) results.

The molar ratios of C:Si in Bering Sea shelf particulate material ranged from 6.4 to 9.6. These ratios are close to those for N-limited growth and do not indicate Si-limitation when compared to the Harrison et al. (1977) ratios. The N:Si ratios for all three regions are below the range of Si-limitation given by the cited study. The coastal and middle domain N:Si ratios suggest N-limitation. The Si:chl-a slopes have a greater range, 16-41, among the three regions than either N:Si or C:Si; again N-limitation is indicated. Assuming that the slopes in Table 8 may be as much as 50% in error, the basic inferences drawn by comparison with Table 9 would remain unchanged. Nitrogen limitation is probably a greater factor in influencing elemental composition in Bering Sea phytoplankton than Si-limitation.

There can be a lag time between the relative uptake of major elements and the resulting cell composition during nonsteady state growth (Slawyk et al., 1978). In cases where elemental ratios are derived from slopes of absolute uptake data, that ratio may have been different from the true particulate ratio. Almost half of the slopes used were from geometric mean regressions of absolute uptakes because the particulate r^2 was not significant. The slopes of C:Si of both particulate and absolute uptake data agreed within 50% for the middle shelf data; the particulate slope was 4.7, the uptake slope was 6.4.

The composition data in Table 8, by itself, are not definitive evidence that N-limitation is a greater factor in middle shelf production than Si-limitation. In support of the composition data, two observations discussed earlier also point to N-limitation as a larger

problem for middle shelf diatoms: 1) the middle shelf also supports nondiatom species, so diatoms must compete for N with other phytoplankton, and 2) nutrient contours from the PROBES A-line in 1979, 1980 and 1981 show nitrate depletion in the surface layer occurring a week or more before silicic acid depletion (Whitledge and Reeburgh, 1980; Reeburgh and Whitledge, 1981 and 1982). Nitrogen and silicon limitation can be a persistent condition in the surface waters of the middle shelf by the end of May.

Along with the changing nutrient regime, the composition of the phytoplankton population also changes. Goering and Iverson (1981) and Kocur (1982) describe the three stages in phytoplankton succession observed in the middle shelf. The spring bloom begins in April in the high nutrient waters of the coastal domain and spreads seaward across the shelf. This Stage I community is largely fast growing, small diatoms such as Chaetoceros debilis, C. concavicornis, C. radians and Thalassiosira aestivalis. By late spring to early summer, larger Stage II diatoms dominate. These are the chain-forming, spine-forming species of Chaetoceros, Thalassiosira, Rhizosolenia, Corethron and Nitzschia. The Stage II species are more resistant to the small grazers of the middle shelf than Stage I species (Iverson *et al.*, 1979; Cooney and Coyle, 1982). The long chains of Rhizosolenia alata, capable of thriving on regenerated N and low concentrations of silicic acid, make up most of Stage III.

During the course of middle shelf succession, the outer shelf is held static by the large grazers able to feed on Stage I and II diatoms

(Kocur, 1982). This selective feeding allows Pheocystis poucheti to dominate outer shelf production and biomass.

Succession in lakes has been related to nutrient levels, water column stability, differential sinking and trophic structure (Tilman, Kilham and Kilham, 1982, cite several references). To explain the success of mixed populations in natural systems, that is, more species than limiting growth factors, researchers have invoked the concept of a species' ability to thrive on different combinations of limiting factors (Tilman, 1976; Tilman, Mattson and Langer, 1981). For example, Turpin and Harrison (1979) demonstrated the degree of dominance between two genera of diatom as a function not of absolute ammonium concentration, but whether ammonium was pulsed or continuously available. This is consistent with the idea of small scale temporal and spatial variability in nutrient regimes. Success in growth can depend on an ability to increase affinity for limiting nutrients during short periods of availability (McCarthy and Goldman, 1979). Batch cultures of Thalassiosira weissflogii can maintain a constant internal pool of dissolved Si even under silicic acid starvation (Binder and Chisholm, 1980). Goldman, McCarthy and Peavey (1979) suggest that flexibility in compositional ratios can allow replication even under limiting conditions.

Paasche (1973a) proposes that during Si-limited growth, uptake may actually be slow and continuous rather than concentrated into a short period just before cell separation (Lewin, 1962; Darley, 1974; Werner, 1977b). This scheme would lengthen the time between divisions,

resulting in slow but steady growth. Adaptions of natural diatom populations to silicic acid limitation have been observed. In Oslo-fjord, Paasche (1980) found thin-walled summer forms of Skeletonema, Chaetoceros and Rhizosolenia. A thin-walled form of Rhizosolenia alata is seen in late bloom (Stage III) Bering Sea samples (Goering and Iverson, 1981).

Thinner frustules and spine reduction increase the sinking rates of diatoms (Smayda, 1970). Harrison et al. (1977) felt sinking rates would also increase under nitrogen limitation, perhaps to a greater degree than frustule reduction. When the nutricline and pycnocline coincide, and both are above the 1% light depth, sinking could help offset nutrient limitation. Chlorophyll-a maxima were found at or just above the mixed layer during calm periods in the spring and summer of 1978.

Silica and Carbon Productivity

Nelson (1975) suggests that for a diatom dominated population whose elemental composition is known and steady in time, silicic acid uptake could provide a better estimate of primary production than uptake of the more labile elements carbon and nitrogen. Several methods have been used to measure production on the Bering Sea shelf. PROBES researchers have generated data on ^{14}C uptake (Iverson et al., 1979), ^{15}N uptake (Sambrotto and Goering, 1981) and the temporal changes in dissolved inorganic carbon (Codispoti et al., 1982) and nutrients (Whitledge and Reeburgh, 1980; Reeburgh and Whitledge, 1981 and 1982).

These methods yield independent estimates of carbon production. This section of the discussion examines how well the silicic acid uptake measurements compare with the changes in silicic acid concentration, and the agreement between ^{14}C based estimates of production and estimates derived from silica production.

Absolute uptake, R_o , is independent of detrital content in a sample (Goering et al., 1973). The integrated R_o 's for silicic acid uptake were used to estimate both silica and carbon production.

Combined silicic acid data from 1979-1980 was contoured as a time series for PROBES A-line Station 5 in the outer domain and Station 14 in the middle domain (T. Whitledge, unpublished data). I have estimated silicic acid disappearance by integrating concentrations to 70 m on a bimonthly grid (Figure 11a,b). The net loss in the middle shelf over the period of March to mid June was 1.925 mol m^{-2} , equivalent to an average daily uptake of $18 \text{ mmol m}^{-2} \text{ d}^{-1}$. This rate is somewhat higher than my April to August average of $14 \text{ mmol m}^{-2} \text{ d}^{-1}$, but the absolute loss of silicic acid is close to my estimated total uptake of 2.15 mol m^{-2} (Table 10). The greater daily rate based on Figure 11a, in part, reflects the greater absolute uptake rates that do occur in May. My period of estimation smooths out those higher rates.

The outer shelf comparison is less satisfying. Total silicic acid loss from April to mid August was 2.09 mol m^{-2} or $17 \text{ mmol m}^{-2} \text{ d}^{-1}$. Both the absolute loss and daily rate are almost double my uptake estimates of 1.23 mol m^{-2} and $10 \text{ mmol m}^{-2} \text{ d}^{-1}$. Two reasons for these differences are: 1) sparse sampling in the outer domain, 5 stations

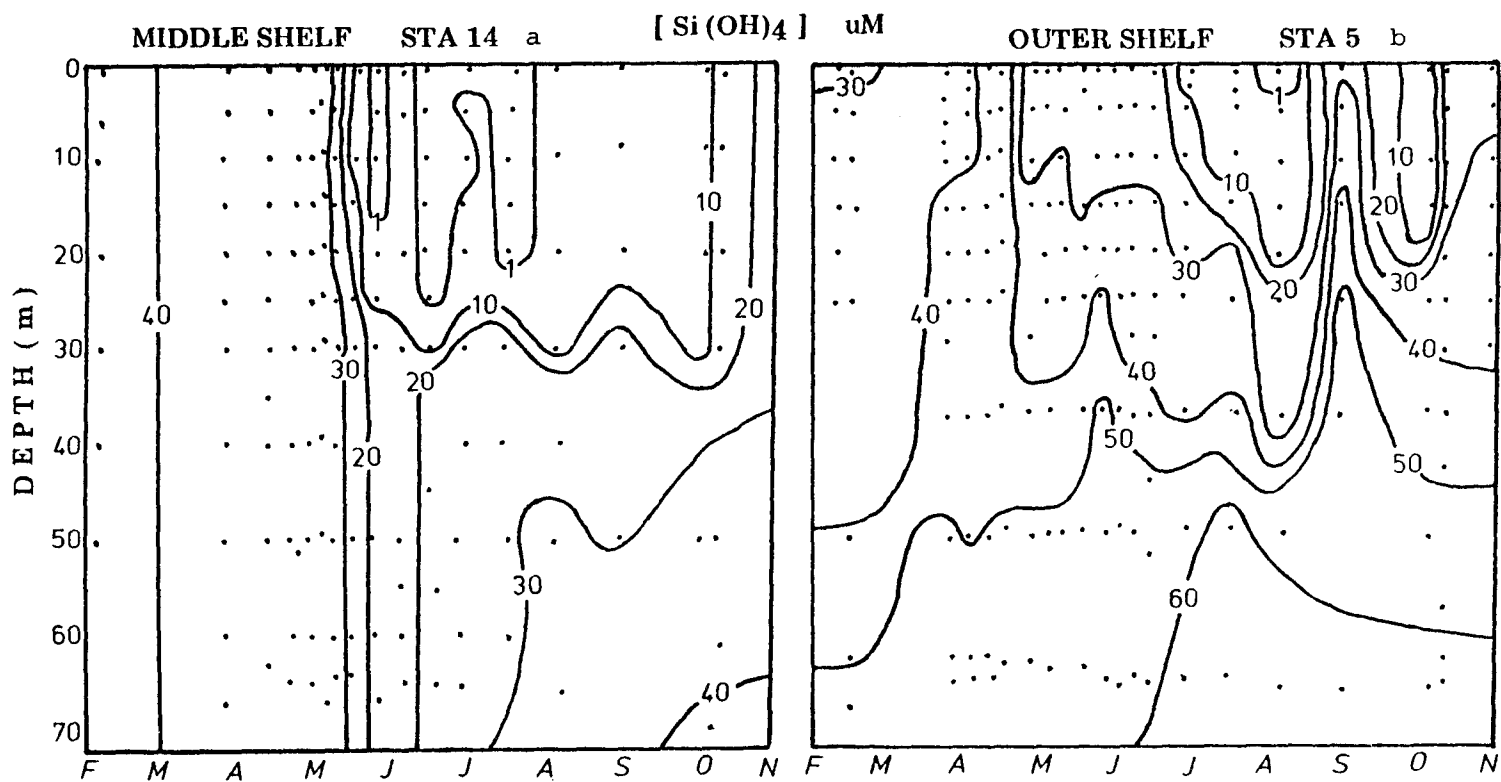


Figure 11a,b. Time series contours of silicic acid at middle domain A-line Station 14 (a) and outer domain A-line Station 5 (b) as drawn from 1979-81 data by T. Whitledge (unpublished data).

Table 10. Data used to estimate the annual production of biogenic silica and carbon on the southeastern Bering Sea shelf. An additional one third of the spring-summer production was included to approximate whole year production. A factor of 6.4 mole C:Si was used to convert Si-uptake to C-uptake.

	Si-UPTAKE mmol Si m ⁻² d ⁻¹	x	days	=	Si-PROD mol Si m ⁻²	C-UPTAKE g C m ⁻² d ⁻¹	C-PROD g C m ⁻²
MIDDLE DOMAIN							
MAY	30		31		0.93	2.3	71.4
APR-AUG	10		122		1.22	0.77	93.7
					2.15		165.1
ANNUAL = (SPR-SUM) + 1/3 (SPR-SUM) =					2.87		220
OUTER DOMAIN							
MAY-AUG	10		123		1.23	0.77	94.5
ANNUAL = (SPR-SUM) + 1/3 (SPR-SUM) =					1.64		126

in 3 years, and 2) the incursion of deeper oceanic water onto the shelf balanced by movement of middle domain water off the shelf (Kinder and Schumacher, 1981a) could mix lower silicic acid water with outer domain water. The first reason makes it difficult to evaluate the second.

Using the middle domain C:Si ratio of 6.4, average carbon productivity for May was $2.3 \text{ g C m}^{-2} \text{ d}^{-1}$ (Table 10). This estimate is close to the bloom value from ^{14}C data, $2.9 \text{ g C m}^{-2} \text{ d}^{-1}$ (R. Iverson, personal communication) but much lower than the $3.6 \text{ g C m}^{-2} \text{ d}^{-1}$ based on changes in total CO_2 (Codispoti *et al.*, 1982).

The average R_o for silicic acid was $\sim 10 \text{ mmol m}^{-2} \text{ d}^{-1}$ for the period of May through July on the outer shelf. Because Pheocystis dominates outer shelf biomass, the C:Si ratio of 9.6 is probably high (Table 8). If I use the middle domain ratio, 6.4, carbon production equals $0.8 \text{ g C m}^{-2} \text{ d}^{-1}$, less than half the $2.0 \text{ g C m}^{-2} \text{ d}^{-1}$ from ^{14}C data (R. Iverson, personal communication).

A Comparison of Biogenic Silica and Silicic Acid Uptake in the Bering Sea and Three Upwelling Systems

There have been few studies involving the direct measurement of silicic acid uptake in natural systems. Some data exist for the Gulf of California (Azam and Chisholm, 1976) and the Antarctic Southern Ocean (Nelson and Gordon, 1982), but most of the research in this area has been conducted in upwelling systems as part of the Coastal Upwelling Ecosystems Analysis Project (Barber, 1977). Silicic acid uptake and dissolution measurements off the coasts of Peru, northwest Africa

and Baja California are summarized in Nelson et al. (1981) and the following discussion deals with those studies.

Integrated particulate silicon in the middle domain of the Bering Sea was generally greater than that observed off northwest Africa, Baja California and Peru (Table 11). Bering Sea surface concentrations are similar to those off northwest Africa however, northwest Africa does get some aeolian input of silica (Nelson and Goering, 1977b) so actual biogenic silica may be somewhat lower than reported.

Unlike particulate silicon, specific uptake rates in the Bering Sea are comparatively low. Specific uptake rates in the upper 10 m ($\sim 0.005\text{--}0.015\text{ h}^{-1}$) are roughly half those measured off northwest Africa and far less than those off Baja (Nelson and Goering, 1978). Surface rates approach those in Peru during strong wind conditions ($>5\text{ m s}^{-1}$) and the few rates available from the Antarctic (Nelson and Gordon, 1982). Like the Antarctic observations, geographic gradients in biogenic silica production across the Bering Shelf reflect a difference in diatom biomass, not a difference in specific uptake velocities.

There are some similarities in the general features of uptake profiles. Upwelling and Bering Sea profiles are fairly uniform, lacking extreme maxima near the surface. Both Bering Sea and upwelling areas exhibit measurable uptake at depths equivalent to the 0.01% SPAR depth, twice the assumed bottom of the euphotic zone. Deep uptake may indicate that cell division occurs at depths below which carbon and

Table 11. Average integrated biogenic silica (integrated to the 1% SPAR depth) in the PROBES study area and three upwelling systems.

SYSTEM	mmol Si m^{-2}	REFERENCE
Bering Sea - coastal domain	169 ± 75	This study.
middle domain	130 ± 62	This study.
outer domain	50 ± 29	This study.
Baja California (3-5/73)	76 ± 31	Nelson & Goering (1978)
Northwest Africa (3-5/74)	78 ± 37	Nelson & Goering (1978)
Peru (3-4/77)	80	Nelson <u>et al.</u> (1981)

nitrogen uptake are severely light limited (Nelson, 1975; Nelson and Goering, 1978).

The occurrence of surface maxima in uptake appeared to be limited to stations from the middle domain during the peak bloom period in early May. The near surface peaks in uptake and particulate silicon seen in the Station 12, 1979 time series (Figure 5) were like the weak wind ($<5 \text{ m s}^{-1}$) maxima off Peru (Nelson et al., 1981). Though I found no clear correlation between wind speed and surface structure in Vo, as in the Nelson et al. (1981) Peru study, the distribution of at least the particulate properties in the middle shelf were linked to upper water column stability. Middle domain waters were strongly stratified by the first week in May, 1979; a result of decreased wind mixing and increased insolation (Whitledge et al., 1981a; Sambrotto et al., unpublished manuscript). During this 5-10 day calm period, there was a large increase in chlorophyll-a with concomittant decreases in nitrate and silicic acid (Whitledge and Reeburgh, 1980; Goering and Iverson, 1981). The stabilization of the still nutrient replete surface layer in early May supported the high silicic acid uptake and resulting accumulation of particulate silicon. This was observed at Station 12, 1979, and some middle domain stations in 1978. Some isolated stations exhibited maxima in Vo and P_{Si} despite recent high winds, perhaps a result of inertial resistance to mixing in the stable surface layer.

The ability to support the greater concentrations of particulate silicon on the Bering Shelf may lie in the prebloom nutrient loading. Table 12 lists the prebloom nitrate and silicic acid concentrations

Table 12. Nutrient concentrations and surface temperatures in the PROBES study area and three upwelling systems.

SYSTEM	NO_3^- uM	Si(OH)_4 uM	Si:N mole	TEMP °C	REFERENCE
NW Africa	20	10	0.5	16	Friederich & Codispoti (1979)
Peru	25	20	0.8	16-19	Walsh (1975)
Baja Calif.	20	20	1.0	13-17	Walsh <u>et al.</u> (1974)
Bering Sea	20	40	2.0	3-6	Whitledge & Reeburgh (1980)

in the PROBES study area and three upwelling systems. Nitrate among all these systems is about the same, but initial silicic acid levels in the Bering Sea are at least twice the concentrations observed in the upwelling systems. Even though specific uptake rates are higher in the upwelling systems, the Bering Shelf can support greater absolute uptake, resulting in the observed high silica production.

In the presence of initially high nitrate and silicic acid, why are Bering Sea specific velocities lower than those in the upwelling systems discussed? Part of the answer may be the differences in upper water column temperatures (Table 12). Eppley (1977) summarizes work in temperature and phytoplankton growth; higher maximum growth rates covary with higher optimum temperatures. Surface layer temperatures are 5-10°C lower in the Bering Sea. Growth rates calculated for the Bering Shelf, based on the uptake of silicic acid (Eppley and Strickland, 1968), were generally less than 0.5 div d^{-1} . Antarctic ice diatoms grow at less than 1 div d^{-1} at optimum temperatures of 4-6°C (Eppley, 1977 cites Bunt, 1968); for Antarctic pelagic diatoms, growth is also less than 1 div d^{-1} (Nelson and Gordon, 1982).

CHAPTER III. A BIOGENIC SILICA BUDGET IN THE OUTER SHELF OF THE BERING SEA

Methods and Materials

Four cores, two in 1979 and two in 1982, were taken from the outer shelf domain (Figure 12 and Table 13). Sediment was retrieved in 6.8-cm (diameter) plastic core liners loaded in a Benthos gravity corer. Capped cores were kept upright on deck, at ambient air temperature ($\sim 10^{\circ}\text{C}$) until sectioned and squeezed. At each location, one core was extruded into six PVC Reeburgh (1967) squeezers and squeezed at wet lab temperature. Resulting interstitial water was collected in 20-ml polyethylene bottles. Samples were kept cold or frozen until analyzed for silicic acid by the automated molybdate method (Armstrong, Stearns and Strickland, 1967; Whitledge et al., 1981b). In 1979 silicic acid concentration was also measured in the overlying water of cores from Stations 2051 and 2057.

A second or companion core was taken at 1982 stations PB-4 and PB-5 for porosity, particulate organic carbon and nitrogen, amorphous silica and ^{210}Pb activity analyses. These cores were cut into 2- and 3-cm sections and frozen in preweighed plastic bags. Each entire section was weighed (to 0.1 g) before and after overnight drying at 65°C . Porosity was calculated by the standard equation;

$$P_o = \frac{[(g \cdot H_2O) / (\text{Rho} \cdot H_2O)]}{[(g \cdot H_2O) / (\text{Rho} \cdot H_2O) + (g \cdot \text{sed}) / (\text{Rho} \cdot \text{sed})]}$$

5

Table 13. Location, depth, bottom and air temperatures for cores collected in the outer domain of the Bering Sea.

STATION		DEPTH	BOT. TEMP.	AIR TEMP.	LOCATION
		m	°C	°C	
2051	5 May 1979	100	4.3	4.5	55 26.3 N 164 38.2 W
2057	12 May 1979	127	4.0	4.4	55 38.0 N 166 37.4 W
PB-4	20 June 1982	144	3.9	6.7	55 20.0 N 167 08.1 W
PB-5	20 June 1982	139	4.0	7.2	55 28.4 N 166 53.1 W

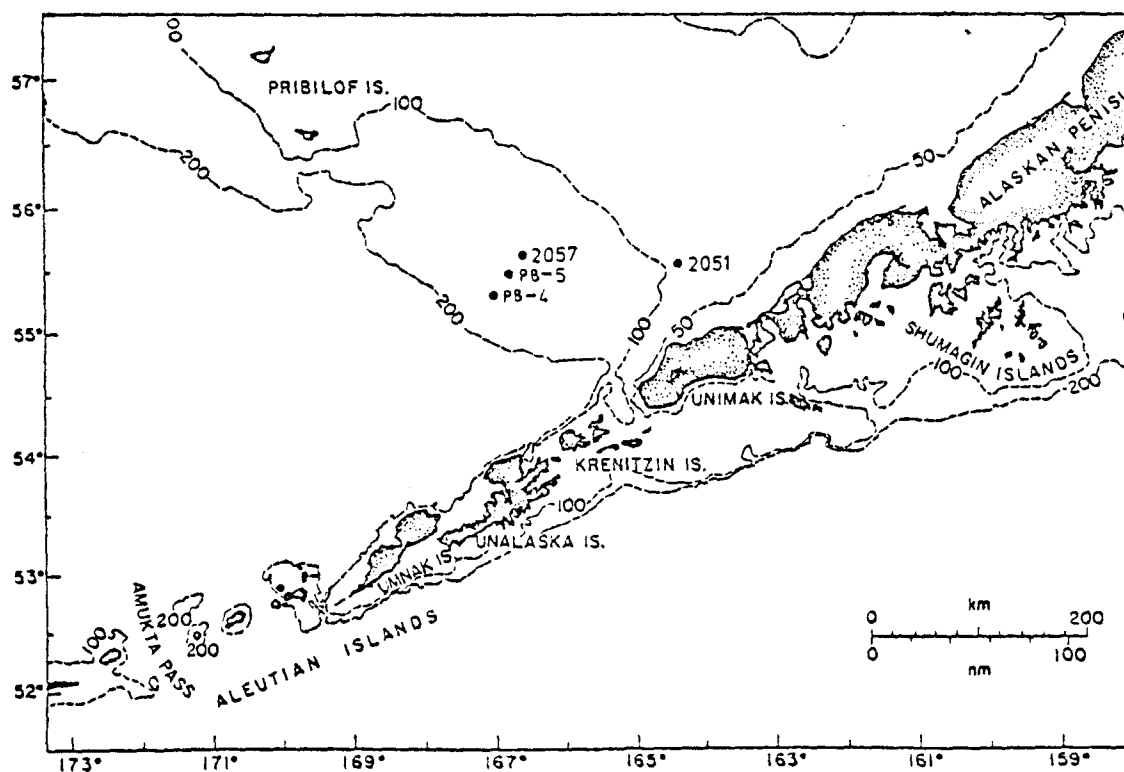


Figure 12. Station locations of cores collected in 1979 and 1982 from the outer domain.

where $g \cdot H_2O$ is the difference between bulk and dry section weights, $Rho \cdot H_2O$ was assumed equal to 1.028 g cm^{-3} for a salinity of 35‰ and 3°C , $g \cdot sed$ is the weight of the dry section, and $Rho \cdot sed$, the dry sediment density, was assumed equal to 2.5 g cm^{-3} .

Ten-mg subsamples of sediment, dried overnight at 100°C , were analyzed for organic carbon and nitrogen using a Perkin-Elmer Model 240C elemental analyzer. The model 240C combusts a sample under an oxygen atmosphere, measuring resulting N_2 and CO_2 gas by thermal conductivity. Reproducibility for both C and N was 0.05%. Samples were not pretreated with acid because a separate determination of total carbonate on a surface sample indicated a carbonate content less than 0.05% (J. Cornwell, personal communication). I considered carbonate content negligible if it was less than sample reproducibility.

I measured the amorphous silica content on dry 50 mg subsamples by the method described by Eggimann, Manheim and Betzer (1980). Sediments in teflon centrifuge tubes were digested in 2 M sodium carbonate at 90°C for 4 h. The resulting solution was divided, one portion for silicic acid analysis, the other acidified for aluminum determination. The treated sediment was leached, the solution split and analyzed for Si and Al as mentioned. The second leach solution was used to determine an Al:Si ratio to correct for Si contributed by clays in the first leach. Eggimann et al. (1980) measured Al by graphite furnace atomic absorption. To reduce analysis time, the sodium carbonate solutions were preconcentrated by evaporation and analyzed by flame atomic absorption.

Three- to four-gram subsamples of dry sediment were prepared for ^{210}Pb counting using the method detailed in Kipphut (1978). Weighed sediment was digested in 100 ml of 6 N HCl with the addition of the ^{208}Po tracer as a check on extraction and plating efficiency. The solid phase was removed by centrifugation, the remaining solution evaporated to 10 ml and then brought back to 100 ml with 1.5 N HCl. To prevent the precipitation of iron phases, powdered ascorbic acid was added until the solution, usually a yellow-brown, no longer lightened in color. The surface of a 1-cm² silver disk was roughened with an abrasive cleanser and placed in the stirred acid solution for 2 h at 75°C. During this time the tracer, ^{208}Po , and the ^{210}Pb daughter, ^{210}Po , plate onto the silver surface. The disk was then rinsed with distilled water and acetone. Total ^{210}Pb activity was measured by the alpha decay of ^{210}Po and efficiency determined by ^{208}Po activity. The counting was done using Si-surface barrier detectors with pulse height analyzers.

The assignment of a supported ^{210}Pb activity was based on the average activity in deeper sections of the core where activity became constant. This average activity was subtracted from the upper layer activities, resulting in excess ^{210}Pb activity. A sedimentation rate was derived from the slope of a linear least squares fit of the natural logarithm of excess ^{210}Pb activity and the cumulative mass of sediment per unit area.

Results

Interstitial silicic acid concentrations in all four core locations were high and scattered, changing by as much as 100 μM between adjacent sections (Figure 13). The combined average core shows the high rate of increase in the top 5 cm, up to 500 μM from the 60 μM of the overlying water. The average core also suggests a fairly constant concentration down to 50 cm. The deepest interstitial concentration measured in a 47-50 cm section from PB-4 was 525 μM , about equal to the concentration at 5 cm. That value is also about half of the ~ 1000 μM considered saturating for amorphous silica in sea water at 3°C (Hurd, 1972; Schink, Guinasso and Fanning, 1975).

The porosities of surface sediment at Stations PB-4 and PB-5 were 0.74 and 0.80, respectively. Both cores show a sharp decrease, about 12% of surface porosity, in the top 6 cm (Figure 14). The profiles of these cores are similar, with PB-4 displaced about 0.5 porosity units lower than PB-5. Porosity decreases sharply in the 21-24 cm section of PB-4.

Surface concentrations of organic C and N, as approximated by the top 2-cm sections, were 1% and 0.2%, respectively. Both elements decreased with depth; concentrations are somewhat higher in the PB-5 core (Figure 15). Like the porosity profile of PB-4, %C decreases in the first 6 cm and again in the 21-24 cm section. In the interval between 6 and 21 cm, %C increases to near surface values. Core PB-5 follows the same trend down to 21 cm.

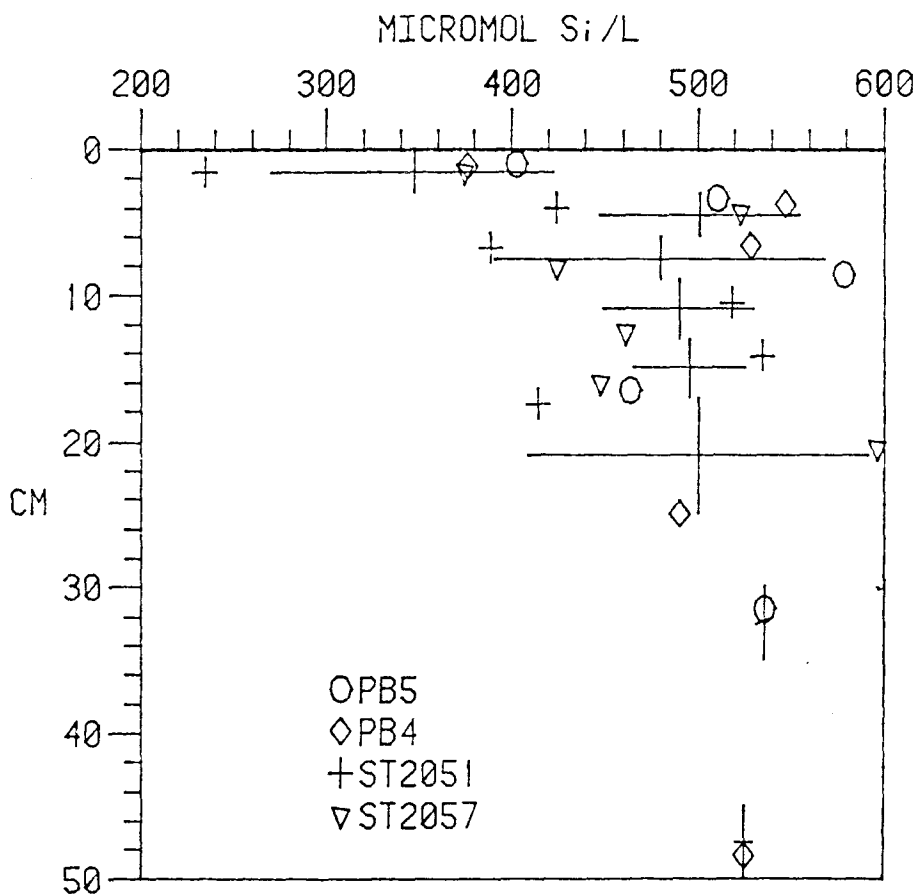


Figure 13. Profiles of interstitial silicic acid concentration in four cores from the outer domain. The large crosses represent an averaged profile; the vertical line is the length of the average section, the horizontal line indicates \pm one standard deviation.

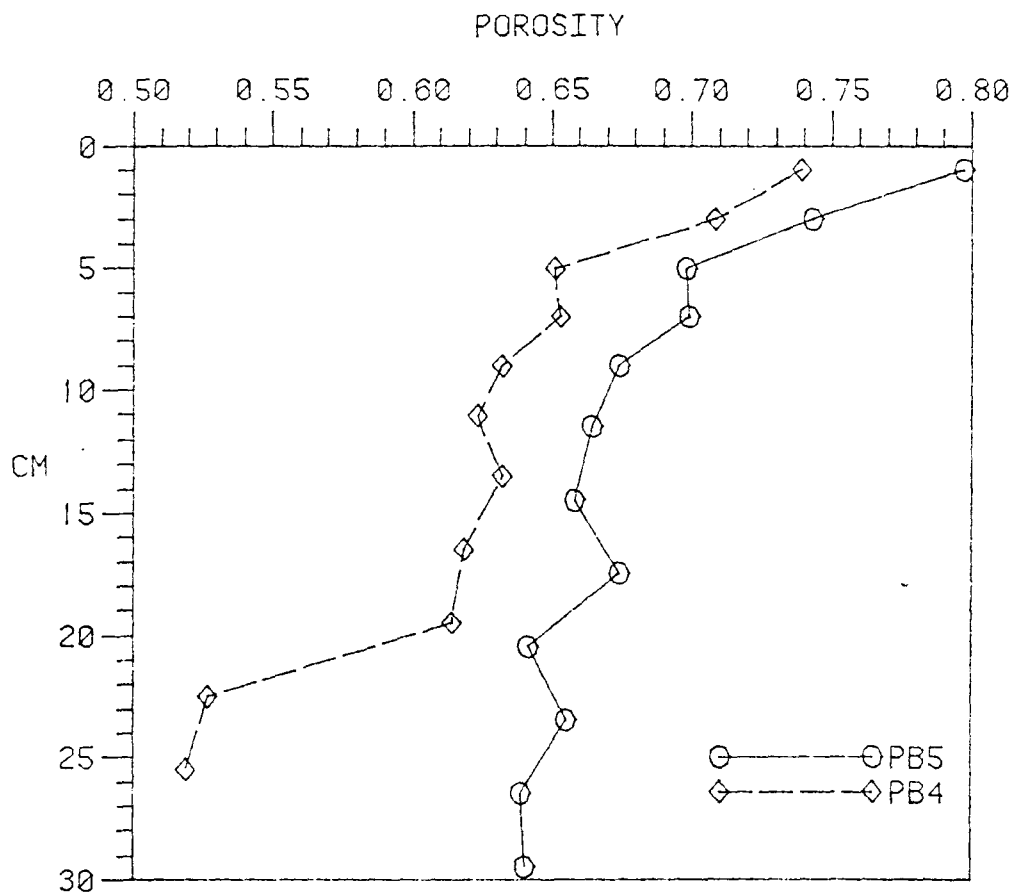


Figure 14. Porosity profiles for 1982 outer domain cores PB-4 and PB-5.

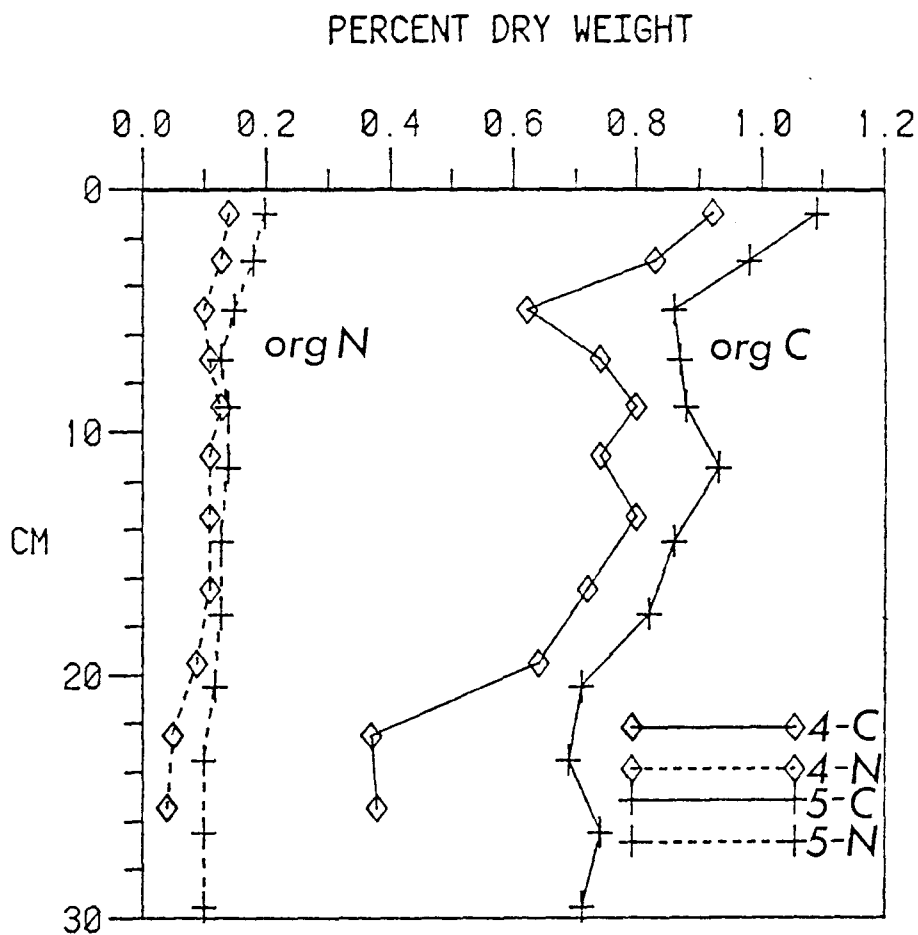


Figure 15. Profiles of percent particulate organic nitrogen (org N) and particulate organic carbon (org C) for 1982 outer domain cores PB-4 and PB-5. The numbers 4 and 5 in the legend correspond to the data for cores PB-4 and PB-5 respectively.

The shapes of the amorphous silica profiles for PB-4 are similar to the %C profiles; decreasing in the top 6 cm, increasing to a mid core maximum and decreasing down the rest of the core (Figure 16a,b). Like %C and %N, amorphous silica content in PB-5 was greater than PB-4. Surface concentrations ranged from 7.5% to 10%; the deepest section analyzed, the 47-50 cm section of PB-4, contained 3.7% silica (Figure 16a).

The results of ^{210}Pb activity analyses are in Figure 17 and Table 14. Sedimentation rates for the outer shelf are 706 and 877 $\text{g m}^{-2} \text{yr}^{-1}$. The linearity in the excess ^{210}Pb plots (Figure 17a,c) is probably an indication of relatively low rates of bioturbation. The infaunal organic carbon content in the outer shelf is much lower than that found in the middle and coastal domains (Haflinger, 1981). The surface unsupported activities and ^{210}Pb deposition rates are within the range of values expected at this latitude (Robbins, 1978).

Discussion

The Flux of Silicic Acid from Sediments

The variability in interstitial silicic acid concentrations between coring locations (and possibly between sections within a core) may be attributed to differences in storage and squeezing temperatures. Sediments originally at 3-5°C, stored and squeezed at ~20°C, have silicic acid concentrations up to 1.5 times those of cold squeezed cores (Fanning and Pilson, 1971; Schink et al., 1974). The correction factor applied by Schink et al. (1974) to warm squeezed cores may not

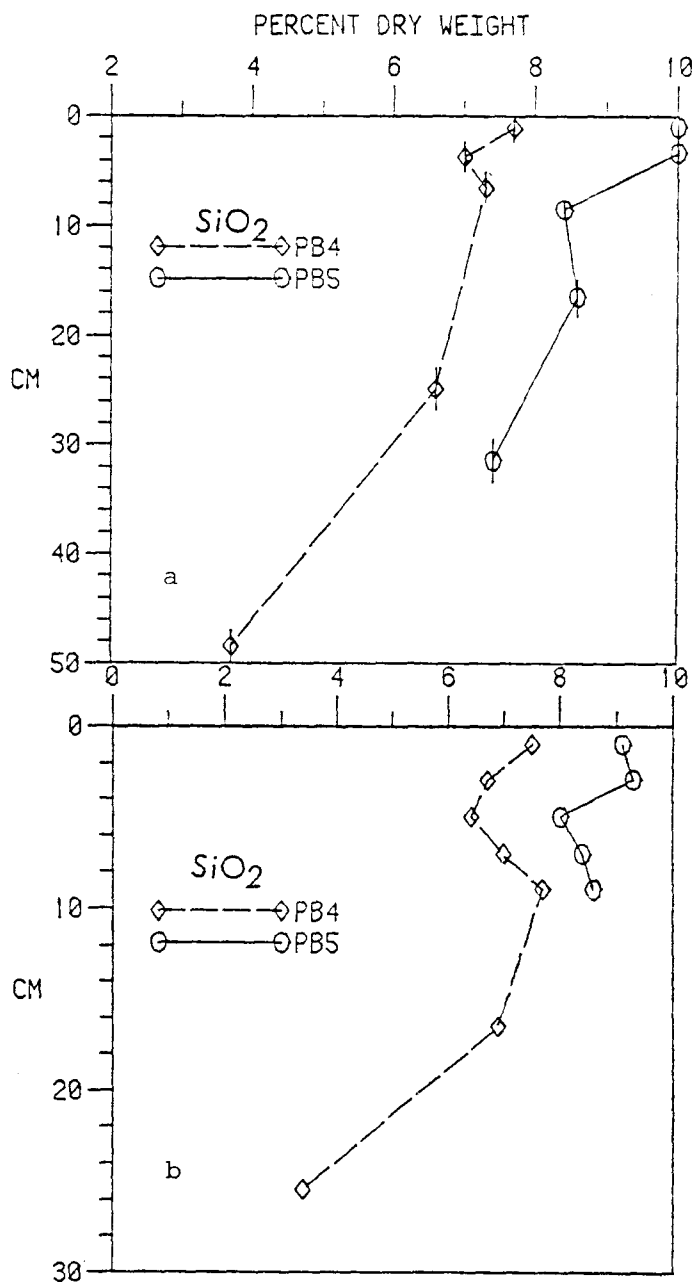


Figure 16a,b. Profiles of percent amorphous silica for the 1982 outer domain cores PB-4 and PB-5. Figure 16a and 16b represent companion cores; Figure 16b was derived from the analysis of the same cores resulting in Figures 14 and 15.

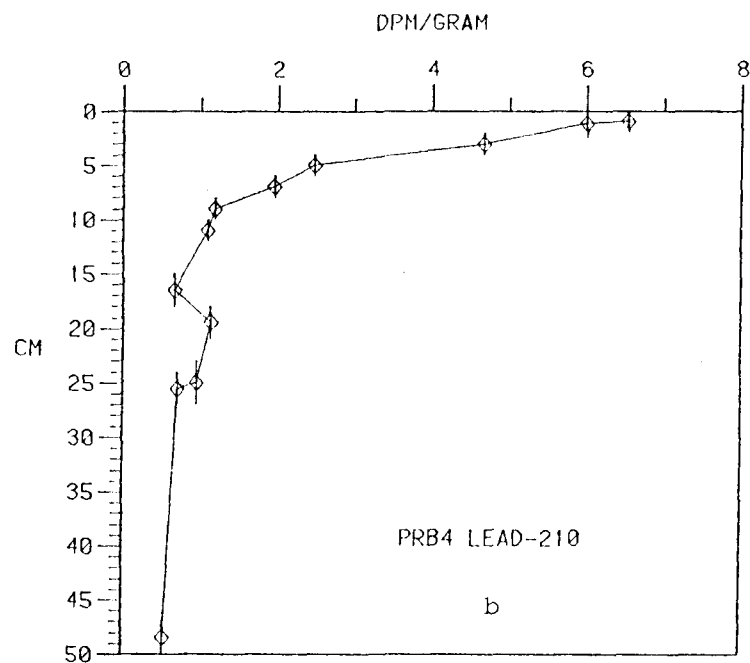
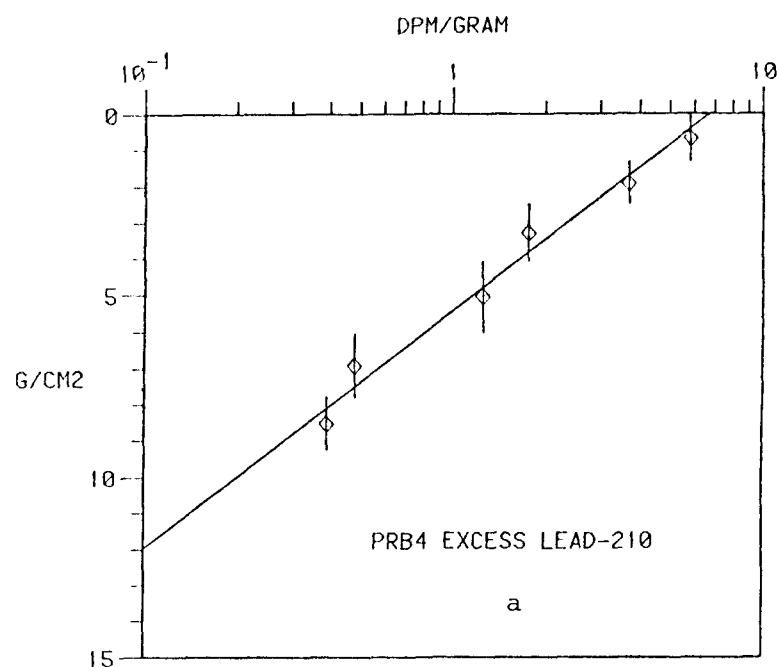


Figure 17a. Excess ^{210}Pb activity (dpm g^{-1}) versus the cumulative mass of sediment (g cm^{-2}) for core PB-4. The line is the linear least squares regression with a slope equivalent to a sedimentation rate of $877 \text{ g m}^{-2} \text{ yr}^{-1}$.

Figure 17b. Profile of total ^{210}Pb activity versus depth in the sediment for core PB-4.

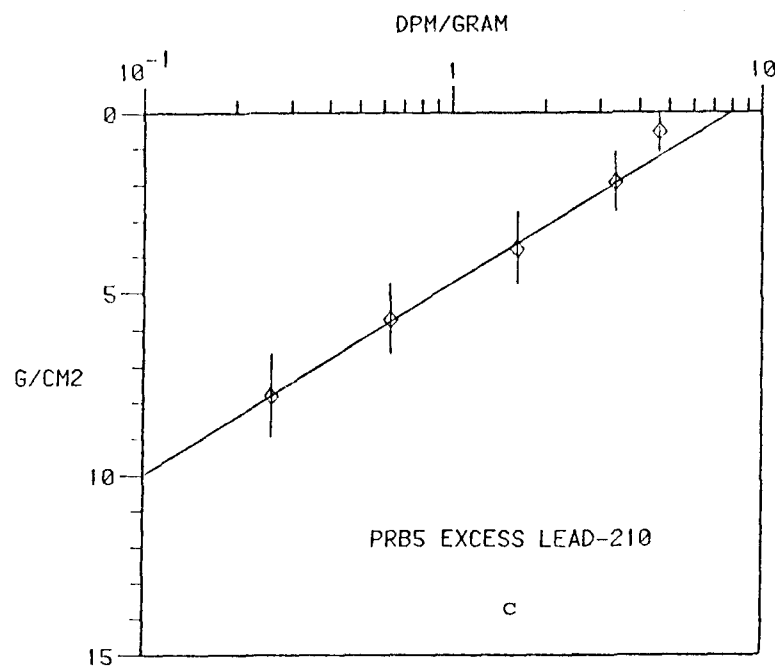


Figure 17c. Excess ^{210}Pb activity (dpm g^{-1}) versus the cumulative mass of sediment (g cm^{-2}) for core PB-5. The line is the linear least squares regression with a slope equivalent to a sedimentation rate of $706 \text{ g m}^{-2} \text{ yr}^{-1}$.

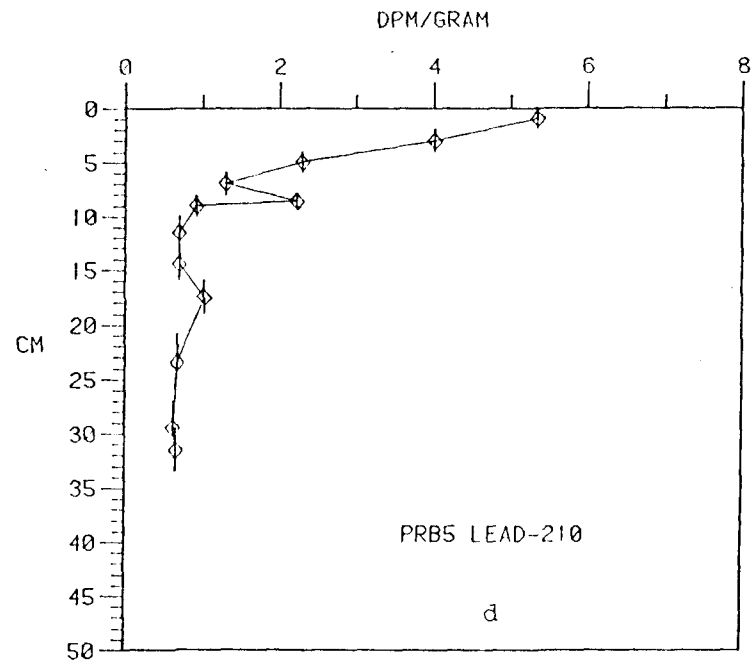


Figure 17d. Profile of total ^{210}Pb activity versus depth in the sediment for core PB-5.

Table 14. Sedimentation rates, ^{210}Pb activities and ^{210}Pb flux rates to surface sediments for outer domain cores PB-4 and PB-5, June 1982. The 95% confidence intervals for sedimentation rates are enclosed in parentheses.

CORE	SURFACE ACTIVITY dpm g^{-1}	SUPPORTED ACTIVITY dpm g^{-1}	SUPPORT DEPTH cm	^{210}Pb FLUX RATE $\text{dpm cm}^{-2} \text{ yr}^{-1}$	SEDIMENTATION (95% INTERVAL) $\text{g m}^{-2} \text{ yr}^{-1}$
PB-4	6.53	0.71 ± 0.17	16.5	0.58	877 (729-1099)
PB-5	5.34	0.67 ± 0.03	11.5	0.50	706 (640-788)

be appropriate for the Bering Sea cores. The temperature of storage for the 1979 cores was only $\sim 0.5^{\circ}\text{C}$ higher than in situ (Table 13). The June 1982 cores were stored at air temperatures $2\text{--}3^{\circ}\text{C}$ higher than in situ. All cores were squeezed at $8\text{--}10^{\circ}\text{C}$, the temperature of the wet lab on the R/V THOMPSON, half of the temperature of processing in the Fanning and Pilson (1971) study. Their correction factor would likely underestimate the silicic acid concentrations of cores squeezed at lower temperatures. The uncorrected data is used with the caution that fluxes of silicic acid calculated using these concentrations represent upper limits.

Fick's First Law for the flux of a dissolved property through bulk sediment is;

$$J = -(P_o) (D_s) (dC/dZ) \quad 6$$

where J is the flux in $\mu\text{mol cm}^{-2} \text{ s}^{-1}$, Z is depth in cm, P_o is porosity, C is concentration in $\mu\text{mol cm}^{-3}$ and D_s is the bulk diffusion coefficient in $\text{cm}^2 \text{ s}^{-1}$ (Berner, 1980). The flux of silicic acid across the sediment-water interface can be approximated by;

$$J = -(P_o) (D_s) [(C_1 - C_o)/Z_1] \quad 7$$

The concentration of silicic acid in the top section is C_1 , the median depth of that section, Z_1 , and P_o is the average porosity of that section. The value of C_o is equal to the concentration of silicic acid in the overlying core water for Stations 2051 and 2057 or the deepest water column value measured for Stations PB-4 and PB-5.

The free solution diffusion coefficient, D_o , for silicic acid in seawater at 3°C is $5.0 \times 10^{-6} \text{ cm}^2 \text{ s}^{-1}$ (Wollast and Garrels, 1971). Aller and Benninger (1981) calculated a D_s equal to $5.4 \times 10^{-6} \text{ cm}^2 \text{ s}^{-1}$ at 4°C using the Stokes-Einstein equation (Li and Gregory, 1974). For marine muds with $P_o > 0.7$, Ulman and Aller (1982) approximate the bulk diffusion coefficient with the equation;

$$D_s = D_o (P_o)^{1.5} = (5.4 \times 10^{-6} \text{ cm}^2 \text{ s}^{-1}) (0.75)^{1.5} \quad 8$$

This value of D_s , $3.5 \times 10^{-6} \text{ cm}^2 \text{ s}^{-1}$, was used in my flux calculations.

Estimated fluxes from the four outer shelf cores range from 114 to $276 \text{ mmol m}^{-2} \text{ yr}^{-1}$ (Table 15), well within the estimates of both modeled and measured fluxes (Table 16). Tsunogai *et al.* (1979) state their estimated input of silicic acid from the sediments, $212 \text{ mmol m}^{-2} \text{ yr}^{-1}$ to the deep Bering Sea as equivalent to ~10% of the biogenic silica production in the surface layer. The mean value from the outer shelf, $200 \text{ mmol m}^{-2} \text{ yr}^{-1}$ represents 12% of the estimated annual uptake (or 16% of the spring-summer uptake).

First order dissolution coefficients for biogenic silica, k in s^{-1} , were calculated using an equation derived by Aller and Benninger (1981, see Table 15).

$$k = [J/P_o(C_e - C_o)]^2 (1/D_s) \quad 9$$

The J value was calculated using equation #7 and C_e is the asymptotic concentration of silicic acid in $\mu\text{mol cm}^{-3}$. In other formulations of the equations used to derive equation #7 (Hurd, 1972; Hurd, 1973; Wollast, 1974; Kamatani and Riley, 1979; Berner, 1980) C_e

Table 15. Silicic acid flux rate estimates and first order dissolution constants based on pore water gradients of silicic acid in outer domain cores PB-4 and PB-5, June 1982. Co is the concentration of silicic acid in the overlying seawater, Cl and Zl are the silicic acid concentration and mean depth of the top section of the core, k(Ce) is the first order constant using the asymptotic concentration and k(Cs) is the constant based on the saturation concentration of amorphous silica at 4°C in seawater. Po is porosity.

CORE	Po	Co	Cl	Zl	FLUX ^a	k(Ce) ^b	k(Cs) ^c
		umol cm ⁻³		cm	mmol m ⁻² yr ⁻¹	x 10 ⁻⁷ s ⁻¹	
2051	0.8*	0.042	0.234	1.5	114	2.2	0.62
2057	0.8*	0.060	0.374	1.5	186	6.4	1.7
PB-4	0.74	0.060	0.376	1.2	216	10.0	2.7
PB-5	0.80	0.060	0.420	1.1	276	14.0	3.8

$$\overline{\text{FLUX}} = 198 \pm 67 \text{ mmol m}^{-2} \text{ yr}^{-1}$$

$$\overline{k}(\text{Ce}) = 8.1 \times 10^{-7} \text{ s}^{-1}$$

$$\overline{k}(\text{Cs}) = 2.2 \times 10^{-7} \text{ s}^{-1}$$

* An estimated value based on the measured porosity of cores PB-4 and PB-5.

^a Calculated using a $D_s = 3.5 \times 10^{-6} \text{ cm}^2 \text{ s}^{-1}$.

^b $C_e = 0.550 \text{ umol cm}^{-3}$.

^c $C_s = 1.0 \text{ umol cm}^{-3}$.

Table 16. A summary of studies estimating or measuring the flux of silicic acid from sediments.

LOCATION	FLUX mmol m ⁻² yr ⁻¹	METHOD	REFERENCE
Deep Equatorial Pacific	41	Modeling pore water.	Hurd (1973)
North Atlantic	83-167	Measured in cores.	Fanning & Pilson (1974)
Deep Bering Sea	212	Modeled Si:O in deep water.	Tsunogai <u>et al.</u> (1979)
Galapagos Rift	142	Sediment traps and sedimentation rates.	Cobler & Dymond (1980)
Long Island Sound (winter)	285-402	Measured in cores.	Aller & Benninger (1981)
Deep Southeastern Pacific	109-439	Modeling pore water.	Wakefield (1982)
Deep Bering Sea	650	Modeling water column.	Toggweiler & Broecker (unpublished manuscript)
Outer Shelf, Bering Sea	114-276	Modeling pore water.	This study.

is actually Cs, the saturation concentration at a given temperature. I have calculated the first order constant both ways, with Cs set to $1.0 \mu\text{mol cm}^{-3}$ and Ce equal to $0.55 \mu\text{mol cm}^{-3}$. The k(Cs) values fall well within the range of constants compiled by Hurd (1973) and Lawson, Hurd and Pankratz (1978) for untreated diatom tests at 4°C. The k(Ce) values are within a factor of ten of those calculated for Long Island Sound sediments (Aller and Benninger, 1981), acid-cleaned Thalassiosira and Rhizosolenia tests (Kamatani and Riley, 1979) and North Sea sediments (Vanderborgh, Wollast and Billin, 1977).

It is not clear to me which formulation is really correct in terms of yielding real first order constants. However, I favor the k(Cs) formulation of equation #7 because these constants are closer to those of more rigorous dissolution studies (Lawson et al., 1978). Both k(Cs) and k(Ce) are based on a calculated flux from the top 2 cm and so represent upper limits.

A convention used to determine pseudo first order coefficients from the vertical distribution of a solid phase was applied to PB-4 and PB-5 amorphous silica data to determine long term dissolution coefficients (i.e., Johnson, Evans and Eisenreich, 1982; Kamatani and Riley, 1979). The relationship between the natural logarithm of solid concentration and the estimated average age of a section is assumed to be linear (Figure 18). The resulting slope is the first order rate constant. The average k for PB-4 and PB-5 was $2.8 \times 10^{-11} \text{ s}^{-1}$, ten times greater than k's for a deep Bering Sea core, $1.9-7.5 \times 10^{-12} \text{ s}^{-1}$ (Kamatani and Riley, 1979). However, the deep Bering Sea k's are based

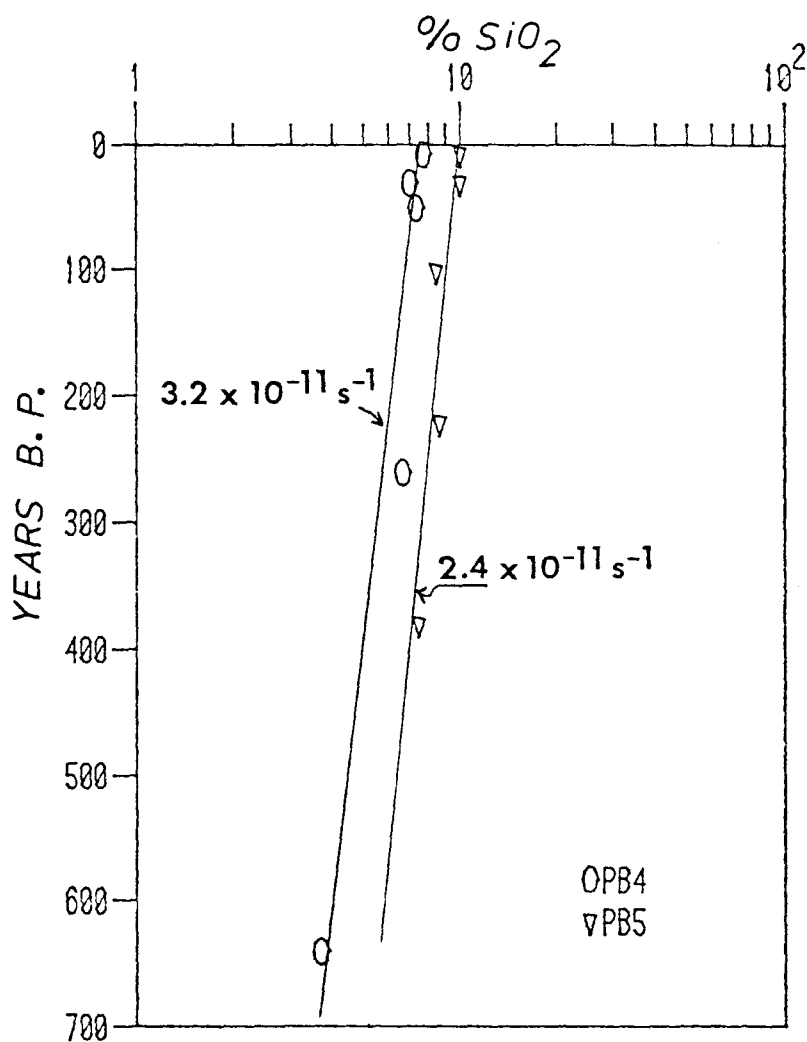


Figure 18. Percent amorphous silica content versus the estimated average age of each core section from the companion cores to PB-4 and PB-5. The lines are the linear least squares regressions with slopes equivalent to first order dissolution constants, k in s^{-1} .

on a core almost 900 cm long. I would expect a greater k for silica in the top 50 cm. Hurd (1973) showed that dissolution constants for biogenic silica in the sediments are 6-8 orders of magnitude less than ones measured for acid cleaned tests. The real sediment k values must then be 4-6 orders of magnitude less than untreated diatoms because fossil tests survive millions of years in the sedimentary record (Schink et al., 1975). Schink et al. (1975) cite T. C. Johnson's work with fossil silica, his k 's are 2.0 to $8.0 \times 10^{-9} \text{ s}^{-1}$. The outer shelf data is consistent with this, the average $k(\text{Cs}) = 2.2 \times 10^{-7} \text{ s}^{-1}$ and the k based on the decrease in core silica = $2.8 \times 10^{-11} \text{ s}^{-1}$.

The Deposition of Carbon and Silica

The similarity among the C, Si and N profiles suggests the section to section variation is a depositional feature, while the overall decrease in all three elements is the result of early diagenesis (Berner, 1980). The deposition rates in Table 17 are meant as approximations to material buried after reactions at the sediment-water interface and now subject to diagenesis.

The recent deposition of silica and carbon is estimated by multiplying the ^{210}Pb sedimentation rate by the $\% \text{SiO}_2$ and $\% \text{C}$ content in the top 2-cm section. The percent biogenic silica in the surface sediments was $\sim 7.5\%$ at PB-4 and 9-10% at PB-5. These values are within the limits of Lisitzin's (1972) global distribution map ($<10\% \text{SiO}_2$). My values for $\% \text{C}$ and $\% \text{N}$ are somewhat higher than those of earlier studies (Lisitzin, 1969; Gardner, Dean and Vallier, 1980). However, surface

Table 17. Data used to estimate the accumulation rate of particulate organic carbon (ACCUM C) and biogenic silica (ACCUM Si) in outer shelf sediments. Percent carbon and silica listed are those measured values from the top section of each core. In one calculation the flux of silicic acid (DISS Si) is subtracted from silica accumulation as a lower limit estimate of burial.

CORE	SEDIMENTATION $\text{g m}^{-2} \text{yr}^{-1}$	%C	ACCUM C $\text{g m}^{-2} \text{yr}^{-1}$	BURIED PRODUCED ^a	%SiO ₂	ACCUM Si $\text{mol m}^{-2} \text{yr}^{-1}$	BURIED PRODUCED	ACCUM-DISS PRODUCED ^b
PB-4	877	0.9	7.9	0.040	7.5	1.10	0.67	0.54 ^c
PB-5	706	1.1	7.7	0.038	9.0	1.05	0.64	0.47 ^d

^a Carbon production = $200 \text{ g m}^{-2} \text{yr}^{-1}$.

^b Silica production = $1.64 \text{ mol m}^{-2} \text{yr}^{-1}$.

^c Dissolved flux = $216 \text{ mmol m}^{-2} \text{yr}^{-1}$.

^d Dissolved flux = $276 \text{ mmol m}^{-2} \text{yr}^{-1}$.

sediments from five outer shelf locations (along the A-line) were analyzed for organic C (acid treated) and N. The results were %C = 1.14 (SD = 0.07) and %N = 0.14 (SD = 0.02) (R. Iverson, unpublished data). Based on the figures in Table 17, as much as 50% of silicic acid uptake and <4% of the carbon uptake becomes buried in the surface sediments.

The silica buried is equivalent to 50% of outer shelf uptake, but it is not clear that what becomes incorporated in the outer shelf sediments originates in outer shelf surface water. Half or more of the outer shelf diatoms are thinly silicified Chaetoceros and Rhizosolenia species (Kocur, 1982). Yet these two genera are not found in great numbers in the sediments (Sancetta, 1981a). The outer shelf sediments contain a mixture of coastal, middle shelf, outer shelf and oceanic species (Sancetta, 1981a and 1981b; Oshite and Sharma, 1974).

Lisitzin (1969) suggests that more heavily silicified neritic and oceanic diatoms have a 10-50% "survival" rate at depths up to 500 m. High interstitial silicic acid and a high sedimentation rate tend to enhance the preservation of recently buried tests (Lewin, 1961). Most of the research looking at remineralization of biogenic silica versus burial has been conducted at locations with bottom depths of 1000-5000 m. Results from these studies show that 80-99% of the surface produced silica dissolves before reaching the sea floor (Hurd, 1973; Heath, 1974; Cobler and Dymond, 1980). In shallower systems like the outer shelf, a higher "survival" rate than that in the deep ocean can be expected. Direct measurements in the Antarctic Southern Ocean show

that 18-55% of the surface produced silica dissolves in the top 100 m (Nelson and Gordon, 1982).

The low rate of regeneration of water column silica in the Peru upwelling system is attributed to the ingestion and eventual packing of diatom tests into fast sinking fecal pellets (Nelson et al., 1981). Large membrane-enclosed fecal pellets physically retard dissolution and accelerate sinking. Schrader's (1971) work with Calanus finmarchicus in the Baltic Sea showed that diatom tests, especially those of larger species of Thalassiosira, sink to the sediments intact in fecal pellets. Members of the genus Chaetoceros are crushed before excretion so once the pellet breaks apart, dissolution is accelerated. Barring horizontal advection, grazing in conjunction with microbial degradation, seems a good explanation for the relatively high deposition of silica and low deposition of particulate organic carbon. Griffiths et al. (1983) measured methane and carbon dioxide production, glutamate uptake and nitrogen fixation (processes associated with microbial activity) in sediments near PB-5. Some of the rates are comparable to those measured in temperate and tropical sediments.

The wet chemical analysis of amorphous silica may overestimate the biogenic silica content. Past volcanic activity on the Aleutian Chain has sprayed ash, including volcanic glass (opal) over the PROBES study area (Lisitzin, 1969). However, even if values are in error by 50%, silica is still being deposited in excess of organic carbon. This high silica deposition may constitute an argument against the advection

of biological material, specifically carbon, off the Bering Shelf (Walsh et al., 1981; Walsh, Premuzic and Whitledge, 1981).

High silica deposition does not, however, argue against advection of biogenic silica onto the outer shelf or concentrating outer shelf silica onto a smaller area. The first ~2 m of outer shelf sediments are contemporary, consisting of Bristol Bay detritus, Kuskokwim drainage suspensions and weathered material from the Alaska Peninsula and Aleutian coast (Sharma, Naidu and Hood, 1972; Sharma, 1974). The distribution of heavy minerals suggests east and north movement of sediment along, and from, the Aleutians (Sharma, 1974). Silt shoreward of the 100 m isobath can be resuspended during winter storms and eventually deposited on the deeper outer shelf. Greater concentrations of diatom frustules are found in sediments beyond the 100-m isobath (Oshite and Sharma, 1974). Analysis of direct current measurements by Schumacher and Kinder (1982, in press) indicates that though energy in the middle shelf and coastal zones is >90% tidal, storm driven (subtidal) currents can have short term speeds of $8-20 \text{ cm s}^{-1}$. Sharma (1974) suggests that storm induced long waves are capable of setting sediment in motion at water depths up to 94 m.

The steady state budget for biogenic silica proposed by Hurd (1973) to estimate water column dissolution is;

$$\begin{aligned} \text{BIOGENIC SILICA PRODUCED} - \text{SILICA BURIED} = & 10 \\ \text{FLUX FROM SEDIMENTS} + \text{WATER COLUMN DISSOLUTION} \end{aligned}$$

My estimate for the amount of silica incorporated into outer shelf surface sediment is based on an average concentration of the top 2 cm. Most of the dissolution at the sediment-water interface may have already occurred. The calculation was done two ways: a) with the SILICA BURIED - FLUX FROM SEDIMENTS term set equal to the mean burial at 2 cm, and b) subtracting the estimated flux from the 2 cm burial rate. Substituting experimental values, equation 10 becomes:

$$\begin{aligned} \text{a) } & 1.64 \text{ mol m}^{-2} \text{ yr}^{-1} \text{ PRODUCED} - 1.05 \text{ mol m}^{-2} \text{ yr}^{-1} \text{ BURIED} = \\ & \quad 0.59 \text{ mol m}^{-2} \text{ yr}^{-1} \text{ DISSOLVED} \\ \text{b) } & 1.64 \text{ PRODUCED} - (1.05 \text{ BURIED} - 0.2 \text{ FLUX}) = \\ & \quad 0.39 \text{ DISSOLVED.} \end{aligned}$$

Roughly 24-36% of the silica produced in the surface dissolves in the water column before burial in the outer shelf. These percentages are within the range, but with a lower limit, of those quoted for the top 100 m of the Antarctic Southern Ocean (Nelson and Gordon, 1982). This budget is summarized in Figure 19.

Total biogenic silica deposition for the entire Bering Sea is estimated to be $2.8 \times 10^{13} \text{ g SiO}_2 \text{ yr}^{-1}$ (DeMaster, 1981). Based on the figures used in the budget, a conservative estimate of total outer shelf deposition is:

$$\begin{aligned} & (1.05 - 0.2 \text{ mol m}^{-2} \text{ yr}^{-1}) (60 \text{ g mol}^{-1}) (4.2 \times 10^{10} \text{ m}^2) = \\ & \quad 2.1 \times 10^{12} \text{ g SiO}_2 \text{ yr}^{-1}. \end{aligned}$$

This is equal to 7.5% of the total estimated accumulation. DeMaster's figure is based on a rate of silica accumulation = $3.83 \text{ mol m}^{-2} \text{ yr}^{-1}$ assumed for half the Bering Sea area.

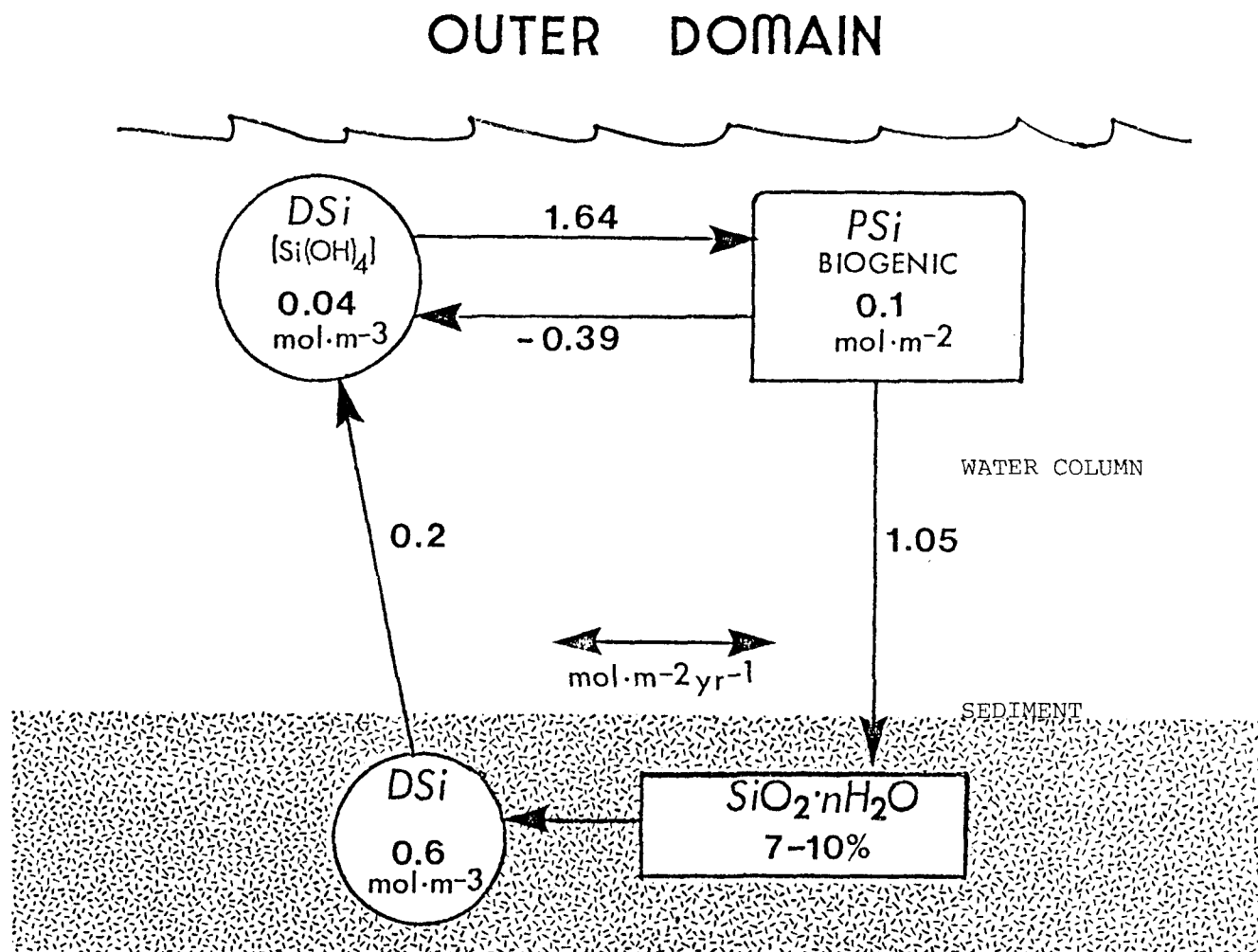


Figure 19. Summary of the biogenic silica budget for the outer domain of the Bering Shelf. The pools indicated are dissolved Si as silicic acid (DSi) and particulate biogenic Si or amorphous Si (PSi); characteristic concentrations are given for each pool. The arrows show the direction and magnitude of Si flux between pools.

CHAPTER IV. SUMMARY, CONCLUSIONS AND RECOMMENDATIONS

This study was composed of two parts; one examining some physiological aspects of silicic acid uptake by diatoms and the other quantifying the inorganic processes and pools of the biogenic silica cycle. Studying the production of biogenic silica involved the direct measurement of silicic acid uptake and the standing stock of diatoms as silica in the euphotic layer. This information was used to describe the vertical and cross-shelf distributions of specific uptake and biogenic silica. Estimates of diatom production as silica and as carbon were made. Factors influencing silicic acid uptake, such as light, water column stability and silicic acid availability were also discussed.

The second part of this study dealt with the fate of biogenic silica after its production. Sediment accumulation, silica content in the sediments and the concentration of silicic acid in outer shelf pore waters were combined to yield estimates of silica burial and dissolution. The synthesis of both parts is a first attempt at quantifying the cycle of biogenic silica on the southeastern Bering Sea shelf.

The distribution of biogenic silica across the Bering Sea shelf reflects the difference in grazing pressure between the well defined hydrographic and biological domains as described by PROBES investigators (Cooney and Coyle, 1982; Dagg et al., 1982; Vidal and Smith, unpublished manuscript). The large copepods of the outer shelf effectively lower particulate silicon concentrations to less than one third those in the relatively ungrazed middle shelf. As specific uptake

velocities are essentially the same in all domains and through most of the bloom period, grazing is probably the major factor influencing the cross-shelf distribution of silica.

The specific uptake rates of silicic acid generally decreased below the 15% SPAR depth. These deeper rates were probably representative of night rates. Although increasing light tended to increase silicic acid uptake, the short term light reductions of night or reductions brought about by moderate wind mixing did not always result in decreased specific uptake.

The occurrence of silicic acid limitation in the middle and coastal domains is confirmed by the Michaelis-Menten response observed in silicic acid kinetic experiments. However, as an influence on the elemental composition of diatom phytoplankton, nitrogen seems the dominant type of nutrient limitation.

The combination of estimated biogenic silica production and a C:Si ratio based on absolute uptake data, resulted in an annual carbon production rate in close agreement with the ^{14}C estimate in the middle shelf. Unfortunately, so few silicic acid uptake experiments were done in the outer shelf that the value for annual silica production in that area is crude at best.

Despite the low specific uptake rates, the Bering Shelf maintains relatively high integrated concentrations of particulate silicon; higher than the Peru, northwest Africa and Baja California upwelling systems. The greater initial silicic acid concentrations in the prebloom shelf waters allow for potentially high accumulations of diatom biomass.

After production, diatom tests sink by passive settling in the middle shelf and inclusion in fecal material in the outer shelf. The sediments in the outer domain are 7-9% amorphous silica (presumed biogenic) and 1-2% combined organic carbon and nitrogen. If biogenic material is not advected on to or away from the outer shelf then up to 50% of the silica production and less than 4% of the carbon production is deposited in surface sediments.

The simple Fickian diffusion model applied to the gradients measured in interstitial silicic acid indicates fluxes equivalent to 12% of the surface production. The mass balance of silica produced, silica buried and silicic acid input from the sediments suggests that ~30% of the surface production dissolves in the water column before burial. This approximate dissolution rate is within the range observed in the Antarctic Southern Ocean (Nelson and Gordon, 1982).

A List of Study Results

1. Specific uptake velocities (V_o) of silicic acid in the upper 10 m of the southeastern Bering Sea shelf range from 0.005 to 0.015 h^{-1} , with rates decreasing sharply below the 15% light depth. No significant differences in integrated specific uptake were observed between the coastal, middle and outer domains.
2. Average integrated concentration of particulate silicon on the middle shelf was 300-400 mmol Si m^{-2} and 100 mmol Si m^{-2} on the outer shelf.

3. Silicic acid uptake in the middle and coastal domains is accurately modeled by the Michaelis-Menten kinetic equation. The mean kinetic constants from six experiments are $K_s = 3.2 \mu\text{M}$ and $V_{\text{max}} = 0.009 \text{ h}^{-1}$.
4. The estimated annual production of biogenic silica on the middle shelf is $2.87 \text{ mol Si m}^{-2} \text{ yr}^{-1}$, equivalent to $220 \text{ g C m}^{-2} \text{ yr}^{-1}$. Annual silica production on the outer shelf is $1.64 \text{ mol Si m}^{-2} \text{ yr}^{-1}$ or $126 \text{ g C m}^{-2} \text{ yr}^{-1}$.
5. The sedimentation rate in the outer domain is $700\text{--}877 \text{ g m}^{-2} \text{ yr}^{-1}$; 7-10% of this material is amorphous silica.
6. Pore waters of outer domain sediments are highly enriched in silicic acid compared to the water column. Diffusive fluxes of silicic acid from surface sediments, based on concentration gradients in the upper 3 cm, are $114\text{--}276 \text{ mmol m}^{-2} \text{ yr}^{-1}$, equivalent to ~12% of the surface silica production. The estimated first order silica dissolution constants (k) are on the order of 10^{-7} s^{-1} in surface sediments and 10^{-11} s^{-1} in deeper sections.
7. Neglecting advection of silica into the outer domain, up to 50% of the surface production is incorporated in the sediments and an estimated 24-36% dissolves in the water column before burial.

Recommendations for Further Study

Estimating whole population primary production is probably best done using the ^{15}N or ^{14}C methods. The ^{30}Si method is relatively time consuming, requiring wet chemical processing before actual isotope

analysis. The value of the silicic acid method is in its ability to partition diatom productivity from the whole population productivity. Outer shelf zooplankton feed largely on diatoms. Determining the amount of carbon produced by diatoms would help quantify the carbon transfer efficiency from the primary to the secondary producers. More ^{30}Si experimentation in conjunction with experiments using germanic acid as an inhibitor of diatom productivity (Thomas, Dodson and Reid, 1978; Davies, Sleep and Harbour, 1982) could establish the proportions of diatom and Pheocystis productivity in the outer shelf.

A flaw in this study was my choosing not to extend the sampling depths for particulate silicon to the bottom. The whole water column distribution of silica might give a clearer indication as to whether diatoms were actually sinking more or less directly to the bottom or being advected off-shelf. Sediment traps deployed at mid depth and near the outer shelf bottom would provide information about the amounts of silica sinking (in addition to organic C and N) for comparison with its estimated accumulation in surface sediments. This data could also be used as another estimate of silica dissolution in the water column.

Further study should be directed at determining the sedimentation rates in the area of the outer front and beyond the shelf break. Repeating the sediment analyses done in this study might quantify how much silica is going to the bottom and where it is being deposited. The wet chemical method for measuring silica cannot distinguish

between biogenic silica and volcanic opal. A microscopic method to visually estimate the content of diatom tests and volcanic opal should be done.

A method for measuring the dissolution of silica is detailed in Nelson (1975) and Nelson and Goering (1975). Dissolution experiments were done in the euphotic layer and at depth intervals down to the bottom. No reliable data resulted because of problems I experienced with the procedure for precipitating the analyte, barium hexafluorosilicate. This procedure has been modified (D. Nelson, personal communication) and dissolution rates may come from the processing of remaining samples. Successful dissolution experiments may help support the proposed idea of reduced water column dissolution in the outer shelf through grazing.

LITERATURE CITED

- Alexander, G. B. 1954. Polymerization of monosilicic acid. J. Am. Chem. Soc. 76(2):2094-97.
- Aller, R. C. and L. K. Benninger. 1981. Spatial and temporal patterns of dissolved ammonium, manganese and silica fluxes from bottom sediments of Long Island Sound, U.S.A. J. Mar. Res. 39(2):295-314.
- Armstrong, F. A. J., C. R. Stearns and J. D. H. Strickland. 1967. The measurement of upwelling and subsequent biological processes by means of the Technicon AutoAnalyzer and associated equipment. Deep-Sea Res. 14:381-389.
- Azam, F. and S. W. Chisholm. 1976. Silicic acid uptake and incorporation by natural marine phytoplankton populations. Limnol. Oceanogr. 21(3):427-435.
- Banse, K. 1977. Determining the carbon-to-chlorophyll ratio of natural phytoplankton. Mar. Biol. 41:199-212.
- Barber, R. T. 1977. The JOINT-1 expedition of the Coastal Upwelling Ecosystems Analysis Program. Deep-Sea Res. 24(1):1-6.
- Berner, R. A. 1980. Early Diagenesis. Princeton University Press, Princeton, N. J.
- Beynon, J. H., R. A. Saunders and A. E. Williams. 1968. The Mass Spectra of Organic Molecules. Elsevier Publishing Co., N. Y.
- Binder, B. J. and S. W. Chisholm. 1980. Changes in the soluble silicon pool size in the marine diatom Thalassiosira weissflogii. Mar. Biol. Lett. 1:205-212.
- Bishop, J. K. B., J. M. Edmond, D. R. Ketten, M. P. Bacon and W. R. Silker. 1977. The chemistry, biology and vertical flux of particulate matter from the upper 400 m of the equatorial Atlantic Ocean. Deep-Sea Res. 24:511-548.
- Broecker, W. S. and T.-H. Peng. 1982. Tracers in the Sea. Eldigio Press, Columbia University, N. Y.
- Cleland, W. W. 1967. The statistical analysis of enzyme kinetic data. Adv. Enzymol. 29:1-32.
- Coachman, L. K. 1982a. Ramblings on sea shelf fronts, with special references to the Bering Sea. p. 34-58. In: Processes and Resources of the Bering Sea Shelf, Vol. II, 1981. University of Alaska, Fairbanks. 785 p.

- Coachman, L. K. 1982b. Flow convergence over a broad, flat continental shelf. Continental Shelf Res. 1(1):1-14.
- Coachman, L. K. and R. L. Charnell. 1979. On lateral water mass interaction - A case study, Bristol Bay, Alaska. J. Phys. Oceanogr. 9(2):278-297.
- Coachman, L. K. and J. J. Walsh. 1981. A diffusion model of cross-shelf exchange of nutrients in the southeastern Bering Sea. Deep-Sea Res. 28(8A):819-846.
- Cobler, R. and J. Dymond. 1980. Sediment trap experiment on the Galapagos Spreading Center, equatorial Pacific. Science 209: 801-803.
- Codispoti, L. A., G. E. Friederich, R. L. Iverson and D. W. Hood. 1982. Temporal changes in the inorganic carbon system of the southeastern Bering Sea during spring 1980. Nature 296:242-245.
- Conover, S. A. M. 1975a. Partitioning of nitrogen and carbon in cultures of the marine diatom Thalassiosira fluviatilis supplied with nitrate, ammonia or urea. Mar. Biol. 32:231-246.
- Conover, S. A. M. 1975b. Nitrogen utilization during spring blooms of marine phytoplankton in Bedford Basin, Nova Scotia, Canada. Mar. Biol. 32:247-261.
- Conway, H. L., P. J. Harrison and C. O. Davis. 1976. Marine diatoms grown in chemostats under silicate or ammonium limitation. II. Transient response of Skeletonema costatum to a single addition of the limiting nutrient. Mar. Biol. 35:187-199.
- Cooney, R. T. 1981. Bering Sea zooplankton and micronekton communities with emphasis on annual production. p. 947-974. In: D. W. Hood and J. A. Calder (eds.), The Eastern Bering Sea Shelf: Oceanography and Resources, Vol. II. University of Washington Press, Seattle.
- Cooney, R. T. and K. O. Coyle. 1982. Trophic implications of cross-shelf copepod distributions in the southeastern Bering Sea. Mar. Biol. 70:187-196.
- Cooper, L. H. N. 1933. Chemical constituents of biological importance in the English Channel, November, 1930 to January, 1932. Part I. Phosphate, silicate, nitrate, nitrite, ammonia. Mar. Biol. Assoc. U. K. 18:677-728.

- Dagg, M. J., J. Vidal, T. E. Whitledge, R. L. Iverson and J. J. Goering. 1982. The feeding, respiration and excretion of zooplankton in the Bering Sea during a spring bloom. Deep-Sea Res. 29(1A):43-63.
- Darley, W. M. 1974. Silicification and calcification, p. 655-675. In: W. D. P. Stewart (ed.), Algal Physiology and Biochemistry. Botanical Monographs No. 10, University of California Press, Berkeley.
- Darley, W. M. and B. E. Volcani. 1971. Synchronized cultures: diatoms. In: A. San Pietro (ed.), Methods in Enzymology. Vol. 23A, Photosynthesis. Academic Press, New York.
- Davies, A. G., J. A. Sleep and D. S. Harbour. 1982. Germanic acid inhibition of carbon fixation in natural phytoplankton assemblages. Limnol. Oceanogr. 27(2):357-361.
- Davis, C. O., N. F. Breitner and P. J. Harrison. 1978. Continuous culture of marine diatoms under silicon limitation. 3. A model of Si-limited diatom growth. Limnol. Oceanogr. 23(1):41-53.
- DeMaster, D. J. 1981. The supply and accumulation of silica in the marine environment. Geochim. Cosmochim. Acta 45:1715-1732.
- Dugdale, R. C. 1972. Chemical oceanography and primary productivity in upwelling regions. Geoforum 11:47-61.
- Edmond, J. M., S. S. Jacobs, A. L. Gordon, A. W. Mantyla and R. F. Weiss. 1979. Water column anomalies in dissolved silica over opaline pelagic sediments and the origin of the deep silica maximum. J. Geop. Res. 84(C12):7809-7826.
- Eggiman, D. W., F. T. Manheim and P. R. Betzer. 1980. Dissolution and analysis of amorphous silica in marine sediments. J. Sed. Pet. 50(1):215-225.
- Emerson, S., R. Jahnke, M. Bender, P. Froelich, G. Klinkhammer, C. Bowser and G. Setlock. 1980. Early diagenesis in sediments from the eastern equatorial Pacific, I. Pore water nutrient and carbonate results. Earth Planet. Sci. Lett. 49:57-80.
- Eppley, R. W. 1977. The growth and culture of diatoms. p. 24-64. In: D. Werner (ed.), The Biology of Diatoms. Botanical Monographs No. 13. University of California Press, Berkeley.
- Eppley, R. W., E. H. Renger and W. G. Harrison. 1979. Nitrate and phytoplankton production in souther California coastal waters. Limnol. Oceanogr. 24(3):483-494.

- Eppley, R. W. and J. D. H. Strickland. 1968. Kinetics of marine phytoplankton growth. p. 23-62. In: M. Droop and E. Ferguson (eds.), Advances in Microbiology of the Sea. Vol. I. Academic Press, New York.
- Fanning, K. A. and M. E. Q. Pilson. 1971. Interstitial silica and pH in marine sediments: some effects of sampling procedures. Science 173:1228-1231.
- Fanning, K. A. and M. E. Q. Pilson. 1974. The diffusion of dissolved silica out of deep-sea sediments. J. Geophys. Res. 79(9):1293-1297.
- Friederich, G. E. and L. A. Codispoti. 1979. On some factors influencing dissolved silicon distribution over the northwest African shelf. J. Mar. Res. 37(2):337-353.
- Gardner, J. V., W. E. Dean and T. L. Vallier. 1980. Sedimentology and geochemistry of surface sediments, outer continental shelf, southern Bering Sea. Mar. Geol. 35:299-329.
- Goering, J. J. and R. L. Iverson. 1979. Primary production, and composition. p. 203-240. In: Processes and Resources of the Bering Sea Shelf. Progress Report, PROBES Phase I, 1977-1978. University of Alaska, Fairbanks. 488 p.
- Goering, J. J. and R. L. Iverson. 1981. Phytoplankton distribution in the southeastern Bering Sea Shelf. p. 933-946. In: D. W. Hood and J. A. Calder (eds.), The Eastern Bering Sea Shelf: Oceanography and Resources, Vol. II. University of Washington Press, Seattle.
- Goering, J. J., D. M. Nelson and J. A. Carter. 1973. Silicic acid uptake by natural populations of marine phytoplankton. Deep-Sea Res. 20:777-789.
- Goldman, J. C., J. J. McCarthy and D. G. Peavey. 1979. Growth rate influence on chemical composition of phytoplankton in oceanic waters. Nature 279(5710):210-215.
- Griffiths, R. P., B. A. Caldwell, W. A. Broich and R. Y. Morita. 1983. Microbial processes relating to carbon cycling in southeastern Bering Sea sediments. Mar. Ecol. Prog. Ser. 10:265-275.
- Haflinger, K. 1981. A survey of benthic infaunal communities of the southeastern Bering Sea. p. 1091-1103. In: D. W. Hood and J. A. Calder (eds.), The Eastern Bering Sea Shelf: Oceanography and Resources, Vol. II. University of Washington Press, Seattle.

- Harrison, P. J., H. L. Conway and R. C. Dugdale. 1976. Marine diatoms grown in chemostats under silicate or ammonium limitation. I. Cellular chemical composition and steady-state growth kinetics of Skeletonema costatum. Mar. Biol. 35:177-186.
- Harrison, P. J., H. L. Conway, R. W. Holmes and C. O. Davis. 1977. Marine diatoms grown in chemostats under silicate or ammonium limitation. III. Cellular chemical composition and morphology of Chaetoceros debilis, Skeletonema costatum and Thalassiosira gravida. Mar. Biol. 43:19-31.
- Heath, G. R. 1974. Dissolved silica and deep-sea sediments. p. 77-93. In: W. W. Hay (ed.), Studies in Paleo-Oceanography. Soc. Econ. Paleontologists and Mineralogists Spec. Pub. No. 20, Tulsa.
- Honjo, S., S. J. Manganini and J. C. Cole. 1982. Sedimentation of biogenic matter in the deep ocean. Deep-Sea Res. 29(5A):609-625.
- Huheey, J. E. 1972. Inorganic Chemistry: Principles of Structures and Reactivity. Harper and Row, Publishers, New York.
- Hurd, D. C. 1972. Factors affecting solution rate of biogenic opal in seawater. Earth Planet. Sci. Lett. 15:411-417.
- Hurd, D. C. 1973. Interactions of biogenic opal, sediment and seawater in the central equatorial Pacific. Geochim. Cosmochim. Acta 37:2257-2282.
- Iverson, R. L., L. K. Coachman, R. T. Cooney, T. S. English, J. J. Goering, G. L. Hunt, Jr., M. C. Macauley, C. P. McRoy, W. S. Reeburgh and T. E. Whitledge. 1979. Ecological significance of fronts in the southeastern Bering Sea. p. 437-466. In: R. J. Livingston (ed.), Ecological Processes in Coastal and Marine Systems. Marine Science Series No. 10, Plenum Press, New York.
- Jahnke, R., D. Heggie, S. Emerson and V. Grundmanis. 1982. Pore waters of the central Pacific Ocean: Nutrient results. Earth Planet. Sci. Lett. 61:233-256.
- Johnson, T. C. 1976. Controls on the preservation of biogenic opal in sediments of the eastern tropical Pacific. Science 192:887-890.
- Johnson, T. C., J. E. Evans and S. J. Eisenreich. 1982. Total organic carbon in Lake Superior sediments: comparisons with hemipelagic and pelagic marine environments. Limnol. Oceanogr. 27(3):481-491.
- Kamatani, A. and J. P. Riley. 1979. Rate of dissolution of diatom silica walls in seawater. Mar. Biol. 55:29-35.

- Kinder, T. H. 1981. A perspective of physical oceanography in the Bering Sea, 1979. p. 5-14. In: D. W. Hood and J. A. Calder (eds.), The Eastern Bering Sea Shelf: Oceanography and Resources, Vol. I. University of Washington Press, Seattle.
- Kinder, T. H. and J. D. Schumacher. 1981a. Hydrographic structure over the continental shelf of the southeastern Bering Sea. p. 31-52. In: D. W. Hood and J. A. Calder (eds.), The Eastern Bering Sea Shelf: Oceanography and Resources, Vol. I. University of Washington Press, Seattle.
- Kinder, T. H. and J. D. Schumacher. 1981b. Circulation over the continental shelf of the southeastern Bering Sea. p. 53-75. In: D. W. Hood and J. A. Calder (ed.), The Eastern Bering Sea Shelf: Oceanography and Resources, Vol. I. University of Washington Press, Seattle.
- Kipphut, G. W. 1978. An investigation of sedimentary processes in lakes. Ph.D. thesis, Columbia University. 179 p.
- Koblentz-Mishke, O. J., V. V. Volkovinski and J. C. Kabanova. 1970. Plankton primary production of the world ocean. p. 183-193. In: W. Wooster (ed.), Scientific Exploration of the South Pacific. Nat. Acad. Sc., Washington, D. C.
- Kocur, C. 1982. Phytoplankton distribution in southeastern Bering Sea shelf waters during spring. M.S. thesis, Florida State University. 47 pp.
- Lawson, D. S., D. C. Hurd and H. S. Pankrantz. 1978. Silica dissolution rates of decomposing phytoplankton assemblages at various temperatures. Am. J. Sci. 278:1373-1393.
- Lewin, J. C. 1961. The dissolution of silica from diatom walls. Geochim. Cosmochim. Acta 21:182-198.
- Lewin, J. C. 1962. Silicification. p. 445-455. In: R. A. Lewin (ed.), Physiology and Biochemistry of Algae. Academic Press, New York.
- Lewin, J. C. and B. E. F. Reimann. 1969. Silicon and plant growth. Ann. Rev. Plant Physiol. 20:289-304.
- Li, Y. -H. and S. Gregory. 1974. Diffusion of ions in sea water and in deep-sea sediments. Geochim. Cosmochim. Acta 38:703-714.
- Lisitsyn (Lisitzin), A. P. 1969. Recent Sedimentation in the Bering Sea. Israel Program for Scientific Translations, Jerusalem.

- Lisitzin, A. P. 1972. Sedimentation in the World Ocean. Soc. Econ. Paleontologists and Mineralogists Spec. Pub. No. 17, Tulsa.
- MacIsaac, J. J. and R. C. Dugdale. 1972. Interactions of light and inorganic nitrogen in controlling nitrogen uptake in the sea. Deep-Sea Res. 19:209-232.
- Mackenzie, F. T. and R. M. Garrels. 1965. Silicates: reactivity with sea water. Science 150:57-78.
- Mackenzie, F. T., R. M. Garrels, O. P. Bricker and F. Bickley. 1967. Silica in seawater: control by silica minerals. Science 155: 1404-1405.
- McCarthy, J. J. and J. C. Goldman. 1979. Nitrogenous nutrition of marine phytoplankton in nutrient-depleted waters. Science 203: 670-672.
- Mechling, J. A. and S. S. Kilham. 1982. Temperature effects on silicon limited growth of the Lake Michigan diatom Stephanodiscus minutus (Bacillariophyceae). J. Phycol. 18:199-205.
- Nelson, D. M. 1975. Uptake and regeneration of silicic acid by marine phytoplankton. Ph.D. thesis, University of Alaska. 157 p.
- Nelson, D. M. and H. Lee Conway. 1979. Effects of light regime on nutrient assimilation by phytoplankton in the Baja California and northwest Africa upwelling systems. J. Mar. Res. 32(2): 301-318.
- Nelson, D. M. and J. J. Goering. 1977a. A stable isotope method to measure silicic acid uptake by marine phytoplankton. Anal. Biochem. 78:139-147.
- Nelson, D. M. and J. J. Goering. 1977b. Near-surface silica dissolution in the upwelling region off northwest Africa, 1977. Deep-Sea Res. 24:65-73.
- Nelson, D. M. and J. J. Goering. 1978. Assimilation of silicic acid by phytoplankton in the Baja, California and northwest Africa upwelling systems. Limnol. Oceanogr. 23(3):508-517.
- Nelson, D. M., J. J. Goering and D. W. Boisseau. 1981. Consumption and regeneration of silicic acid in three coastal upwelling systems. p. 242-256. In: F. A. Richards (ed.), Coastal Upwelling. Coastal and Estuarine Sci. No. 1, Amer. Geophys. Union, Washington, D. C.

- Nelson, D. M. and L. I. Gordon. 1982. Production and pelagic dissolution of biogenic silica in the Southern Ocean. Geochim. Cosmochim. Acta 46:491-501.
- Niebauer, H. J. 1982. PROBES: Processes and Resources of the Bering Sea Shelf Data Report PDR 82-007, Weather Data for PROBES Cruises 1978-1981. University of Alaska, Fairbanks.
- Niebauer, H. J., C. P. McRoy, J. J. Goering and R. L. Iverson. 1982. PROBES: Processes and Resources of the Bering Sea Shelf Data Report PDR 82-009, 1978-1981 Productivity Data. University of Alaska, Fairbanks. 225 p.
- Oshite, K. and G. D. Sharma. 1974. Distribution of recent diatoms on the eastern Bering Shelf. p. 541-552. In: D. W. Hood and E. J. Kelley (eds.), Oceanography of the Bering Sea. Occasional Pub. No. 2, University of Alaska, Fairbanks.
- Paasche, E. 1973a. Silicon and the ecology of marine plankton diatoms. I. Thalassiosira pseudonana (Cyclotella nana) grown in a chemostat with silicate as a limiting nutrient. Mar. Biol. 19:117-126.
- Paasche, E. 1973b. Silicon and the ecology of marine plankton diatoms. II. Silicate-uptake kinetics in five diatom species. Mar. Biol. 91:262-269.
- Paasche, E. 1980. Silicon content of five marine plankton diatom species measured with a rapid filter method. Limnol. Oceanogr. 25(3):474-480.
- Paasche, E. and I. Ostergren. 1980. The annual cycle of plankton diatom growth and silica production in the inner Oslofjord. Limnol. Oceanogr. 25(30):481-494.
- Reeburgh, W. S. 1967. An improved interstitial water sampler. Limnol. Oceanogr. 12:163-165.
- Reeburgh, W. S. and T. E. Whitledge. 1981. Nutrient dynamics and distribution in the southeast Bering Sea. p. 121-160. In: Processes and Resources of the Bering Sea Shelf. Progress Report, 1980, Vol. I. University of Alaska, Fairbanks. 456 p.
- Reeburgh, W. S. and T. E. Whitledge. 1982. Nutrient dynamics and distribution in the southeast Bering Sea. p. 93-128. In: Processes and Resources of the Bering Sea Shelf. Progress Report, 1981, Vol. I. University of Alaska, Fairbanks. 379 p.
- Rhee, G. -Yull. 1978. Effects of N:P atomic ratios and nitrate limitation on algal growth, cell composition and nitrate uptake. Limnol. Oceanogr. 23(1):10-25.

- Ricker, W. E. 1973. Linear regressions in fishery research. J. Fish. Board Can. 30:409-434.
- Robbins, J. A. 1978. Geochemical and geophysical applications of radioactive lead. p. 287-393. In: J. Nriagu (ed.), The Biogeochemistry of Lead in the Environment. Elsevier, Amsterdam.
- Russell-Hunter, W. D. 1970. Aquatic Productivity. Macmillan Pub. Co., Inc., New York.
- Sambrotto, R. N. and J. J. Goering. 1981. Some aspects of the pelagic springtime ecosystem over the southeastern Bering Sea. p. 487-522. In: Processes and Resources of the Bering Sea Shelf. Progress Report, 1980, Vol. II. University of Alaska, Fairbanks. 668 p.
- Sambrotto, R. N., H. J. Niebauer, R. L. Iverson and J. J. Goering. 1983. Water column stability and the development of the spring phytoplankton bloom on the southeast Bering Sea middle shelf. Unpublished manuscript.
- Sancetta, C. 1981a. Diatoms as hydrographic tracers: example from Bering Sea sediments. Science 211:279-281.
- Sancetta, C. 1981b. Oceanographic and ecological significance of diatoms in surface sediments of the Bering and Okhotsk Seas. Deep-Sea Res. 28(8A):789-817.
- Sayles, F. L. 1981. The composition and diagenesis of interstitial solutions - II. Fluxes and diagenesis at the water-sediment interface in the high latitude North and South Atlantic. Geochim. Cosmochim. Acta 45:1061-1086.
- Schink, D. R., K. A. Fanning and M. E. Q. Pilson. 1974. Dissolved silica in the upper pore waters of the Atlantic Ocean floor. J. Geophys. Res. 79(15):2243-2250.
- Schink, D. R., N. L. Guinasso, Jr. and K. A. Fanning. 1975. Processes affecting the concentration of silica at the sediment-water interface of the Atlantic Ocean. J. Geophys. Res. 80(21):3013-3031.
- Schrader, H. -J. 1971. Fecal pellets: role in sedimentation of pelagic diatoms. Science 174:55-57.
- Schumacher, J. D. and T. H. Kinder. 1983. Low-frequency current regimes over the Bering Sea Shelf. J. Phys. Oceanogr. In press.

- Sharma, G. D. 1974. Contemporary sedimentary regimes of the eastern Bering Sea. p. 517-552. In: D. W. Hood and E. J. Kelley (eds.), Oceanography of the Bering Sea. Occasional Pub. No. 2, University of Alaska, Fairbanks.
- Sharma, G. D. 1979. The Alaskan Shelf. Springer-Verlag, New York.
- Sharma, G. D., A. S. Naidu and D. W. Hood. 1972. Bristol Bay: model contemporary graded shelf. Amer. Pet. Geol. Bull. 56(10):2000-2012.
- Siever, R., K. C. Beck and R. A. Berner. 1965. Composition of interstitial waters of modern sediments. J. Geol. 73(1):39-73.
- Simpson, T. L. and B. E. Volcani. 1971. Silicon and Siliceous Structures in Biological Systems. Springer-Verlag New York, Inc., New York.
- Slawyk, G. 1979. ¹³C and ¹⁵N uptake by phytoplankton in the Antarctic upwelling area: results from the Antiprod I cruise in the Indian Ocean sector. Aust. J. Mar. Freshwater Res. 30: 431-438.
- Slawyk, G., Y. Collos, M. Minas and J. -R. Grall. 1978. On the relationship between carbon-to-nitrogen composition ratios of the particulate matter and growth rate of marine phytoplankton from the northwest African upwelling area. J. Exp. Mar. Biol. Ecol. 33:119-131.
- Smayda, T. J. 1970. The suspension and sinking of phytoplankton in the sea. Oceanogr. Mar. Biol. Rev. 8:353-414.
- Smayda, T. J. 1971. Normal and accelerated sinking of phytoplankton in the sea. Mar. Geol. 11:93-104.
- Sullivan, C. W. 1976. Diatom mineralization of silicic acid. I. Si(OH)₄ transport characteristics in Navicula pelliculosa. J. Phycol. 12:390-396.
- Sullivan, C. W. 1977. Diatom mineralization of silicic acid. II. Regulation of Si(OH)₄ transport rates during the cell cycle of Navicula pelliculosa. J. Phycol. 13:86-91.
- Sullivan, C. W. 1980. Diatom mineralization of silicic acid. V. Energetic and macromolecular requirements for Si(OH)₄ mineralization events during the cell cycle of Navicula pelliculosa. J. Phycol. 16:321-328.

- Thomas, W. H. and A. N. Dodson. 1972. On nitrogen deficiency in tropical Pacific oceanic plankton. II. Photosynthetic and cellular characteristics of a chemostat-grown diatom. Limnol. Oceanogr. 17(4):515-523.
- Thomas, W. H., A. N. Dodson and F. M. H. Reid. 1978. Diatom productivity compared to other algae in natural marine phytoplankton assemblages. J. Phycol. 14:250-253.
- Tilman (Titman), D. 1976. Ecological competition between algae: experimental confirmation of resource-based competition theory. Science 192:463-465.
- Tilman, D., S. S. Kilham and P. Kilham. 1982. Phytoplankton community ecology: the role of limiting nutrients. Ann. Rev. Ecol. Syst. 13:349-372.
- Tilman, D., M. Mattson and S. Langer. 1981. Competition and nutrient kinetics along a temperature gradient: an experimental test of a mechanistic approach to niche theory. Limnol. Oceanogr. 26(6):1020-1033.
- Toggweiler, J. R. and W. S. Broecker. 1983. Geochemistry of the deep Bering Sea. Unpublished manuscript.
- Tsunogai, S., M. Kusakabe, H. Iizumi, I. Koike and A. Hattori. 1979. Hydrographic features of the deep water of the Bering Sea — the sea of silica. Deep-Sea Res. 26(6A):641-659.
- Turpin, D. H. and P. J. Harrison. 1979. Limiting nutrient patchiness and its role in phytoplankton ecology. J. Exp. Mar. Biol. Ecol. 39:151-166.
- Ullman, W. J. and R. C. Aller. 1982. Diffusion coefficients in nearshore marine sediments. Limnol. Oceanogr. 27(3):552-556.
- Vanderborgh, J. -P., R. Wollast and G. Billin. 1977. Kinetic models of diagenesis in disturbed sediments. Part I. Mass transfer properties and silica diagenesis. Limnol. Oceanogr. 22(5):787-793.
- Vidal, J. and S. H. Smith. 1983. Biomass, growth and development of populations of herbivorous zooplankton in the southeastern Bering Sea during spring. Submitted to Deep-Sea Res.
- Wakefield, S. J. 1982. Silica distribution in interstitial waters and sediments from the southeastern Pacific. Sed. Geol. 31:13-31.

- Walsh, J. J. 1975. A spatial simulation model of the Peru upwelling ecosystem. Deep-Sea Res. 22:201-236.
- Walsh, J. J., J. C. Kelley, T. E. Whitledge, J. J. MacIsaac and S. A. Huntsman. 1974. Spin-up of the Baja California upwelling ecosystem. Limnol. Oceanogr. 19(4):553-572.
- Walsh, J. J., E. T. Premuzic and T. E. Whitledge. 1981. Fate of nutrient enrichment on continental shelves as indicated by the C/N content of bottom sediments. p. 13-50. In: J. C. J. Nihoul (ed.), Ecohydrodynamics. Elsevier Scientific Pub. Co., New York.
- Walsh, J. J., G. T. Rowe, R. L. Iverson and C. P. McRoy. 1981. Biological export of shelf carbon is a sink of the global CO₂ cycle. Nature 291:196-201.
- Werner, D. 1977a. Introduction with a note on taxonomy. p. 1-17. In: D. Werner (ed.), The Biology of Diatoms. Botanical Monographs Vol. 13, University of California Press, Berkeley.
- Werner, D. 1977b. Silicate metabolism. p. 110-149. In: D. Werner (ed.), The Biology of Diatoms. Botanical Monographs Vol. 13, University of California Press, Berkeley.
- Whitledge, T. E., R. T. Cooney, R. L. Iverson and J. J. Walsh. 1981a. Some aspects of the pelagic springtime ecosystem over the southeastern Bering Sea Shelf. p. 633-668. In: Processes and Resources of the Bering Sea Shelf. Progress Report, 1980, Vol. II, University of Alaska, Fairbanks. 668 p.
- Whitledge, T. E., S. C. Malloy, C. J. Patton and C. D. Wirick. 1981b. Automated Nutrient Analysis in Seawater. Brookhaven Nat. Lab. Pub. 51398, Upton, New York. 216 p.
- Whitledge, T. E. and W. S. Reeburgh. 1980. Nutrient dynamics and distribution in the southeast Bering Sea. p. 101-143. In: Processes and Resources of the Bering Sea Shelf. Progress Report, 1979, Vol. I. University of Alaska, Fairbanks. 367 p.
- Willey, J. D. 1978. Release and uptake of dissolved silica in seawater by marine sediments. Mar. Chem. 7:53-65.
- Wollast, R. 1974. The silica problem. p. 359-392. In: E. D. Goldberg (ed.), The Sea. Vol. 5, John Wiley and Sons, New York.
- Wollast, R. and R. M. Garrels. 1971. Diffusion coefficient of silica in seawater. Nature Phys. Sci. 229(3):94.

APPENDIX A. Station locations, silicic acid uptake data and biogenic silica concentrations at selected PROBES productivity stations. Stations were grouped by location in a domain or near a front. The list below, in conjunction with Figure 1a, gives the approximate location of each station.

COASTAL DOMAIN (INCLUDING THE INNER FRONT)

Station 2019 1979	Station 4030 1980
" 2073 "	
" 3017 "	
" 3069 "	

MIDDLE DOMAIN (INCLUDING THE MIDDLE FRONT)

Stations east of the A-line:	Stations west of the A-line:
Station 1147 1978	Station 2061 1978
" 2030 "	" 2065 "
" 2041 "	" 3044 "
" 3044 "	" 3077 "
	" 3086 "
	" 4034 "

Stations at or near PROBES 12:

Station 2012 1979	Station 4012 1980
" 2044 "	" 4039 "
" 2077 "	" 4070 "
" 3026 "	" 4090 "
" 3097 "	

OUTER DOMAIN

Station 2051 1978	Station 2057 1979	Station 4131 1981
" 3031 "	" 3009 "	
	" 3044 "	

OUTER FRONT (AND OCEANIC DOMAIN)

Station 3001 1979	Station 4105 1980	Station 4052 1981
" 3036 "		" 4124 "

APPENDIX A. Continued.

Silicic acid uptake data and biogenic silica concentrations at selected PROBES productivity stations.

	%SPAR	Z m	Vo h ⁻¹	PSi mmol m ⁻³	Ro mmol m ⁻³ d ⁻¹
Station 1147	100	0	0.0066	9.6	1.514
	50	2	0.0085	7.7	1.584
29 April 1978	30	4	0.0051	10.7	1.308
56 3.5 N 164 58.2 W	15	7	0.0052	8.7	1.080
MIDDLE DOMAIN	5	11	-	11.3	-
	1	17	0.0037	8.5	0.756
	0.1	26	0.0006	11.1	0.168
	0.01	34	-	-	-
0.01% INTEGRATION (m ⁻² basis)			0.110	341	18.76
Station 2030	100	0	0.0026	6.9	0.434
	50	2	0.0087	7.4	1.541
12 May 1978	30	3	0.0021	7.7	0.386
55 35.3 N 163 52.1 W	15	4	0.0014	6.1	0.204
MIDDLE DOMAIN	5	7	0.0019	8.2	0.377
	1	10	0.0032	8.2	0.638
	0.1	15	0.0015	8.5	0.312
	0.01	20	0.0011	9.1	0.233
0.01% INTEGRATION (m ⁻² basis)			0.047	160.4	9.36
Station 2041	100	0	0.0025	7.2	0.437
	50	2	0.0111	14.0	3.720
14 May 1978	30	4	0.0031	6.8	0.509
55 35.6 N 164 14.3 W	15	6	0.0023	7.6	0.418
MIDDLE DOMAIN	5	9	0.0027	7.5	0.490
	1	14	0.0018	8.0	0.353
	0.1	21	0.0019	8.6	0.386
	0.01	28	0.0017	10.7	0.449
0.01% INTEGRATION (m ⁻² basis)			0.077	243.5	18.3

APPENDIX A. Continued.

	<u>%SPAR</u>	<u>Z</u> <u>m</u>	<u>Vo</u> <u>h⁻¹</u>	<u>PSi</u> <u>mmol m⁻³</u>	<u>Ro</u> <u>mmol m⁻³ d⁻¹</u>
Station 2051	100	0	0.0042	2.2	0.221
	50	1	0.0037	2.1	0.118
16 May 1978	30	2	0.0042	2.0	0.207
55 42.4 N 166 17.0 W	15	4	0.0045	2.1	0.225
OUTER DOMAIN	5	6	0.0035	1.4	0.121
	1	9	0.0031	2.1	0.154
	0.1	14	0.0024	2.3	0.113
	0.01	18	0.0032	1.3	0.081
0.01% INTEGRATION (m ⁻² basis)			0.059	35.0	2.58
Station 2061	100	0	0.0082	9.7	1.920
	50	2	0.0094	9.3	2.083
18 May 1978	30	4	0.0092	10.0	2.230
56 41.5 N 167 49.9 W	15	6	0.0085	9.7	1.982
MIDDLE DOMAIN	5	9	0.0058	10.9	1.502
	1	14	0.0033	10.6	0.840
	0.1	21	0.0024	11.6	0.667
	0.01	28	0.0017	13.4	0.550
0.01% INTEGRATION (m ⁻² basis)			0.132	308.0	33.14
Station 2065	100	0	0.0072	8.7	1.503
	50	2	0.0049	9.7	1.141
19 May 1978	30	3	0.0044	9.4	0.993
56 24.2 N 168 36.0 W	15	6	0.0049	9.8	1.152
MIDDLE DOMAIN	5	9	0.0041	9.6	0.945
	1	13	0.0013	-	-
	0.1	19	0.0007	9.1	0.153
	0.01	26	0.0003	9.1	0.066
0.01% INTEGRATION (m ⁻² basis)			0.061	243	16
Station 3031	100	0	0.0031	1.9	0.144
	50	4	0.0043	1.8	0.190
31 May 1978	30	7	0.0050	2.2	0.269
56 1.2 N 166 1.1 W	15	11	0.0047	2.5	0.281
OUTER DOMAIN	5	18	0.0065	3.4	0.538
	1	27	0.0041	6.0	0.600
	0.1	40	0.0019	5.0	0.230
	0.01	54	0.0003	5.8	0.041
0.01% INTEGRATION (m ⁻² basis)			0.181	251.7	17.70

APPENDIX A. Continued.

	<u>%SPAR</u>	<u>Z</u> <u>m</u>	<u>Vo</u> <u>h⁻¹</u>	<u>PSi</u> <u>mmol m⁻³</u>	<u>Ro</u> <u>mmol m⁻³ d⁻¹</u>
Station 3044	100	0	0.0075	1.0	0.175
	50	5	0.0071	1.0	0.166
2 June 1978	30	8	0.0068	1.0	0.156
55 53.0 N 165 13.1 W	15	13	0.0040	0.6	0.062
MIDDLE DOMAIN	5	21	0.0067	1.2	0.192
	1	32	0.0035	8.8	0.739
	0.1	48	0.0010	7.9	0.182
	0.01	64	0.0004	5.3	0.053
0.01% INTEGRATION (m ⁻² basis)			0.230	312.4	17.28
Station 3077	100	0	0.0053	1.5	0.192
	50	4	0.0047	1.7	0.192
6 June 1978	30	7	0.0054	1.7	0.214
56 27.2 N 166 27.7 W	15	12	0.0075	1.8	0.331
MIDDLE DOMAIN	5	19	0.0060	2.1	0.305
	1	29	0.0079	2.4	0.463
	0.1	43	0.0015	12.7	0.454
	0.01	58	0.0001	8.0	0.216
0.01% INTEGRATION (m ⁻² basis)			0.262	317.8	18.79
Station 3086	100	0	-	9.9	-
	50	1	-	10.6	-
7 June 1978	30	3	-	10.8	-
56 56.0 N 166 54.0 W	15	5	-	11.4	-
MIDDLE DOMAIN	5	9	-	11.2	-
	1	14	-	9.0	-
	0.1	21	-	8.9	-
	0.01	28	-	10.2	-
0.01% INTEGRATION (m ⁻² basis)			-	278.6	-
Station 4034	100	0	0.0076	4.4	0.804
	50	3	0.0058	5.3	0.737
24 June 1978	30	5	0.0049	5.4	0.641
57 17.0 N 166 39.0 W	15	8	0.0044	5.5	0.574
MIDDLE DOMAIN	5	12	0.0029	6.6	0.468
	1	19	0.0000	5.6	0.000
	0.1	30	0.0002	5.8	0.031
	0.01	38	0.0002	10.2	0.046
0.01% INTEGRATION (m ⁻² basis)			0.053	235.8	12.40

APPENDIX A. Continued.

	<u>%SPAR</u>	<u>Z</u> m	<u>Vo</u> h^{-1}	<u>PSi</u> mmol m^{-3}	<u>Ro</u> $\text{mmol m}^{-3} \text{d}^{-1}$
Station 2012	100	0	0.0082	16.4	3.233
	50	2	0.0076	13.4	2.455
4 May 1979	30	3	0.0071	17.7	3.022
56 32.8 N 165 7.2 W	15	5	0.0072	17.1	2.947
MIDDLE DOMAIN	5	9	0.0032	19.3	1.478
	1	14	0.0032	18.2	1.394
	0.1	20	0.0020	17.9	0.864
	0.01	28	-	-	-
0.01% INTEGRATION (m^{-2} basis)			0.10	497	41.2
Station 2019	100	0	0.0048	11.6	1.330
	50	3	0.0055	10.5	1.380
5 May 1979	30	6	0.0050	12.5	1.500
57 35.0 N 163 23.0 W	15	9	0.0057	13.0	1.781
COASTAL DOMAIN	5	15	0.0040	14.6	1.402
	1	24	0.0022	15.1	0.811
	0.1	36	0.0004	15.4	0.151
	0.01	47	0.0015	16.9	0.540
0.01% INTEGRATION (m^{-2} basis)			0.127	680.1	43.01
Station 2044	100	0	0.0053	16.1	2.035
	50	2	0.0047	15.6	1.757
9 May 1979	30	3	0.0069	19.0	3.149
56 34.7 N 165 7.8 W	15	5	0.0097	19.1	4.464
MIDDLE DOMAIN	5	8	0.0045	24.6	2.657
	1	12	0.0032	20.6	1.574
	0.1	17	0.0016	20.5	0.775
	0.01	23	0.0003	14.5	0.096
0.01% INTEGRATION (m^{-2} basis)			0.081	449.7	41.02
Station 2057	100	0	0.0128	1.4	0.425
	50	5	-	-	-
12 May 1979	30	8	0.0259	0.6	0.394
55 38.0 N 166 37.4 W	15	12	0.0061	0.6	0.089
OUTER DOMAIN	5	20	-	-	-
	1	30	0.0015	2.1	0.077
	0.1	45	0.0012	1.2	0.036
	0.01	60	0.0050	1.0	0.108
0.01% INTEGRATION (m^{-2} basis)			0.452	70.5	8.69

APPENDIX A. Continued.

	%SPAR	Z m	Vo h ⁻¹	PSi mmol m ⁻³	Ro mmol m ⁻³ d ⁻¹
Station 2073	100	0	0.0035	9.1	0.751
	50	2	0.0045	6.7	0.725
14 May 1979	30	4	0.0039	7.8	0.739
57 35.0 N 165 23.0 W	15	6	0.0042	7.7	0.778
COASTAL DOMAIN	5	10	0.0023	9.0	0.497
	1	15	0.0011	10.2	0.278
	0.1	20	-	9.4	-
	0.01	30	-	7.8	-
0.01% INTEGRATION (m ⁻² basis)			0.054	262	14.15
Station 2077	100	0	0.0124	17.3	5.153
	50	2	0.0149	14.8	5.273
16 May 1979	30	3	0.0102	15.5	3.797
56 32.8 N 165 7.1 W	15	5	0.0159	15.6	5.947
MIDDLE DOMAIN	5	8	0.0041	14.6	1.454
	1	13	0.0036	16.5	1.411
	0.1	19	0.0015	16.2	0.571
	0.01	25	0.0008	8.8	0.170
0.01% INTEGRATION (m ⁻² basis)			0.137	374.9	50.93
Station 3001	100	0	0.0119	7.7	2.188
	50	2	0.0112	8.2	2.207
25 May 1979	30	4	0.0116	7.4	2.060
54 51.3 N 167 53.1 W	15	6	0.0095	7.7	1.754
OUTER FRONT	5	9	0.0096	6.3	1.443
	1	14	0.0065	3.6	0.563
	0.1	20	0.0037	1.7	0.152
	0.01	28	-	-	-
0.01% INTEGRATION (m ⁻² basis)			0.181	107	25
Station 3009	100	0	0.0019	1.6	0.072
	50	3	0.0041	0.8	0.074
26 May 1979	30	6	0.0054	0.8	0.098
56 5.3 N 165 54.6 W	15	9	0.0037	0.7	0.062
OUTER DOMAIN	5	14	0.0023	0.6	0.031
	1	22	0.0014	0.7	0.026
	0.1	32	0.0017	0.9	0.038
	0.01	43	0.0004	1.3	0.012
0.01% INTEGRATION (m ⁻² basis)			0.091	36.8	1.78

APPENDIX A. Continued.

	<u>%SPAR</u>	<u>Z</u> <u>m</u>	<u>Vo</u> <u>h⁻¹</u>	<u>PSi</u> <u>mmol m⁻³</u>	<u>Ro</u> <u>mmol m⁻³ d⁻¹</u>
Station 3017	100	0	0.0026	4.3	0.268
	50	3	0.0031	4.7	0.349
27 May 1979	30	6	0.0030	4.7	0.332
57 17.4 N 163 53.2 W	15	9	0.0027	4.7	0.302
COASTAL DOMAIN	5	14	0.0022	5.0	0.270
	1	22	0.0037	12.5	1.123
	0.1	32	0.0000	12.1	0.000
	0.01	43	0.0000	10.1	0.000
0.01% INTEGRATION (m ⁻² basis)			0.081	380.2	9.9
Station 3026	100	0	0.0073	1.8	0.304
	50	2	0.0073	1.5	0.268
28 May 1979	30	4	0.0089	1.5	0.316
56 32.9 N 165 8.1 W	15	6	0.0066	1.4	0.221
MIDDLE DOMAIN	5	10	0.0042	3.8	0.396
	1	16	0.0030	6.7	0.492
	0.1	24	0.0005	7.2	0.092
	DARK	40	0.0015	6.4	0.233
	DARK	50	0.0002	8.8	0.004
0.01% INTEGRATION (m ⁻² basis)			0.110	163	7
Station 3036	100	0	0.0108	2.8	0.730
	50	4	0.0121	2.4	0.706
29 May 1979	30	7	0.0074	3.0	0.530
55 0.8 N 166 36.0 W	15	12	0.0021	1.1	0.055
OUTER FRONT	5	19	0.0008	1.3	0.024
	1	30	0.0002	1.7	0.007
	0.1	46	0.0002	1.0	0.005
	0.01	63	0.0003	1.3	0.010
0.01% INTEGRATION (m ⁻² basis)			0.122	94.0	6.86
Station 3069	100	0	0.0026	3.3	0.206
	50	4	0.0030	3.3	0.240
1 June 1979	30	7	0.0026	3.6	0.220
57 30.0 N 164 15.2 W	15	11	0.0027	3.4	0.214
COASTAL DOMAIN	5	18	0.0023	3.5	0.197
	1	27	0.0012	10.7	0.319
	0.1	41	0.0006	17.8	0.274
	0.01% 48	-	-	-	-
0.01% INTEGRATION (m ⁻² basis)			0.078	441	10.5

APPENDIX A. Continued.

	<u>%SPAR</u>	<u>Z</u> <u>m</u>	<u>Vo</u> <u>h⁻¹</u>	<u>PSi</u> <u>mmol m⁻³</u>	<u>Ro</u> <u>mmol m⁻³ d⁻¹</u>
Station 3044	100	0	-	1.4	-
	50	4	-	1.0	-
30 May 1979	30	6	-	1.4	-
55 50.1 N 167 5.2 W	15	10	-	1.4	-
OUTER DOMAIN	5	16	-	1.6	-
	1	24	-	0.6	-
		40	-	0.7	-
	0.01	50	-	0.3	-
0.01% INTEGRATION (m ⁻² basis)			-	43.2	-
Station 3097	100	0	0.0076	2.8	0.509
	50	1	0.0053	4.2	0.528
4 June 1979	30	2	0.0063	2.2	0.341
57 5.4 N 167 23.0 W	15	4	0.0068	2.8	0.466
MIDDLE DOMAIN	5	6	0.0056	4.8	0.636
	1	9	0.0049	5.7	0.672
	0.1	13	0.0038	6.1	0.559
	0.01	17	0.0024	7.9	0.463
0.01% INTEGRATION (m ⁻² basis)			0.086	91.7	9.33
Station 3117	100	0	0.0060	0.6	0.094
	50	2	-	0.9	-
8 June 1979	30	6	0.0029	1.1	0.077
57 30.1 N 164 15.1 W	15	11	0.0030	2.1	0.151
COASTAL DOMAIN	5	20	0.0031	6.3	0.470
	1	32	0.0012	10.6	0.302
	0.1	49	0.0002	21.3	0.084
	0.01	below the bottom			
0.1% INTEGRATION (m ⁻² basis)			0.107	424.3	11.79
Station 4012	100	0	0.0026	13.7	0.859
	50	2	-	-	-
23 May 1980	30	4	0.0028	12.2	0.835
56 32.1 N 165 8.5 W	15	6	0.0029	12.9	0.890
MIDDLE DOMAIN	5	9	0.0024	13.9	0.828
	1	14	0.0013	7.0	0.214
	0.1	21	0.0009	16.7	0.363
	0.01	28	-	-	-
0.01% INTEGRATION (m ⁻² basis)			0.045	369	12.32

APPENDIX A. Continued.

	<u>%SPAR</u>	<u>Z</u> <u>m</u>	<u>Vo</u> <u>h⁻¹</u>	<u>PSi</u> <u>mmol m⁻³</u>	<u>Ro</u> <u>mmol m⁻³ d⁻¹</u>
Station 4030	100	0	0.0053	9.4	1.202
	50	2	0.0057	9.2	1.258
25 May 1980	30	4	0.0053	9.3	1.178
57 8.5 N 164 8.0 W	15	7	0.0034	10.3	0.845
COASTAL DOMAIN	5	10	0.0028	8.8	0.600
	1	16	0.0016	10.4	0.391
	0.1	24	0.0015	11.9	0.425
	0.01	32	0.0003	23.9	0.180
0.01% INTEGRATION (m ⁻² basis)			0.074	385.6	18.74
Station 4039	100	0	0.0036	7.2	0.622
	50	3	0.0031	7.2	0.529
26 May 1980	30	5	0.0031	6.9	0.518
56 32.1 N 165 8.0 W	15	7	0.0027	5.1	0.334
MIDDLE DOMAIN	5	11	0.0022	8.4	0.448
	1	18	0.0017	9.2	0.378
	0.1	26	0.0011	15.1	0.390
	0.01	36	-	-	-
0.01% INTEGRATION (m ⁻² basis)			0.062	384	11.15
Station 4070	100	0	0.0074	11.2	1.975
	15	5	-	14.4	-
30 May 1980	5	7	0.0061	18.1	2.659
57 2.0 N 165 51.0 W	1	11	0.0056	20.1	2.683
MIDDLE DOMAIN	0.1	16	0.0008	13.6	0.250
	0.01	22	0.0013	7.8	0.247
	DARK	50	0.0009	5.9	0.130
	DARK	64	0.0008	5.8	0.118
0.01% INTEGRATION (m ⁻² basis)			0.093	321.4	35.7
Station 4090	100	0	-	2.1	-
	50	6	-	1.2	-
2 June 1980	30	10	-	6.5	-
56 32.0 N 165 8.0 W	15	16	-	2.0	-
MIDDLE DOMAIN	5	25	-	1.5	-
	1	38	-	4.1	-
	0.1	58	-	6.1	-
	0.01	70	-	-	-
0.01% INTEGRATION (m ⁻² basis)			-	290	-

APPENDIX A. Continued.

	%SPAR	Z m	Vo h ⁻¹	PSi mmol m ⁻³	Ro mmol m ⁻³ d ⁻¹
Station 4105	100	0	0.0060	3.2	0.458
	50	2	-	-	-
5 June 1980	30	3	0.0069	3.2	0.528
54 52.0 N 167 53.0 W	15	4	-	-	-
OUTER FRONT	5	7	0.0028	3.9	0.262
	1	10	-	-	-
	0.1	15	0.0002	4.5	0.019
	0.01	20	-	-	-
0.01% INTEGRATION (m ⁻² basis)			0.05	79	4.2
Station 4052	100	0	0.0147	10.0	3.358
	50	2	0.0150	10.1	3.658
7 July 1981	30	3	0.0085	10.8	2.203
54 51.0 N 167 50.1 W	15	5	0.0109	11.0	2.861
OUTER FRONT	5	7	0.0054	4.9	0.631
	1	11	0.0016	2.5	0.096
	0.1	17	0.0005	2.4	0.031
	0.01	22	0.0009	3.2	0.070
0.01% INTEGRATION (m ⁻² basis)			0.101	111.8	20.78
Station 4124	100	0	0.0068	1.2	0.190
	50	5	0.0076	0.9	0.168
19 July 1981	30	8	0.0033	1.0	0.082
55 46.0 N 169 22.1 W	15	13	0.0042	1.0	0.101
OUTER FRONT	5	20	0.0010	1.0	0.024
	1	31	0.0002	1.6	0.010
	0.1	46	0.0000	2.9	0.000
	0.01	62	-	-	-
0.01% INTEGRATION (m ⁻² basis)			0.097	84	2.352
Station 4131	100	0	0.0023	0.4	0.024
	50	5	0.0027	0.4	0.024
20 July 1981	30	8	0.0034	0.3	0.024
55 29.4 N 166 50.5 W	15	13	-	-	-
OUTER DOMAIN	5	20	0.0023	0.5	0.029
	1	31	0.0014	1.0	0.036
	0.1	47	0.0003	0.5	0.005
	0.01	62	-	-	-
0.01% INTEGRATION (m ⁻³ basis)			0.090	35.6	1.22

APPENDIX B. The equations from the linear geometric mean regressions of carbon, nitrogen and chlorophyll-a versus silicon. Both particulate and uptake data are from discrete depths. The range given for v is the 95% confidence interval of the slope.

COASTAL DOMAIN $\text{mg Si m}^{-3} = 41.0 \text{ mg chl-a m}^{-3} - 13.1 \quad r^2 = 0.71$

$$v = 32.1-49.9$$

$$\text{mmol NO}_3^- \text{ m}^{-3} \text{ d}^{-2} = 0.70 \text{ mmol Si m}^{-3} \text{ d}^{-1} - 0.07 \quad r^2 = 0.64$$

$$v = 0.52-0.88$$

$$\text{mmol C m}^{-3} \text{ d}^{-1} = 9.09 \text{ mmol Si m}^{-3} \text{ d}^{-1} - 0.86 \quad r^2 = 0.74$$

$$v = 3.94-14.24$$

MIDDLE SHELF $\text{mg Si m}^{-3} = 16.0 \text{ mg chl-a m}^{-3} + 109 \quad r^2 = 0.72$

$$v = 14.0-18.0$$

$$\text{mmol N m}^{-3} = 0.51 \text{ mmol Si m}^{-3} + 0.54 \quad r^2 = 0.71$$

$$v = 0.44-0.58$$

$$\text{mmol C m}^{-3} \text{ d}^{-1} = 6.41 \text{ mmol Si m}^{-3} \text{ d}^{-1} - 1.59 \quad r^2 = 0.74$$

$$v = 5.03-7.79$$

$$\text{mmol C m}^{-3} = 4.72 \text{ mmol Si m}^{-3} + 1.95 \quad r^2 = 0.65$$

$$v = 3.58-5.86$$

OUTER FRONT $\text{mg Si m}^{-3} = 22.6 \text{ mg chl-a m}^{-3} + 16.8 \quad r^2 = 0.92$

$$v = 19.2-26.0$$

$$\text{mmol NO}_3^- \text{ m}^{-3} \text{ d}^{-1} = 1.30 \text{ mmol Si m}^{-3} \text{ d}^{-1} - 0.35 \quad r^2 = 0.72$$

$$v = 0.99-1.71$$

$$\text{mmol C m}^{-3} \text{ d}^{-1} = 9.58 \text{ mmol Si m}^{-3} \text{ d}^{-1} + 1.03 \quad r^2 = 0.71$$

$$v = 6.44-12.72$$